



UiT The Arctic University of Norway

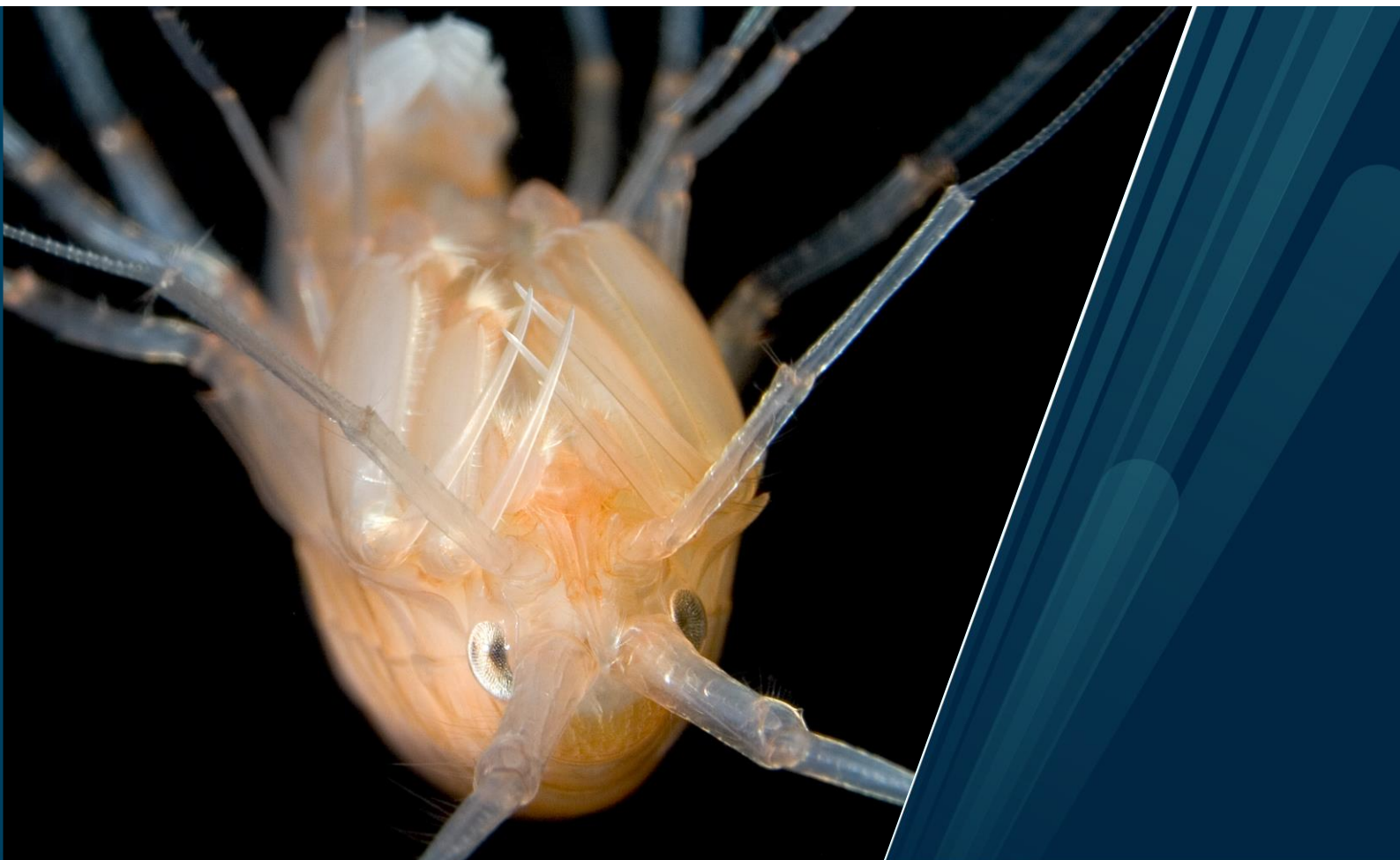
Faculty of Biosciences, Fisheries and Economics

Living on the dark side? Investigations into under-ice light climate and sympagic amphipods

Rupert Harald Krapp

A dissertation for the degree of Philosophiae Doctor

June 2022



**“Living on the Dark Side? Investigations into under-ice light
climate and sympagic amphipods»**

Synthesis of the submitted manuscripts and published articles

By Rupert Harald Krapp

February 2022

Submitted for evaluation as PhD thesis at UiT The Arctic University of Norway

Table of Contents

Acknowledgements	4
Abbreviations and definitions used here	5
List of papers and publication status	6
Declaration of contributions	7
Abstract	8
Background and personal motivation	9
Introduction and setting	12
Sea ice as structuring element: living medium, moving structure and resource filter	13
Climate change induced sea ice decrease and its implications	14
The sympagic domain – a unique feature of the ice-covered oceans	16
Sympagic amphipods in the Arctic	17
Importance of the sea-ice cover for the underwater light climate in polar ecosystems	21
Light climate and its physical definitions	21
Ultraviolet radiation and stratospheric ozone	23
Purpose of this study	26
Scientific approach and methodology	27
Presentation of papers	29
Discussion	32
UV radiation tolerance and protective adaptations in sympagic amphipods	31
Effects of UVR on Arctic sea ice-associated amphipods (paper I)	33
Photoprotective substances	35
Photoprotection through pigment acquisition in sea ice amphipods (pps II & III)	37
Effects of UVR on Antarctic ice-associated ecosystems	40
The ecological role of Antarctic sympagic amphipods (paper IV)	41
Current technical challenges in under-ice sampling and possible future solutions	44
Conclusions	46
Bibliography	47
List of published articles included and discussed in this synthesis	59
Appendix	60

Acknowledgements

This study has been made possible through the financial support of the Deutsche Forschungsgemeinschaft (DFG) through individual grants awarded to me under the Polar Research Programme (Polarforschungsprogramm), as well as general support by the Alfred-Wegener-Institute for Polar and Marine Research (AWI), and by the University Centre in Svalbard (UNIS). I would like to express my deepest gratitude to Prof. Dr. Spindler at the University of Kiel and the AWI, for introducing me to the Polar regions and for supporting me in my years in Kiel, and to Prof. Dr. Jørgen Berge, for supervising and supporting me for all these years at UNIS and on Svalbard. I could not have wished for better supervisors and mentors.

I also have to thank my wife Maria, my children, and the rest of my family, for supporting and tolerating my sometimes weird working hours, and for encouraging and inspiring me throughout these years. Last but not least, I would like to thank my scientific diving partners, especially Jørgen Berge and Hauke Flores, for their support during countless hours spent under the sea ice in the Arctic and Antarctic, and the incredibly professional crews of the research vessels R/V Helmer Hanssen and R/V Polarstern.

Abbreviations and definitions used here

6-4 PP	6-4 pyrimidone photoproducts
AUV	autonomous underwater vehicle
CDOM	chromophoric dissolved organic matter
CFCs	chlorofluorocarbons
CIE	Commission International d'Eclairage
CO₂	carbon dioxide
CPDs	cyclobutane pyrimidine dimers
DNA	deoxyribonucleic acid
DOC	Dissolved organic carbon
DOM	Dissolved organic matter
ECMWF	European Centre for Medium-Range Weather Forecasts
FYI	First-year ice
HPLC	high-performance liquid chromatography
IRIS	International Research Institute of Stavanger AS
ISPOL	Ice Station Polarstern
MAA	mycosporine-like amino acids
MDA	malondialdehyde
MOSAiC	Multidisciplinary drifting Observatory for the Study of Arctic Climate
MYI	Multi-year ice
O₃	ozone or trioxygen
ODS	ozone-depleting substances
PAR	photosynthetically active radiation
ROS	reactive oxygen species
ROV	remotely operated vehicle
SUIT	Surface- and under-ice trawl
TBA	thio-barbituric acid
TOSC	total oxyradical scavenging capacity
UVI	ultraviolet radiation index
UVR	ultraviolet radiation
VIS	Visible spectrum, range of wavelengths visible to the human eye

List of papers and publication status

Paper 1: Krapp et al (2009): Antioxidant responses in the polar marine sea-ice amphipod *Gammarus wilkitzkii* to natural and experimentally increased UV levels

(Rupert H. Krapp, Thierry Baussant, Jørgen Berge, Daniela M. Pampanin, Lionel Camus)

Published in AQUATIC TOXICOLOGY (2009)

PAPER 2: Fuhrmann et al (2011): The adaptive significance of chromatophores in the Arctic under-ice amphipod *Apherusa glacialis*

(Mona M. Fuhrmann, Henrik Nygård, Rupert H. Krapp, Jørgen Berge, Iris Werner)

Published in POLAR BIOLOGY (2010)

Paper 3: Krapp & Berge (in prep): Total content of Mycosporine-like amino acids (MAAs) in the sympagic amphipods *Gammarus wilkitzkii*, *Onisimus nanseni*, *O. glacialis*, and *Apherusa glacialis* under Arctic pack ice during different seasons

(Rupert H. Krapp, Jørgen Berge)

Manuscript in preparation

Paper 4: Krapp et al (2008): Sympagic occurrence of Eusirid and Lysianassoid amphipods under Antarctic pack ice

(Rupert H. Krapp, Jørgen Berge, Hauke Flores, Bjørn Gulliksen, Iris Werner)

Published in DEEP-SEA RESEARCH II (2008)

A 5th paper is also included in the appendix of this synthesis, as it has been a product of the data collection efforts on the Antarctic under-ice light climate. But since its main thrust is not directly relevant for sympagic amphipods, but rather on the origins and biogeochemistry of chromophoric dissolved organic matter (CDOM), I have chosen to include it in the appendix, rather than the main thesis.

Paper 5: Norman et al (2011): The characteristics of dissolved organic matter (DOM) and chromophoric dissolved organic matter (CDOM) in Antarctic sea ice (Deep-Sea Res II, 2011)

Declaration of contributions

	Paper 1	Paper 2	Paper 3	Paper 4
Concept and idea	RK, LC, JB	MF, HN, RK, JB	RK, JB	RK, HF, JB, IW
Study design and methods	RK, LC, TB, DP	MF, HN, RK	RK	RK, HF, JB
Data gathering and interpretation	RK, TB, LC, DP	MF, HN, RK, JB	RK, JB	RK, JB, HF, BG
Manuscript preparation	RK, JB, TB, LC, DP	MF, HN, RK, JB, IW	RK, JB	RK, JB, HF, BG

RK = Rupert Krapp

HF = Hauke Flores

JB = Jørgen Berge

BG = Bjørn Gulliksen

TB = Thierry Baussant

HN = Henrik Nygård

LC = Lionel Camus

DP = Daniela Pampanin

MF = Mona Fuhrmann

IW = Iris Werner

Abstract

The manuscripts of the dissertation presented here encompass several aspects of adaptations in ice-associated amphipods, focussing mainly on their ability to cope with increased light levels, including the ultraviolet radiation (UVR), under thinner or more dispersed sea ice. A decrease in multi-year ice (MYI) in the Arctic, and a concurrent reduction in stable habitat for ice-associated species, is a substantial threat to the ecosystem in the Arctic Ocean, as these amphipods act as a key trophic link between primary production inside and under sea ice, and higher trophic levels. In a shift from thicker multi-year ice to thinner and less coherent first-year ice, the changes in under-ice light levels may be considered as the second-most significant factor, after the loss of the habitat itself. This thesis has as its overarching ambition to contribute to our understanding of how this change may affect the organisms living in association with the Arctic sea ice.

While the reduction in stratospheric ozone and the resulting seasonal increases in ultraviolet radiation (UVR) have been halted and to some extent reversed, the recovery period is calculated to be protracted, and might even be affected negatively by the ongoing warming of the troposphere through the ongoing emission of greenhouse gases.

So both the direct and indirect effects of UVR on sea ice-associated amphipods have been proven to be a significant factor, especially in the context of a reduction in both thickness and extent of the Arctic sea ice cover. The effects of pigment ingestion and accumulation have also been of particular interest, as well as the capacity of organisms to cope with and adapt to elevated, radiation-induced oxidative stress.

Another aspect of this thesis has been to investigate hitherto unknown and potentially overlooked aspects of the distribution and occurrence of ice-associated amphipods in the Antarctic.

This study contributed to altering the previously held assumption that ice-associated amphipods in Antarctic waters were predominantly originating from the shallow benthos and were thus able to interact with sea ice only when it is over relatively shallow depths.

One of the papers presented in this thesis documents several pelagic amphipod species living in close association with sea ice. Hence, an important conclusion from this is that there is a pelago-sympagic component of Antarctic amphipods in the Weddell Sea.

Background and personal motivation

Efforts in the scientific exploration of the high Arctic and the Antarctic have for a long time predominantly followed the pathways that had already been developed for economic exploration and exploitation. Due to the substantial costs and risks involved, such economically motivated efforts seemed for the most part to have been focused on those areas and aspects with the highest feasibility, accessibility and greatest potential gains. The same logic appears to be pertinent to the scientifically motivated efforts in polar research.

This approach might well have caused the ecological understanding of the polar oceans to be based on a certain degree of generalizations, assumptions and to some degree through extrapolations of patchy data.

The ice-covered waters of the Arctic and Antarctic were previously assumed to be a “desert” and of little biological or ecological concern, until scientists in the late 80’s decided to spend a significant amount of additional effort and proceeded to develop the required tools and skills to investigate them (Gulliksen & Lønne, 1991). Russian scientists initiated some of the first detailed studies of the Arctic sea ice in the 80’ and early 90’s (Melnikov, 1997), and were later followed by Norwegian scientists (see e.g. Swadling and Arndt 2005). What they found was that there is a lot of life to be found under, around and even inside the sea ice, which we now know to be home and shelter for a complex community of protists, ice algae, crustaceans, and even fish which are strongly adapted to, and associated with, the dynamic and heterogeneous sea ice in the polar oceans (Legendre et al. 1992).

Similarly, the polar night, i.e. the period of several months during which no direct sunlight reaches the high polar latitudes, was long believed to be a period of minimal biological activity, a time of dormancy or even complete absence of any life forms who could avoid it by migrating away from it (Berge et al., 2015a). Upon closer examination, recent investigations found unexpected levels not only of a diverse biological presence, but also high levels of activity and interactions (Berge et al., 2015b), with predators hunting their prey above and below the waters (Berge et al., 2020).

What these two examples show is that it is often worth it to take a closer look, and to spend the extra effort on investigating matters that seem to already have a simple answer.

In the matter of this study, I started out with a deep fascination for the life under the sea ice, particularly for the amphipod species that I had learnt about during my student years at the University Center in Svalbard, UNIS. Amphipods are something that I had been familiar with since my childhood, as they can be found on virtually any beach, under almost any rock, or in any piece of kelp blown ashore. Chances are, that most people who have ever been to a beach, have encountered a good number of species of amphipods.

What makes amphipods under sea ice especially intriguing in an ecological context, is that they represent an important trophic link between the sea ice biota and the underlying water masses. And what intrigued me about their presence under the sea ice was just how heterogenous the structure, thickness, age composition, snow cover, and the resulting light levels under the ice were. From personal experience, diving under various types of sea ice, I knew that it looked a bit like flying an aircraft under broken cloud cover, with strong variations in light intensities varying on the scales of meters (personal observation). And while there was strong evidence that some species seemed to be more often present under the deepest, and thus darkest, areas of the sea ice, on deep ice “keels” and under rafted floes, other species seemed to have a clear preference for the opposite, for the brightest, most light-exposed and shallowest parts of the floes, including the fully sunlight-exposed floe edges (Hop et al, 2000).

So given that amphipods must cope with a considerable variability in light climate, the question formed if there might also be an element of light stress detectable, given that the polar areas, and the Antarctic waters in particular, have been subjected to elevated levels of ultraviolet radiation (UVR), which is known to be harmful on a range of levels.

Another question that had attracted my attention was whether you could also find amphipods under sea ice around the Antarctic. There had been quite a few records of some benthic amphipod species reaching the land-fast sea ice over shallow waters near the Antarctic coasts, but little was known about amphipods under sea ice found over deep water, like in the central Weddell Sea. Indeed, when I finally managed to join a dedicated sea ice research expedition on the German Research vessel “Polarstern”, I met with a senior scientist who had spent her career investigating the sea ice biology in the Antarctic waters. She calmly

informed me over a cup of coffee in the ship's salon that she had never in over 20 years found any amphipods under the ice over deep waters.

But when we finally reached our designated area of research for the ISPOL drift expedition and had established a dive hole in the middle of an ice floe, the first dive revealed that there were amphipods in every direction, swiftly swimming away from the divers.

The following thesis is presenting the accumulated results of my publications on the effects of UVR on Arctic sea ice amphipods, on coping strategies found to handle UVR-induced stress or damage, and on our results of investigations into Antarctic sea-ice associated amphipods from the Weddell and Lazarev Seas in the Antarctic.

Introduction and setting

The main ambition of the study has been to examine the ecology and distribution of under-ice amphipods in an era of abrupt climate change. The first aspect to address was the effect of a changing light climate, including ultraviolet radiation (UVR), on these key invertebrate species living in the Arctic sea ice habitat. Therefore, the physical properties and heterogeneity of sea ice as well as the overlying snow cover, and the importance of the resulting underwater light climate and its physical properties were considered to be of central importance.

However, the complexity of such a task clearly exceeded the scope of such a study in all its physical, optical and technical aspects. In order to address some of the key implications of the under-ice light climate, the direct access to the actual habitat of the sea ice undersurface through scientific diving was an essential factor. This access method allowed for a highly species-specific as well as site-specific approach of sampling, where suitable light and UVR sensors could be deployed to the exact sites where the studied amphipod species had been found.

After thus establishing some *in situ* baseline data on visible (VIS) and ultraviolet (UV) light levels, the next step was then able to progress to controlled radiation exposure experiments in the laboratory. These experiments focused on the mechanisms of UV-induced light stress, which is known to induce oxyradicals in the aquatic environment and thus oxidative stress inside the exposed organisms.

Another objective was to investigate the presumed presence of photo-protective substances known to occur in similar organisms in the Antarctic, called mycosporine-like amino acids (MAA's), and established baseline data for the occurrence of MAA's in Arctic sympagic amphipods as well.

Stemming from the idea of photoprotective pigments mentioned above arose the idea to address the ecological and photoprotective role of chromatophores, or pigment-containing compartments in the body tissues of *Apherusa glacialis*, one of the Arctic sympagic amphipods.

Additionally, in order to relate the work not only to the Arctic, but also to the Antarctic, another interesting approach was to examine the potential presence of ice-associated amphipods in some of the less studied offshore areas in the Southern Ocean.

While logistical constraints prevented us from pursuing all of the mentioned objectives in the Antarctic sea-ice environment to the same extent as had been done in the Arctic, the identification of several Antarctic sympagic amphipods from the Weddell and Lazarev Seas contributed significantly to the understanding of amphipods in the Antarctic sea ice environment.

Sea ice as structuring element: living medium, moving structure and resource filter

Sea ice is a major structuring factor of the ecology of the Arctic and Antarctic seas, providing a substrate for a complex community of sympagic or ice-associated organisms. These organisms are ranging in size from bacteria, various invertebrates to marine mammals (Bradstreet and Cross 1982, Horner 1985). Macias-Fauria and Post (2017) divide the ecological impacts of Arctic sea ice into direct and indirect effects. The three direct effects identified by them are the role of sea ice as a living medium and matrix, as a transport and mobility structure, and as a resource filter. While the indirect effects are more relevant on a larger scale, the direct effects are evidently important on an individual, species and community level. As they aptly described it, the sea ice is much more than just a substrate. It provides a wide scale of salinity regimes, from melt ponds to hypersaline brine channels, and a matrix of cracks, channels, pockets and protrusions that can act as refuge, nursing ground and multifaceted substrate. As it drifts with wind and ocean currents, the sea ice is constantly transformed in its physical properties and can also act as a potent transport agent from the continental shelf areas to the deep central Arctic ocean, and further on to the Northern North Atlantic via the Fram Strait. Last but not least, sea ice acts as a resource filter in several ways, by regulating both the transmission of sunlight into the underlying waters, by retaining biomass in its interior matrix, by establishing and stabilising surface stratification of the under-ice water through melting processes, and by acting as a particle filter.

While the sea ice in the Barents and Bering Seas is predominantly made up of annual or first-year ice (also abbreviated as FYI), which forms and decays on a seasonal basis and is

typically absent during the peak of summer, the central deep basin of the Arctic Ocean and its adjacent seas typically contain a significant proportion of multi-year ice (MYI), which means ice that has been retained throughout one or several seasonal melting periods, and thus is present also in the summer months. So a considerable amount of older, thicker and typically more deformed sea ice is typically found throughout the summer in areas of the Arctic, where conditions favour retention and continuous development.



Fig. 1: scientific diver sampling sea ice fauna under heavy multi-year ice (© G Johnsen)

Climate change induced sea ice decrease and its implications

However, recent studies have shown that the proportion of MYI is decreasing significantly in the Arctic, and both sea ice extent and sea ice thickness have been decreasing consistently in the Arctic during the past decades. Notz & Stroeve (2016) have clearly shown that there is a robust linear relationship between monthly-mean September sea-ice area and cumulative carbon dioxide (CO₂) emissions.

It is therefore to be expected that the total amount of MYI will continue to decrease in future seasons, and that FYI will be the predominant sea ice type also in the central Arctic Ocean. This may potentially have wide-ranging ramifications for the sea ice-associated fauna and flora, and particularly for species that have been described to be closely associated with multi-year ice.

Recent analyses show an accelerated annual sea ice loss during winter months in the Arctic, from -2.4% / decade for the period of 1979-1999, to -3.4%/from 2000 onwards. The same study projects that the Arctic Ocean will become sea-ice free throughout August and September for an additional 800 ± 300 Gt of CO₂ emissions, while it would become ice-free from July to October for an additional 1400 ± 300 Gt of CO₂ emissions (Stroeve and Notz 2018).

A series of studies have tracked the dynamics of sea ice loss over time (Stroeve et al, 2007; Stroeve et al, 2012; Stroeve et al, 2014; Notz and Stroeve, 2016). Stroeve et al (2007) found that there seems to be an accelerating downward trend of sea ice extent, citing -9.1% per decade 1953 – 2006, while over the decade or so just prior to their study (1995 – 2006), observed trends were even larger at -17.9 ± 5.9 %/decade. Stroeve et al (2012) pointed towards a clear shift in both spring and fall sea ice age distribution, where the percentages of older ice classes have been reduced significantly since the 1980's, from about 2.33 million km² (30%) of older ice, i.e. 5 years or older, to 1.4 million km² (18%) by 1996 (see also Maslanik et al, 2007), and less than 700.000 km² by 2010. And Stroeve et al (2014) concluded that there was a significant increase in the length of the melt season, by as much as 5 days per decade in the entire Arctic in the period from 1979 to 2013, while several areas (the Kara, Laptev, East Siberian, Chukchi, and Beaufort seas) were shown to have 6 to 11 days per decade in later autumn freeze-up.

Notz and Stroeve (2016) calculated the linear relationship between the 30-year running mean of September sea-ice areas, and cumulative carbon dioxide emissions, and found that observed Arctic sea-ice loss directly follows the trend of anthropogenic CO₂ emissions, where one metric ton of CO₂ emissions implied a sustained loss of 3 ± 0.3 square meters of September sea-ice area. According to their calculations, the Arctic sea-ice could be lost completely following the emission of another 1000 gigatons of CO₂. Current emissions were estimated as 35 Gt CO₂ per year at the time of their publication and have not decreased much in the last years. This means that the limit of 1000 Gt could be reached by 2050.

In the Antarctic, the overall picture seems to be quite different, as there are only few and quite limited areas with multi-year sea ice. While there overall has been a gradual but uneven increase in Antarctic sea-ice extent until 2014, recent studies now show that there has been a drastic decrease since then, at rates far exceeding those seen in the Arctic (Turner et al, 2016, Parkinson, 2019). As Antarctic ice-associated species have developed in a far more dynamic

sea-ice regime with annual fluctuations far exceeding the rates of growth and decay of Arctic sea-ice, it can be assumed that they will be much better adapted to alternate between sympagic and pelagic lifestyles. Therefore, it seems harder to draw conclusions for the ecological ramifications of the Antarctic sea-ice dynamic.

The sympagic domain – a unique feature of the ice-covered oceans

The Arctic sea-ice has been studied for over 150 years, and some notable publications include C. G. Ehrenberg's classical work on ice flora from 1841, and Fritjof Nansen's studies of protozoans found in Arctic pack ice 1906. Recent improvements in sampling equipment as well as ice-going research vessels has allowed researchers to better understand the role that sea-ice plays in the ecology of the polar oceans. As it attracts and supports a vast range of creatures ranging from protists to cetaceans, it effectively adds a third domain to the polar oceans, but with strong links and vital interactions with the underlying pelagic, as well as the benthic realm.

This unique feature of ice-covered waters is far more than just a "platform" for ice-associated organisms like seals and polar bears. Under the surface, it can also form a convoluted structure of sea ice floes that can be pushed and "rafted" together into a multi-level structure with an astonishing variety of nooks and crannies, ledges, ridges, keels and even "caves" offering protection and shelter. But even the very substance of the sea ice itself is not just a solid slab of frozen water, rather it can instead be best understood as a complex matrix due to the presence of brine channels inside the ice. This process of brine formation and rejection is central to the understanding of the physical structure of sea ice and is based on the crystallization process of sea water, during which salt ions which cannot be incorporated into the crystal structure, are trapped in brine pockets which eventually connect to form brine channels. And it is this matrix of amount brine channels, pockets and cracks, which is offering protection and substrate to a wide range of organisms, ranging from microbes, single-celled algae, to small invertebrate animals.

Common for them is that they have adapted to life under or even inside the sea ice matrix, seeking shelter from potential predators, grazing, or preying on other organisms in the ice, or in close association with it.

The ice-associated, or sympagic, macrofaunal community is defined to be > 5 mm. The term “sympagic fauna” has superseded the less precise term “sub-ice fauna”, as it better reflects the direct association of these organisms with the sea ice undersurface and its topography of brine channels, ridges, and spaces in between rafted sea ice floes.

Another common way of categorizing the sympagic fauna has been to separate between autochthonous and allochthonous species. The term autochthonous, meaning native to the place where found, often also used as autochthonous sympagic, is applied to those organisms whose entire life cycle is considered to be tightly associated with sea ice. Allochthonous species are then those species originating from a place other than where found, is then applied to those assumed to be spending only part of their life cycle in tight association with sea ice. These allochthonous origins can be either the benthic or pelagic realms, and such species are thus often classified as benthic-sympagic or pelago-sympagic, respectively.

Sympagic amphipods in the Arctic

In terms of biomass, the Arctic sympagic invertebrate fauna is dominated by amphipods (Lønne & Gulliksen, 1991). These organisms are occupying a range of trophic strategies, encompassing herbivorous, detritivorous, necrophagous, and carnivorous food sources. Most species seem to show a certain extent of food choice plasticity, but interspecific trophic niche overlap appears to be low (Arndt et al, 2005).

The largest and most conspicuous sympagic amphipods are typically gammarid amphipods, in particular the large, and relatively long-lived *Gammarus wilkitzkii* (Birula 1897) which can grow to up to 5 cm as adult and reach a lifespan of 5-6 years (Carey 1985; Gulliksen 1984, Poltermann et al., 2000). The much smaller calliopioid *Apherusa glacialis* (Hansen, 1888) is the most frequent ice amphipod, and is described to be a herbivore with a short, 2-year life cycle. However, due to its small size, its contribution to the total under-ice biomass is rather low. The lysianassoid species *Onisimus glacialis* (G. O. Sars, 1900) and *O. nansenii* (G. O. Sars, 1900) also occur frequently, but are generally much less abundant than *A. glacialis* and *G. wilkitzkii* (Hop and Pavlova 2008). Their lifespans are described as 3-4 years (Arndt & Beuchel, 2006).

For those species, in the literature most often regarded as autochthonous-sympagic, the year-round access to sea ice in their habitat is considered to be of paramount importance.

Therefore, multi-year ice (MYI), or sea ice that persists throughout the melting periods of summer and fall, is a key prerequisite for these organisms. The role of sea ice ridges as refugia for sea ice amphipods has long been postulated, especially for *G. wilkitzkii*, and has been addressed in Gradinger, Bluhm and Iken (2010).

However, there is mounting evidence that at least one of these species, *A. glacialis*, might in fact be living significant parts of their life cycle in a pelagic stage (Kunisch et al. 2020). Here the authors concluded from a comprehensive data survey on pelagic occurrences of *A. glacialis* that this species appears to be capable to inhabit the water column at any time of the year, both in shallow depths and in deep water, and even in areas where sympagic food sources were presumably available. While similar findings of ice-associated amphipods in deeper water layers have been interpreted as “dead ends” of the respective life cycle, and thus lost to further contributions towards the population, the fact that gravid females were consistently found at depth strengthened the possibility that there could be a seasonal vertical migration from the sea ice to deeper waters and back to the sea ice, which has been previously overlooked. Two conceptual models were put forward by Kunisch et al (2020), one in which adult *A. glacialis* of both sexes were distributed both under sea ice and in the water column throughout the year, with females undergoing vertical movement to the ice during winter to release their offspring from the brood pouch, and the other alternative where only female *A. glacialis* were going through a seasonal migration away from the ice during the polar night. While there remains a level of uncertainty about these life history traits, in large part also due to an undersampling of the Polar Night, there appears to be some evidence that *A. glacialis* is likely to be able to adapt to an environment changing towards a future ice-free Arctic ocean.

Berge et al. (2012) have postulated that the southward export of sea ice with the trans-polar drift, moving from the Arctic Ocean through the Fram Strait, might not be a one-way ticket for all of the sea ice fauna, as previously assumed. During a mid-winter cruise in 2012, they found notable amounts of live individuals of the sympagic amphipod *Apherusa glacialis*, at various depths below 200m depth in the water column of the Fram Strait. These depths are corresponding with the northward flowing Atlantic deep-water current and might thus offer a return pathway to the central Arctic Ocean. Interestingly, more than half of the females of *A.*

glacialis were found to be ovigerous, and lipid levels were found to be reasonably high in all individuals of all age classes, supporting the previously documented midwinter reproduction of this species (Poltermann, Hop & Falk-Petersen 2000).

Based upon the oceanography of the Arctic and these mid-winter observations, Berge et al. (2012) therefore proposed a new conceptual model, one that effectively closes the life cycle of *A. glacialis* from their southward export with the sea ice drifting out of central Arctic, to a poleward return journey, by sinking down and then returning with the deep Atlantic current flowing northward within the Eurasian part of the Arctic. So rather than a dead end and net export, such a pelagic phase may instead be an important part of this amphipod's life history. In combination with the timing of reproduction and the aggregation of sufficient lipid reserves, this strategy would both counteract the export into the North Atlantic and enhance the opportunity for females return and to release their young in productive and ice-covered areas of the Arctic Ocean. Compared to the average surface drift speeds around 2 km / day of sea ice flowing south through the Fram Strait, such deep-water return currents have been measured to speeds of up to 9 km / day. In this new conceptual model, a 2- to 3-month period at the right depth would certainly be sufficient to balance out a 9-month period of surface drift, attached to the sea ice. This would also make sense from both a food availability perspective, as well as in terms of predator avoidance, since the sea ice during the Polar night offers limited to no feeding opportunities for this ice algal grazer, while at the same time ensuring very low detectability by visual predators.

Also, for *Gammarus wilkitzkii* there are at least circumstantial evidence in the form of ciliated epibionts that indicate that the species is able to survive extended ice-free periods in the intertidal, and hence that its status as an autochthonous-sympagic species is overestimated (Arndt et al 2005).

There are also several benthic amphipod species that can be encountered under sea ice under shallow water (Gradinger and Bluhm, 2010). But intriguingly, some of these amphipods have also been found over deep waters and have then been presumed to have drifted there with the sea ice over some time. Some of these benthic species, such as *Gammaracanthus loricatus* (Sabine, 1824), *Anonyx nugax* (Phipps, 1774) and *A. sarsi* (Steele & Brunel, 1968) are therefore considered allochthonous-sympagic and thus termed benthosympagic.

In contrast to this, *Pleusymtes karstensi* (J.L. Barnard, 1959), which was otherwise considered a shallow benthic species, might actually belong to the autochthonous group of sympagic amphipods, and might have been underrepresented in previous sampling efforts, as it closely resembles juvenile *G. wilkitzkii*, unless closely examined under a microscope. The occurrence of these species in sympagic samples was studied in MacNaughton et al (2007), and the authors concluded that *Eusirus holmii* (Hansen, 1887), otherwise known as a bathypelagic species, might be another allochthonous pelago-sympagic species (Arndt & Swadling 2006).

The trophic role of sympagic amphipods has been recognised as key links in the energy transfer from the sea ice– associated primary production to higher trophic levels, effectively repackaging the microalgal biomass for vertebrate predators such as polar cod (*Boreogadus saida* Lepechin, 1774), little auk (*Alle alle* Linneus, 1758), black and Brünnich’s Guillemot (*Cepphus grylle* Linneus, 1758, *Uria lomvia* Linneus, 1758), as well as ringed seals (*Pusa hispida* Schreber, 1775) (Weslawski et al. 1994). Their role is also summarized well in Bluhm et al. (in SEA ICE, D Thomas, 3rd edition, 2017).

Importance of the sea-ice cover for the underwater light climate in polar ecosystems

The sea-ice cover of the Arctic seas acts like a highly efficient lid or physical barrier, for incoming solar radiation, and it is thus of great importance in regulating the amount of light penetrating into the surface waters. The complex physical properties of sea ice, ranging from ice thickness, including freeboard and draft, to snow cover, and especially the extent of brine channel formation and brine or particle inclusion, are of tremendous importance not just for its role as biological habitat, but also due to their optical properties. All of the above-mentioned elements are acting as strong filtering and scattering elements, thus modifying the total light transmission from the atmosphere into the ocean (Katlein et al, 2015). This filter function of sea ice has wide-ranging implications on a global scale, directly affecting the energy budget of the polar oceans. While the surface albedo has been the most accessible and thus well-studied feature, recent investigations into the relative contribution of ice type and ice thickness has shown that transmittance through first-year ice (FYI) can be almost three larger than through multi-year ice (MYI), while the energy absorption has been measured to be 50% larger in FYI than in MYI (Nicolaus et al, 2012).

Light climate and its physical definitions

The biological and ecological significance of light in general, (Johnsen, 2012) and for the polar regions (Sakshaug et al., 2009, Pavlov et al., 2019, Berge et al. (eds), 2020) is well-defined and reviewed. For the purpose of this synthesis, we adopt the concept of light climate from Cohen et al. (2020). They define light climate through its intensity, spectrum and duration of light for a given location. An abbreviated summary of their definition follows here.

The intensity of light can be measured as either radiance, or the amount of photons emitted per unit area per second, or irradiance, which describes the amount of photons received per unit area. Measurements of irradiance are either recorded in energy units (W m^{-2}) or quantal units ($\text{photons s}^{-1} \text{m}^{-2} / \mu\text{mol photons s}^{-1} \text{m}^{-2}$). The latter type of measurement is obviously most common in the context of light climate as an ecological factor for sea ice organisms.

The spectral composition of light is of particular interest in the present thesis. Therefore, the following definitions are of relevance here. Solar radiation is commonly divided into an

ultraviolet (UV) component, measured in the range of 100 to 400 nm, the visible component, which corresponds to photosynthetically active radiation (PAR), in the range of 400 to 700 nm, and the infrared part of the spectrum, from 700 to 2000 nm. Solar UV wavelengths below 280 nm are not able to penetrate through the stratosphere, but both the UVB (280 to 320 nm) and especially the UVA part, with a range from 320 to 400 nm, are important for ecological processes, and are able to penetrate into the water column to a certain extent.

The duration of light exposure is the last important parameter of interest for biological organisms. Cohen et al. (2020) defined the duration of light in terms of its photoperiod, or the day length or “photophase” of a 24h diel cycle compared to the dark portion or “scotophase”. An important and open question in this definition is the separation level or threshold between these two parts of the diel cycle. While this can be based on active versus inactive periods, linked to day and night in some biological processes such as photosynthesis, the reverse may be true for processes such as diel vertical migration. For organisms like sea ice amphipods, where light is crucial for grazing, predation or predator avoidance, their species-specific light sensing ability is therefore of considerable interest.

However, in the context of this study, the actual duration of radiation exposure received by these motile organisms is the hardest to quantify, as it would require a highly site-specific and yet sustained measurement of the above-mentioned parameters, intensity and spectral composition. As the amphipod species studied here are relatively motile, they are likely to alter the degree of intensity that reaches them constantly, and due to the changing angle of the sun, the spectral composition will also change significantly throughout the day. It would therefore be interesting if one could develop or identify a biological dosimeter, for example through a in-vivo staining technique, which could address this with adequate resolution. For now, we will have to approximate duration of light exposure through the simplified assumption that amphipods are remaining exposed to ambient light of the same intensity and spectral composition for a set part of the diurnal cycle, the photophase as defined above.

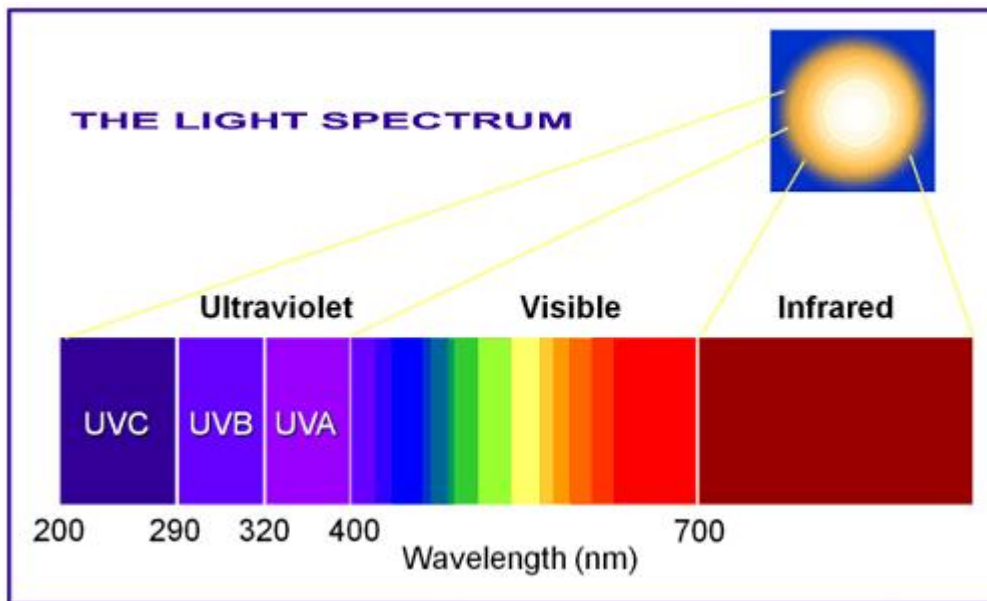


Fig. 2: Schematic overview over the wavelength categories of the light spectrum.

Source: Government of British Columbia, Health & Safety.

Ultraviolet radiation and stratospheric ozone

In ice-covered waters, a very large amount of the incoming solar radiation is being reflected by snow on the sea ice surface or absorbed by the snow and ice before it can reach the underside of the sea ice and the sea water under the ice. Therefore, life forms in ice-covered marine systems are generally considered to be adapted to low light levels, and thus also low UVR levels. Being adapted to a low-light environment, and hence also an environment with low UV radiation, might potentially also mean that the organisms living there are less resistant to increased levels of UV radiation following a reduction of the Arctic sea ice cover and thickness. This is one of the main hypotheses that forms the basis for this thesis (see section 4).

According to the definition by the Commission International d’Eclairage (CIE), the UVB portion of the solar spectrum is defined as 280 to 315 nm. However, in the ecological literature the separation between UVA and UVB is more commonly set to 320 nm. In this thesis I will follow the latter and more conventional definition. Though less energetic than UVB, UVA radiation and transmitted freely through the atmosphere, it is also still considered

to cause some damage, for example sunburn and skin aging in humans. The UVB portion is more energetic than the UVA portion, and can therefore be much more harmful to biomolecules, including cell membranes and DNA molecules, but is quite strongly attenuated through the atmosphere, and is typically absorbed by stratospheric ozone concentrations in what is commonly known as the “ozone layer”. This layer is found in a region of the lower part of the stratosphere, from approximately 20 km to 30 km altitude, where solar UVB radiation creates elevated levels of oxygen molecules in triplet form (O_3). This layer of elevated ozone concentrations is variable in its seasonal and spatial distribution around the globe, owing to stratospheric wind patterns known as the Brewer-Dobson circulation (Butchart, 2014). In short, this circulation model predicts that while most of the stratospheric ozone is produced over the tropics, a stratospheric circulation pattern transports it upward and poleward and eventually downward, thus redistributing the ozone towards mid-to-high latitudes. Recent research indicates that this circulation will increase in response to projected changes in greenhouse-gas concentrations (Garcia & Randel, 2008), and changes are predicted at a rate of up to 3% per decade during the first half of the twenty-first century (Butchart & Scaife, 2001).

However, certain circulation patterns in the upper polar atmosphere (known as Polar Vortex) occur during the respective winter and spring seasons over Antarctica, and to a lesser extent over the central Arctic, and can provide a certain degree of isolation for the air masses in these regions, leading to what is known as seasonal low-ozone periods over the Antarctic, and also over the Arctic. While the formation of such ozone “holes” is expected to end by the middle of this century, due to the slow but steady breakdown of the chlorofluorocarbons (CFC's) and other man-made ozone-depleting chemicals, there will still be significant seasonal depletions of the stratospheric ozone layer over the Antarctic for some years to come. In 2020, also the stratospheric ozone levels over the central Arctic reached a record low during the month of March, with the lowest point with 205 Dobson units on March 12. In comparison, the lowest March ozone value observed in the Arctic is usually around 240 Dobson units (sources: nasa.gov and ECMWF COPERNICUS climate change service). Recent research carried out during the MOSAiC expedition by von der Gathen et al (2021) found that climate change favors the formation of polar stratospheric clouds, which in turn facilitate stratospheric ozone loss. Their model calculations suggest that this could cause conditions favorable for significant seasonal loss of Arctic ozone column O_3 to persist until the end of this century, with a potential to even worsen as well.

Apart from the ozone layer, there are a number of other factors determining the level of UVB and UVA radiation reaching the Earth's surface, including solar elevation, season, aerosol and pollutant gases, albedo, and cloud cover. Further penetration of these wavelengths into the water column is strongly attenuated by dissolved organic matter (DOM, especially chromophoric dissolved carbon (CDOM), as well as other suspended particles and phytoplankton (Hargreaves, 2007, Prasil et al, 2003).

Purpose of this study

In this thesis, I wanted to investigate the physiological effects of light and UVR on sympagic amphipods. The main approaches to achieve this goal were to study selected species' capacity to counteract negative light-induced effects, such as scavenging of reactive oxygen species (ROS), as well as any photo-protective strategies such as absorption of harmful radiation through the dietary uptake of protective pigments, or through the development of chromatophores. The main reason for choosing sympagic amphipod species was their central position in the sea ice ecosystem and their considerable exposure to both direct irradiation and irradiated water masses. In addition, their relative accessibility, body size and relative abundance was making them well suitable for laboratory experimentation, and previous knowledge on their species-specific dietary differences and strategies in habitat use allowed for a good experimental design.

As one must assume that the impact of UVR must be even greater in the area of the Southern Ocean directly affected by the seasonal ozone depletion known as the "ozone hole", this study aimed to expand this approach in a similar way to the Antarctic sympagic community as well. As a first step, I was motivated to search for and identify any sea ice amphipods under Antarctic sea-ice as well, as there had previously been only very few investigations reporting on this group of organisms in this context.

I was able to contribute towards this goal during a designated sea ice cruise on R/V Polarstern into the central Weddell Sea (ISPOL), and I was later able to collaborate with other researchers who had performed similar studies in the Lazarev Sea. Our efforts proved that several species of amphipods could be found in close association with Antarctic sea ice over deep water, providing new evidence for pelago-sympagic coupling in the Antarctic ecosystem.

Although technical limitations of our sampling efforts prevented us from performing the same experimental and physiological studies on live animals to a statistically significant degree, I remain convinced that the close and immediate association of Antarctic sympagic amphipods to the sea ice that we have documented, will be an important and interesting field for further investigations, including the relevant adaptations to the light climate under the Antarctic sea ice.

Scientific approach and methodology

A first step of this study focused on understanding the role of UVR and its effects in a biological context. This topic was approached by collecting field measurements of PAR and UVR *in situ*, documenting large spatial heterogeneity due to complex sea ice structure. As sea ice is not uniformly thick, but highly variable in age, thickness, and structure, while light penetration is also highly dependent on snow cover on top of the ice as well, the resulting under-ice light levels were found to be highly variable as well.

As a next step, I investigated suitable experimental and laboratory methods, and performed experimental lab exposures of sea ice amphipods to natural low-level, high-level and elevated level intensities of UVR, in close collaboration with researchers at IRIS / UiS. We developed experimental *in vivo* exposure setups with one amphipod species (*Gammarus wilkitzkii*) which was the most accessible species to collect, keep in captivity, and process in the lab. To study direct versus indirect effects, we had unirradiated controls, directly irradiated exposures, and a third setting where a similar set of exposure tanks was irradiated, and the water flow then led to separate tanks kept in complete darkness, containing organisms. We then investigated and quantified the effects of those exposure experiments through several types of assays, named TOSC and MDA.

The TOSC assay stands for total oxyradical scavenging capacity assay, was developed by Winston et al (1998) and the protocol was described in Regoli and Winston (1999).

The MDA assay stands for malondialdehyde assay and is one of the most common biomarkers for lipid peroxidation. It is based on the reaction of malondialdehyde (MDA) with thio-barbituric acid (TBA), generating a product that can be measured colorimetrically (Fernandez et al., 1997). Based on the experiences with such exposures, our next study included experimental lab exposures of sea ice amphipods known to have chromatophores to various light and UVR regimes. The effects of these exposures were quantified by visually assessing changes in chromatophore size and extent, and the light response in chromatophores was documented.

Inspired by studies on a group of photoprotective pigments called mycosporine-like amino acids in the Southern Ocean, our study also collected and analyzed samples of various amphipod species for specific pigment content, in early spring, summer and autumn. The

resulting samples were analyzed by high-performance liquid chromatography (HPLC) and compared with standards derived from algal monocultures.

This study documented a strong seasonal trend and linked uptake and concentration of MAAs in various amphipod species dependent on their specific diets. This was the first study of these compounds in Arctic sea ice amphipods.

The other part of this study, focusing on investigating Antarctic sympagic amphipods, employed several established methods of sampling under Antarctic ice, as well as applying new sampling tools, notably a novel under-ice trawl known as SUIIT (surface-and-under-ice-trawl), as well as scientific diving and the deployment of small inspection-class ROV's under ice (ROV=remotely-operated underwater vehicle). Once samples were obtained, they were kept alive for feeding experiments and live observations, and finally processed for taxonomical analysis.

Presentation of papers

Paper I: Antioxidant responses in the polar marine sea-ice amphipod *Gammarus wilkitzkii* to natural and experimentally increased UV levels

This paper showed that *G. wilkitzkii*, the most dominant of the Arctic sympagic amphipod species, has considerable tolerance to natural UV radiation. This can be expected from a species that is relatively mobile and spends considerable time both on shallow floe edges and under deep ice ridges, thereby encompassing strong gradients in irradiation. Our research showed further that UV radiation may act both directly on the body tissue of exposed organisms, but also indirectly, through the formation of oxyradicals through the decay of dissolved organic matter (DOM) present in these typically well-stratified surface waters. The results of this study have proven that *G. wilkitzkii* has a considerably higher capacity to tolerate and neutralise oxidative stress if sampled in summer as compared to winter conditions. It has also shown that during experimental exposure to elevated UV radiation levels, the total oxyradical scavenging capacity can be severely depleted.

This study was a baseline study on the susceptibility of the Arctic sea ice amphipod *Gammarus wilkitzkii* to UV radiation and UV-induced oxyradical stress.

Paper II: The adaptive significance of chromatophores in the Arctic under-ice amphipod *Apherusa glacialis*

This paper showed that the chromatophores that are present in these amphipods are susceptible to light levels, and therefore they have in all likelihood an adaptive and photoprotective function for this species. This study showed a physiological colour change in response to short-term light exposure, through the pigment dispersal from red-brown chromatophores in the tissue covering the body, as well as in the internal organs. Exposure in the PAR range (400-700nm) with high light intensities was the main trigger for this type of response, with a reversal of the pigment dispersal during a following period of darkness. Experiments showed no statistically significant change in coloration in response to different background colours, or to UV radiation. While one could observe some effects in response to UV radiation, the sample size was insufficient to make this statistically valid. This study showed for the first time that chromatophores present in the Arctic sea ice amphipod

Apherusa glacialis can provide a functional response to high light levels, and likely provide both photoprotection and crypsis.

Paper III (in prep): Total MAA content in summer and winter in the Arctic under-ice amphipod Gammarus wilkitzkii, and comparison in between this and other species

Our results show that the UV-protective substances belonging to the class of mycosporine-like amino acids (MAAs) are present and appear to play a role also in Arctic amphipods.

Our preliminary findings indicate that sea ice algae grazers likely benefit from the ingestion and retention of such MAA's. There is also a marked seasonal trend in the MAA content in such sea ice algal grazers, which fits well with the onset of the spring phytoplankton bloom. When comparing typical algal grazers with omnivore/grazers and scavengers, the algal grazers contained the highest relative concentration of MAAs.

Unfortunately, technical difficulties in chemical resolution of our sample contents prevented us from identifying the contributing MAA types, and lack of supporting data on the MAA producing sea ice algae prevented us from identifying the nutritional sources and types.

This material in prep provides a baseline on the total MAA content in Arctic sea ice amphipods.

Paper IV: Sympagic occurrence of Eusirid and Lysianassoid amphipods under Antarctic pack ice

During three Antarctic expeditions (2004, ANT XXI-4 and XXII-2; 2006, ANT XXIII-6) with the German research icebreaker R/V Polarstern, six different amphipod species were recorded under the pack ice of the Weddell Sea and the Lazarev Sea. These cruises covered Austral autumn (April), summer (December) and winter (August) situations, respectively. Five of the amphipod species recorded here belong to the family Eusiridae (*Eusirus antarcticus* Thomson, 1880, *E. laticarpus* Chevreux, 1906, *E. microps* Walker, 1906, *E. perdentatus* Chevreux, 1912, and *E. tridentatus* Bellan-Santini & Ledoyer, 1974), while the last belongs to the Lysianassoidea, genus *Cheirimedon* (cf. *femoratus* Pfeffer, 1888). The results from this study suggest that the underside of Antarctic pack ice serves at least temporarily as a habitat for Eusirid amphipods. Although this could not be determined with

certainty, we believe that their origin for the reported oceanic occurrences is most probably the pelagic habitat, from which they can colonize the sea ice during favourable conditions. It is thus puzzling that none of these amphipods were found in any of the extensive concurrent zooplankton sampling efforts, which did record a number of isopods, as well as scinid and hyperiid amphipods of similar size classes. One explanation might be that the transition to a sympagic life style had been initiated prior to our sampling period.

For the Lysianassoid *Cheirimedon* cf. *femoratus* which also was found by this study, such a pelagic origin seems less likely, but since the species determination is still uncertain for the sampled material, it cannot be completely ruled out.

Discussion

UV radiation tolerance and protective adaptations in sympagic amphipods

Direct effects of UV radiation are induced by the absorption of energy in especially vulnerable molecules like nucleic acids, which in turn disrupt DNA replication and translation processes within the cells. Photo-induced DNA-damage comprises cyclobutane pyrimidine dimers (CPDs), exclusively in the UVB range, and also other lesions formed at lower rates such as pyrimidine 6-4 pyrimidone photoproducts (6-4 PP) (Buma et al. 2006). Generally, wavelengths below 302 nm cause more damage than higher wavelengths.

Melanomas (skin damage) and cataracts (eye damage) are not only present in humans but also shown for fish (Nairn et al. 1996) and amphibians (Little & Fabacher 2003). Ultimately, accumulated DNA damage will result in increased mortality which has been shown in both zooplankton and fish eggs (Kouwenberg et al. 1999 a+b, Lesser et al. 2006). Targets are key proteins e.g. antioxidant catalase (Butow et al. 1994, Cheng et al. 1981, Zigman et al. 1996), lens proteins (Weinreb & Dovrat 1996), and rubisco, the key enzyme of photosynthesis (Hidema et al. 1996). Under favourable natural conditions UVR damage and repair are balanced, however ozone depletion (UVB increase) or insufficient energy supplies can bias this equilibrium.

As the presence of natural UV radiation has been an integral component of the evolution of terrestrial and aquatic organisms and ecosystems, researchers have found a wide range of tolerances and adaptive mechanisms, including exposure avoidance, photo-protective screening compounds, quenching of free radicals, and damage repair mechanisms (Sommaruga 2001, Jain et al, 2004).

Exposure avoidance obviously requires a certain motility, and presents those organisms capable of undertaking vertical migrations with the trade-off between radiation exposure avoidance on the one hand, as well as most likely also visual predator exposure avoidance, and access to feeding opportunities on the other hand, which often are restricted to the high-light zones. Other avoidance mechanisms might be less energetically demanding, such as moving towards more shaded areas of the same benthic or sympagic environment, by moving either under the canopy of macroalgae, or under thicker portions of the sea ice cover. In the context of sympagic amphipods, the former mechanism, i.e. diel vertical migrations, has been

ruled out, but the latter might be accessible to some species to some extent (Hop et al; 2000, Gradinger & Bluhm, 2004).

However, it is to my knowledge unresolved and questionable whether the preference for deeper and darker areas on ice floe ridges for p.e. *G. wilkitzkii*, and the contrasting preference for *A. glacialis* for much more light-exposed floe edges, is mostly determined by food availability than by radiation avoidance strategies. Fuhrmann et al. (2011) discussed the trade-off between transparency and crypsis versus photoprotection through dispersed pigments in chromatophores on *A. glacialis*. While the contraction of pigments will make the animal's body more transparent and thus less conspicuous to visual predators like polar cod, the downside is presumably less photoprotection from these pigments, while dispersed pigments make the animal's body more visible in a high-light environment against a mostly white background. Also, the movement of such pigments is of course energy demanding. While this study initially aimed at collecting data furthering our understanding of the aspect, technical constraints in attaining sufficient sample sizes from high-light sample sites versus low-light sample sites have so far prevented us from this.

Effects of UVR on Arctic sea ice-associated amphipods (paper I)

The detrimental effects of ultraviolet radiation have been well-documented in Antarctic zooplankton and fish larvae, (Malloy et al, 1997), on Antarctic echinoderms under sea ice (Lesser et al, 2004) as well as on Arctic zooplankton and fish eggs (Kouwenberg et al, 1999). All of these studies have demonstrated that both the Antarctic and the Arctic marine ecosystems are strongly influenced by ultraviolet radiation, even in the presence of sea ice cover. A recent review on the effect of ultraviolet radiation on the life stages of fish (Alves and Agusti, 2020) has summarized these effects to range from increased mortality, developmental abnormalities, behavioral and metabolic changes, to tissue lesions, physiological changes and immune system modulation, impairment of molecular and cellular processes in the early developmental stages as well as in juveniles and adults.

Our research on the total oxyradical scavenging capacity showed that *G. wilkitzkii* certainly has a considerable tolerance for exposure to oxidative stress, most likely caused indirectly through the creation of reactive oxygen species (ROS) by way of photolysis of DOM in the

exposed surface waters between ice floes and under thin ice with little or no snow cover. Our experimental exposures also confirmed the hypothesis that exposure to UV-irradiated water was at least as important as direct exposure of the organisms to the UV radiation. This can be explained by the formation of ROS in the water which then act upon the organisms immersed in it. So even though organisms like *G. wilkitzkii* show photonegative behaviour, ie they avoid exposure to direct sunlight, they are likely exposed to oxyradicals nonetheless, as long as there is sufficient area in between floes, where the sunlight reaches the surface waters.

While we were not able to investigate the other Arctic sympagic amphipod species, we can assume that they would be exposed to similar conditions and thus would have to deal with the same level of oxidative stress. A compounding issue for especially *A. glacialis* seems to be that its recorded lifestyle suggests that it is more prominently exposed to direct radiation as well, as it is most often found along well-irradiated floe edges or under thinner parts of ice floes where light conditions are most favorable for ice algae on which it grazes. The observations of the other Arctic sympagic species suggests that they can employ avoidance strategies to a much larger extent by preferring thicker and less irradiated floes, ridges or cracks between rafted floes.

The timing of the seasonal maximum of ultraviolet radiation reaching the Arctic is also crucial here, as the Northern Spring combines the environmental factors of higher sun angles, increased surface reflectivity through greater snow and cloud cover, and enhanced stratospheric ozone depletion with the biological factors of little or no algal-derived protective pigmentation and low food availability in general.

In such a scenario, it seems reasonable to conclude that a further development towards a sea ice situation which is both decreasing in area coverage and thinning in average ice thickness is going to pose an increased challenge to sea ice amphipods in terms of habitat loss, and lower quality of habitat. At the same time, there is still a considerable amount of long-lived CFC's in the stratosphere, and research by Andrady et al (2017, in: United Nations Environment Programme, Progress Report, 2016) indicates that there are strong interactions between seasonal ozone depletion and man-made climate change processes on a global scale. One well-documented consequence of man-made climate change processes is the warming of the troposphere, which leads to concurrent cooling of the lower stratosphere. Since a key component to the effectiveness of ozone-depleting substances (ODS) like CFC's and others is

the temperature in the lower stratosphere, one must therefore conclude that man-made global warming can also influence the seasonal ozone depletion, even if the long-term trend in the reduction of ODS remaining in the stratosphere is negative. This is especially true for the situation in the Antarctic (Hartmann et al, 2000).

In conclusion, this study provides some evidence that the ultraviolet radiation is a significant stressor for Arctic sympagic amphipods, and one that is likely to increase in the future. While we have not been able to replicate similar experimental exposures of Antarctic amphipods while measuring their responses, there is a host of other such studies on other organisms exposed to elevated UVR.

And since the seasonal ozone depletion is much more pronounced in the Antarctic than in the Arctic, it stands to reason that these effects will also be very important for Antarctic amphipods.

Photoprotective substances

Photo-protective screening compounds, which typically are being acquired through dietary uptake and then retained, have been found in different amphipod species in various extent and forms, and can be found as carapace pigmentation, chromophores, and pigmentation of soft tissue within the carapace structure. See also paper III (Fuhrmann et al, 2011) on this topic. One prominent and well-studied group of pigments which have relevant UV-protective properties are mycosporine-like amino acids (MAAs) (Carreto et al, 1990, Karentz et al, 1991).

Mycosporine-like amino acids (MAAs) can be found in marine organisms from the poles to the tropics, ranging from bacteria to vertebrates (Karentz et al. 1991, Karentz 2001, Dunlap & Shick 1998). MAAs are derivatives of mycosporines, compounds identified in the mycelia of fungi. More than 30 different types of MAAs have been identified (Singh et al, 2008), and they are commonly perceived as “microbial sunscreen”, although their intracellular functions may also include antioxidant properties, and have been found to help with cellular resistance to desiccation (Wright et al, 2005), osmotic stress (Oren & Gunde-Cimerman, 2007) and heat stress (Michalek-Wagner & Willis, 2001).

In crustaceans, at least 10 different MAAs and the chemical precursor gadusol have been identified so far, with shinorine, porphyra 334, mycosporine- glycine, palythenic acid and palythine being the most dominant substances. UV-protection by MAAs in animals is clearly shown, though stimulation of uptake and accumulation still varies from species to species and results are sometimes contradictory (Banaszak et al, 2006).

Other common pigments found in crustaceans are melanins and carotenoids. While the former class of substances typically absorbs in all UVR and PAR wavelengths, which makes it beneficial to non-photosynthetic, heterotrophic organisms, e.g. fresh water Cladocera (Zellmer 1995), the latter class seems to absorb mostly in the visible range, with absorption maxima around 480 nm. While the cover certainly extends beyond its peak absorbance, carotenoids seem to primarily act as a photoprotective pigment class for photosynthetic autotrophic organisms, in the protection against excessive PAR radiation. But due to their absorption well into the UVA, it is also a popular component in sunburn-protecting sun

lotions for human consumption. Both pigment classes have been shown to have antioxidant properties (Vershinin, 1999, Sarangarajan & Apte, 2005, Yao & Qi, 2016).

Photoprotection through pigment acquisition in sea ice amphipods (papers II & III)

My investigations into photoprotective pigment content in four Arctic sympagic amphipod species (Krapp, unpublished) has confirmed that there are some substances present with the absorption characteristics of mycosporine-like amino acids. While technical issues prevented us from isolating and identifying these substances, our study has shown both a strong seasonal trend of pigment content, as well as highest prevalence of pigments in the herbivorous species *A. glacialis*, with lower amounts in the omnivorous *G. wilkitzkii*, and the lowest amounts in carnivorous-detritivorous species *O. nansenii* and *O. glacialis*.

These UV-protective substances are known to have an important photoprotective role as they efficiently absorb potentially harmful UV radiation, as well as act in a strong antioxidant role (Rastogi et al, 2017). They have previously been described mainly from a variety of Antarctic invertebrate species, notably including krill, but also echinoderms, crustaceans, and even fish (Karentz, 1994). In the Arctic, there are to date only a few studies on MAAs in sea ice environments, notably the Baltic Sea (Uusikivi et al., 2010; Piiparinen et al., 2015), the Canadian Arctic (Elliott et al., 2015) and the southern Nansen Basin north of Svalbard (Kauko et al, 2017). Ha et al (2012) documented several MAAs in phytoplankton samples collected in and around Kongsfjorden, Svalbard, and Ha et al (2018) documented MAA synthesis and size-dependent contents from the Beaufort Sea as well.

MAA-like signatures have also been documented in particle absorption samples from sea ice (Uusikivi et al., 2010; Fritsen et al., 2011; Mundy et al., 2011; Piiparinen et al., 2015; Taskjelle et al., 2016).

Their role has been well-studied in Arctic macro-algae and in certain benthic amphipod species grazing on these algae, which due to such a relatively shallow benthic lifestyle also are exposed to potentially harmful UV radiation (Obermüller et al, 2005). These and earlier studies found that the grazers were gaining a clear benefit from ingesting and retaining these pigments for the photoprotection against harmful levels of UV radiation.

It is reasonable to assume that such photoprotective pigments are important not only for the sea ice algal community, but also for the sea ice amphipod community, as members of the latter live in close connection with the former. And while amphipods are mobile and thereby able to reduce exposure to some extent by moving to less exposed sites, their ice-associated lifestyle prevents them from escaping potential exposure altogether.

During spring melt and the formation of melt ponds, the amount of incident PAR, (400–700 nm) transmitted through sea ice has been reported to exponentially increase over just a few weeks from <1 to 5–22% and from <1 to 21–67% under white ice (i.e. drained surface ice above the local water table) and melt ponds, respectively (Ehn et al. 2011, Mundy et al. 2014). As Elliott (2015) pointed out, this transition coincides with the timing of peak downwelling irradiance resulting in exposure of sea ice and associated communities to high levels of UV radiation and PAR.

Although there are certainly several substances in sea ice known to absorb UVR to some extent, notably colored dissolved organic matter, or CDOM (Perovich et al., 1998; Belzile et al., 2000; Uusikivi et al., 2010, Kauko et al, 2017), which of course also would include MAAs released from destroyed algal cells after an osmotic shock or similar, one can still conclude that the incident UVR transmitted through sea ice will also follow the trends documented above, resulting in a dramatic increase of intensity.

Based on these studies and our own results, we can assume that dietary acquisition is the source of these photoprotective pigmentation also in the sea ice amphipods studied here.

The presence of chromatophores has so far only been documented in *A. glacialis* and not in other sea ice species. Unless there are in fact chromatophores present in other species with absorption characteristics that are not apparent in the visible spectrum, we must assume that these are only present in this one species as documented. And while it appears to have a dual role, its importance in helping with crypsis is likely more relevant than its importance as photoprotection. Therefore, we can conclude for now that dietary pigment acquisition is likely the main source of photoprotective pigmentation.

It is a clear indication of the importance of photoprotection for sea ice amphipods that the species most regularly recorded from highly irradiated floe edges and melt ponds have been shown to have both the strongest signature in terms of UV-absorbing compounds, as well as possessing chromatophores. And while our study (Fuhrmann et al., 2011) could not confirm

the response of these chromatophores to UVR exposure by means of statistical tests, due to the insufficient sampling size, it is nonetheless reasonable to assume that the observed reaction in chromatophore appearance serves mainly for photoprotection against UVR, as it is well-known that this part of the radiation has been proven harmful to organisms.

Previous research by Hop et al, (2000) has shown that *Apherusa glacialis* appears frequently on the more irradiated portions of the sea ice floes, as in floe edges and under relatively thin ice, as well as in under-ice domes. The other species (*G. wilkitzkii*, *O. nanseni*, *O. glacialis*) are more often found under thicker ice and appear thus to utilize the sea ice differently, mainly because they are not as directly dependent on sea ice algae as their main food source. So, it appears plausible that a more omnivore / detritivore / carnivore foraging strategy allows these species to avoid direct light stress to a much larger extent than in the case of *A. glacialis*.

Intriguingly, however, at least *G. wilkitzkii* has been shown in our studies to have a considerable tolerance available to deal with oxyradical stress, which is presumed to be a proxy for light stress. Clearly more studies are necessary to quantify this to a better degree, but there are two possible explanations for this, based on the assumption that avoidance is considered to be the main strategy to deal with light stress. One possibility is that ambient oxyradical levels in the water layer just under the sea ice is requiring this high level of oxyradical tolerance. So, in other words, even when the organisms can minimize their direct exposure to harmful radiation, they are still exposed to considerable levels of oxyradicals in their environment, through advection and dispersion of the sea water that is well irradiated in some areas.

The other alternative is that these animals which are preying on more exposed species like *A. glacialis* and *Calanus* spp are actually ingesting prey items with high concentrations of oxyradicals in their body tissue.

Effects of UVR on Antarctic ice-associated ecosystems

It has long been accepted that the detrimental effects of CFC's on the ozone layer, especially over Antarctica, have been slowly but steadily reduced in the decades since the adoption of the Montreal Protocol on Substances that deplete the Ozone Layer in 1987. Previously, a significant downward trend in the ultraviolet radiation index (UVI) of 5.5% per decade has been reported, thanks mainly to the reduction in CFC emissions since the adoption of the Montreal Protocol. The ultraviolet index is a dimensionless index calculated from high-resolution hyperspectral measurements which then are weighed with the McKinlay-Diffey action spectrum of erythema and scaled to 40 W/m².

However, a recent paper by Bernard and Stierle (2020) has addressed concerns that long-term drifts in calibrations implemented at three key sites, namely South Pole, Arrival Heights, and Palmer Station, have led to misrepresentations of reported UVI data. After readjusting these calibrations, they found that those reported decadal trends in UVI had in fact to be reduced by 1.5 to 2.3 %, which is a significant reduction. So, in fact, the decrease in UVI is still significant, but is progressing at a smaller rate than previously assumed. Furthermore, they also stated that this decrease is valid for the Antarctic summer months only. The data for the Antarctic spring months (October and November) do not yield any significant reductions of UVI yet, due to the large variability caused by the seasonal ozone depletion known as the ozone hole.

So, in essence, there is still cause for concern for the Antarctic marine ecosystem as there is still considerable UVR exposure during ozone hole conditions, and the reduction of UVI per decade has been found to be slower than had been assumed previously.

Another important aspect of the effects of UVR on sea ice was investigated by the biogeochemistry group of Thomas et al who were also present during the ISPOL expedition to the western Weddell Sea. They investigated the characteristics of dissolved organic matter (DOM) and chromophoric dissolved organic matter (CDOM) in Antarctic sea ice.

Dissolved organic carbon is the largest reservoir of organic carbon in the aquatic environment and a key component in marine biogeochemistry (Thomas et al, 2010). Typically, the marine DOM pool is fed from both terrestrial, or allochthonous and marine, or autochthonous material derived from the biosynthesis (Nelson and Siegel, 2002). But a unique feature of the

ice-covered region of Southern Ocean is the absence of major terrestrial inputs in the form of rivers, which are a dominant feature of the Arctic Ocean and sub-polar regions which are also dominated by seasonal sea ice cover. Therefore, the DOM found in sea ice formed in the Southern Ocean is predominantly marine or autochthonous, and as their study showed, likely originates from primary production within the sea ice.

A part of their field investigations during the ISPOL expedition was a CDOM photo-bleaching experiment, where my main contribution in the field was to provide the visible and ultraviolet light measurements during the in-situ exposure experiment of sea ice brine over a 120-hour period. Their study, to which I was invited to contribute as co-author, indicated that there is a likely source of CDOM from mycosporine-like amino acids (MAAs) generated in sea ice, and that Antarctic sea ice melt contributes as a significant source of autochthonous CDOM and labile DOC to the Antarctic Ocean.

In their estimations, they also compared the potential contribution to the local carbon budget based on the dissolved organic carbon (DOC) content measured in their combined studies. They arrived at an annual DOC input estimate of 8 Tg C from sea ice to Antarctic surface waters (Norman et al, 2011). In comparison, Arctic river catchments are thought to represent a similar size of the seasonal Antarctic sea ice melt zone, and they have been estimated by Raymond et al (2007) to provide an input of 16 Tg C. If one considers the fact that those Arctic rivers receive material from a diverse and substantial tundra vegetation, the sea ice derived DOC figures for the Antarctic seasonal sea ice zone are quite impressive in that comparison.

This In summary, sea ice-derived CDOM is not only major contributing factor in the marine carbon cycle of Southern Ocean but is also significantly influencing the optical properties of surface waters, and through its presumed source materials including mycosporine-like amino acids, it is also directly contributing to UV protection as well as attenuation of PAR (Nunez-Pons et al, 2018).

The ecological role of Antarctic sympagic amphipods (paper IV)

The results of our own study on Eusirid and Lysianassoid amphipods under Antarctic pack ice have indicated that the pack ice undersurface serves at least temporarily as habitat for

these organisms. Previous to this study, the species in question have been considered to belong to the pelagic community, and most reports of sympagic amphipods have concentrated on other species occurring in the coastal fast-ice zone (Gulliksen and Lønne, 1991, Arndt and Swadling, 2006). Our primary study area, the central Weddell Sea, can be considered to be one of the most productive sectors of the Southern Ocean (Arrigo et al. 1997, 2008), as well as the sector with the highest year-round retention of sea ice cover and thus largest percentage of multi-year ice (Steer et al., 2008).

One of the tremendous advantages of the multi-disciplinary approach of the ISPOL expedition, which provided the main sampling access to this study, is that the sampling stations on the one hand were positioned over an area with considerable water depths (from 1300 – 1900 m, Krapp et al., 2008), while the expedition on the other hand also performed a consistent and regular sampling regime directed at the zooplankton and environmental parameters (temperature, salinity, chl a) in the water column from 1000m up to the surface (Schnack-Schiel, 2008). The total absence from these amphipod species in any of these pelagic zooplankton samples supports thus our assumption that these amphipods had been closely associated with the sea ice under-surface for some time at the time of sampling and did not migrate or alternate between these two zones.

Further investigations by Flores et al (2011) and by David et al (2017) have since supported the hypothesis that there are several Antarctic amphipods spending at least part of their life cycle under offshore Antarctic sea ice.

Flores et al (2011) proposed a conceptual model of a pelago-sympagic mode of life for the Antarctic amphipod *Eusirus laticarpus*, with an ascent phase from the pelagic during the winter, a sympagic phase during the late winter and spring, and a descent phase during the melting season, which coincides with the release of the juveniles. However, since available material on the abundance and trophic role of these organisms is still scarce, it is currently not possible to resolve the ecological role with a good level of resolution and certainty.

A more recent study by David et al (2017) contributed yet more documentation on the sympagic lifestyle of certain amphipods. Although both krill and copepods dominate in terms of abundance, with the latter also dominating the under-ice community in terms of abundance (Schnack-Schiel et al, 2001, Kiko et al 2008), amphipods nevertheless contribute

significantly in terms of total biomass. The species *Eusirus laticarpus* is also here mentioned as ice-associated and listed as the most abundant amphipod in this sample set.

One challenging aspect should be mentioned here with regards to taxonomic resolution of the *Eusirus* species found by these, and previous studies. Several species reported in previous publications have been re-analyzed and either synonymized or described as separate species. This will be of particular relevance for any attempts to data-mine such taxonomic data from previous publications but might also be challenging for new fieldwork and sample collection. The species *E. tridentatus* (Bellan-Santini and Ledoyer, 1974), and *E. microps* (Walker, 1906) have been described as separate species by Barnard and Karaman (1991), but synonymized by de Broyer and Jazdzewski (1993). Also, the species *E. antarcticus* and *E. laticarpus* have been considered separate species by De Broyer (1983), but synonymized by Barnard and Karaman (1991). There is, however, a more recent taxonomic paper available from Andres et al (2002) which clearly distinguishes and maintains all above-mentioned species and names, and we used this one for our purposes.

In summary, this thesis and further investigations have indicated mounting evidence for the presence of seasonally ice-associated amphipods also in the Antarctic sea ice. As their foraging strategies suggest that they may occupy similar trophic strategies based on sea ice-derived biomass (like ice algae and sympagic copepods) as they do in the Arctic sea ice environment, while also contributing with a considerable amount of the total biomass found under the sea ice, Antarctic ice-associated amphipods might well be a hitherto unnoticed trophic link from the sea ice to both the pelagic, but also to “topside” air-breathing predators, like sea birds and seals.

Current technical challenges in under-ice sampling and possible future solutions

One central technical challenge in sea ice research in general, and thus also for sea ice biology in particular, is how to approach the dilemma of high spatial resolution for quantitative efforts versus the need to cover larger areas, for a better understanding of patchiness, regional and large-scale variability. The other challenge is the temporal aspect: the in-situ availability of sufficient individuals or biomass that can be sampled during a sea ice station of a typical scientific cruise into sea ice is necessarily limited, while the temporal availability of those organisms throughout longer time intervals, ideally throughout the progress of one or more seasons is so far generally lacking and can often only be addressed by data mining from the literature.

The solution to both challenges has so far been to increase the effort in terms of manpower and ship time to extend the access on-site to extended periods. The recently completed MOSAiC expedition (mosaic-expedition.org) is an impressive and unique example of this approach.

Scientific diving under sea ice has immensely increased our access to this very demanding habitat type, compared with traps, pumps, net hauls or video systems deployed from “topside”. However, the operational range limits and safety-related limitations of diver-operated sampling tools are confining us to relatively small areas of sampling footprint, and to short intervals of time. Some technological advances such as the SUIT trawl (Flores et al, 2011) have ameliorated this to some extent, but while such a trawl is covering a much larger area than previous methods, it can only address point (a) to some extent, and works only for species that are large enough to get retained in the net, but not motile enough to escape the trawl opening.

The use and ability of remotely operated vehicles has developed rapidly in recent years, and this is likely going to supplement and extend the direct access to the sea ice habitat much more than scientific diving could, both in times of area covered, and effective sampling time per deployment. Also the development of long-term moorings and autonomous samplers is also a very promising avenue towards broadening our temporal access, possibly even allowing unprecedented year-round access to certain parameters in the near future.

Ideally, one could wish for the development of an autonomous sampling system comprised of a stable in-ice or under-ice mooring system with a suite of sensors, including at a minimum

sediment and baited organism traps capable of storing their sampled contents for long deployment intervals, in order to address the challenge of long-term access.

As for the challenge of access to larger areas, I believe that the greatest potential will be harvested from the technological development in autonomous underwater vehicles (AUVs) and their navigational capabilities, which will enable such sensor platforms to sweep closer to the sea under-ice surface and detect physical and biological parameters with greater precision and over larger areas than have been accessible by ROV's or scientific divers so far.

Conclusions

In this study, I have covered a wide range of aspects related to the effects of the ultraviolet part of sunlight on the sea ice amphipods in the Arctic. Both the direct light-induced stress in the form of oxyradical formation, which can occur both in the organisms themselves as well as in the surrounding surface waters, and several types of photoprotective pigmentation could be documented in detail here. The results of both the *in situ* material collected, and the experimental exposures to UVR, showed a considerable capacity to mitigate the UV-induced stress induced in the form of oxyradical formation. This proves that these organisms are adapted to a highly variable light climate under the Arctic sea-ice.

From our data, it also seems evident that the amphipods in question have a considerable capacity to protect themselves from such harmful radiation by shielding themselves from it with the help of photoprotective pigments belonging to the mycosporine-like amino acids. These pigments are also highly useful in an antioxidant role.

The evidence of such photoprotective pigments had not been verified in Arctic sympagic amphipods to date, while substantial research has been done in Arctic benthic amphipods already. This invites further research into the exact composition, as well as the sources of these pigments in the sympagic context.

Also the possible function of chromatophores studied in *Apherusa glacialis* in a photoprotective role, as well as in crypsis, contributed an interesting aspect of the range of adaptations that sympagic amphipods require to cope with such a dynamic environment and light climate.

An additional research focus of this study was the presence of Antarctic sea ice amphipods under offshore sea ice, and the results presented in this study confirmed that there are indeed several amphipod species present under the sea ice of the Weddell and Lazarev Seas. These species have previously been described as pelagic but should from now on be considered pelago-sympagic. This stands in interesting contrast to the other amphipod species found previously under Antarctic sea ice, which had been sampled over shallow water depths and had been confirmed to originate from the benthos. This goes to show that there are still some aspects of the ecology of the polar areas which have not been accessible to dedicated investigations until recently, and thus might still hold some unexpected elements and contributions to our ecological understanding of the polar oceans.

Bibliography

- Andres, H. G., A. N. Lörz, and A. Brandt. A common but undescribed huge species of *Eusirus* Krøyer, 1845 (Crustacea, Amphipoda, Eusiridae) from Antarctica. *Mitt aus dem Hamb Zool Museum und Institut* 99 (2002): 109-126.
- Alves RN, Agustí S (2020) Effect of ultraviolet radiation (UVR) on the life stages of fish. *Rev Fish Biol Fish* 30:335–372. <https://doi.org/10.1007/s11160-020-09603-1>
- Arndt CE, Beuchel F (2006) Life history and population dynamics of the Arctic sympagic amphipods *Onisimus nanseni* Sars and *O. glacialis* Sars (Gammaridea: Lysianassidae). *Polar Biol* 29:239–248. <https://doi.org/10.1007/s00300-005-0045-x>
- Arndt CE, Brandt A, Berge J (2005a) Mouthpart-atlas of arctic sympagic amphipods— trophic niche separation based on mouthpart morphology and feeding ecology. *J Crustacean Biol* 25:401–412. <https://doi.org/10.1651/c-2544>
- Arndt CE, Fernandez-Leborans G, Seuthe L, et al (2005b) Ciliated epibionts on the Arctic sympagic amphipod *Gammarus wilkitzkii* as indicators for sympago–benthic coupling. *Mar Biol* 147:643–652. <https://doi.org/10.1007/s00227-005-1599-4>
- Arndt CE, Swadling KM (2006) Crustacea in Arctic and Antarctic sea ice: distribution, diet and life history strategies. *Adv Mar Biol* 51:197–315. [https://doi.org/10.1016/S0065-2881\(06\)51004-1](https://doi.org/10.1016/S0065-2881(06)51004-1)
- Banaszak AT, Barba Santos MG, LaJeunesse TC, Lesser MP (2006) The distribution of mycosporine-like amino acids (MAAs) and the phylogenetic identity of symbiotic dinoflagellates in cnidarian hosts from the Mexican Caribbean. *J Exp Mar Bio Ecol* 337:131–146. <https://doi.org/10.1016/j.jembe.2006.06.014>
- Belzile C, Johannessen SC, Gosselin M, et al (2000) Ultraviolet attenuation by dissolved and particulate constituents of first-year ice during late spring in an Arctic polynya. *Limnol Oceanogr* 45:1265–1273. <https://doi.org/10.4319/lo.2000.45.6.1265>

- Berge J, Daase M, Renaud PE, et al (2015a) Unexpected levels of biological activity during the polar night offer new perspectives on a warming Arctic. *Curr Biol* 25:2555–2561. <https://doi.org/10.1016/j.cub.2015.08.024>
- Berge J, Geoffroy M, Daase M, et al (2020) Artificial light during the polar night disrupts Arctic fish and zooplankton behaviour down to 200 m depth. *Commun Biol* 3:102. <https://doi.org/10.1038/s42003-020-0807-6>
- Berge J, Renaud PE, Darnis G, et al (2015b) In the dark: A review of ecosystem processes during the Arctic polar night. *Prog Oceanogr* 139:258–271. <https://doi.org/10.1016/j.pocean.2015.08.005>
- Berge J, Varpe O, Moline MA, et al (2012) Retention of ice-associated amphipods: possible consequences for an ice-free Arctic Ocean. *Biol Lett* 8:1012–1015. <https://doi.org/10.1098/rsbl.2012.0517>
- Bernhard G, Stierle S (2020) Trends of UV radiation in Antarctica. *Atmosphere (Basel)* 11:795. <https://doi.org/10.3390/atmos11080795>
- Bradstreet MSW, Cross WE (1982) Trophic relationships at high arctic ice edges. *Arctic* 35:. <https://doi.org/10.14430/arctic2303>
- Buma AGJ, Wright SW, van den Enden R, et al (2006) PAR acclimation and UVBR-induced DNA damage in Antarctic marine microalgae. *Mar Ecol Prog Ser* 315:33–42. <https://doi.org/10.3354/meps315033>
- Butchart N (2014) The brewer-Dobson circulation. *Rev Geophys* 52:157–184. <https://doi.org/10.1002/2013rg000448>
- Butchart N, Scaife AA (2001) Removal of chlorofluorocarbons by increased mass exchange between the stratosphere and troposphere in a changing climate. *Nature* 410:799–802. <https://doi.org/10.1038/35071047>
- Butow B, Wynne D, Tel-Or E (1994) Response of catalase activity to environmental stress in the freshwater dinoflagellate *Peridinium gatunense*1. *J Phycol* 30:17–22. <https://doi.org/10.1111/j.0022-3646.1994.00017.x>

- Carey AG (2018) Marine Ice Fauna: Arctic. In: Sea Ice Biota. CRC Press, pp 173–190
- Carreto JJ, Carignan MO, Daleo G, Marco SGD (1990) Occurrence of mycosporine-like amino acids in the red-tide dinoflagellate *Alexandrium excavatum*: UV-photoprotective compounds? *J Plankton Res* 12:909–921.
<https://doi.org/10.1093/plankt/12.5.909>
- Cheng L, Kellogg EW, Packer L (1981) Photoinactivation of catalase. *Photochem Photobiol* 34:125–129. <https://doi.org/10.1111/j.1751-1097.1981.tb09334.x>
- Cox GFN, Weeks WF (1974) Salinity variations in sea ice. *J Glaciol* 13:109–120.
<https://doi.org/10.3189/s0022143000023418>
- David C, Schaafsma FL, van Franeker JA, et al (2017) Community structure of under-ice fauna in relation to winter sea-ice habitat properties from the Weddell Sea. *Polar Biol* 40:247–261. <https://doi.org/10.1007/s00300-016-1948-4>
- Dunlap WC, Shick JM (1998) Review-ultraviolet radiation-absorbing mycosporine-like amino acids in coral reef organisms: A biochemical and environmental perspective. *J Phycol* 34:418–430. <https://doi.org/10.1046/j.1529-8817.1998.340418.x>
- Ehn JK, Mundy CJ, Barber DG, et al (2011) Impact of horizontal spreading on light propagation in melt pond covered seasonal sea ice in the Canadian Arctic. *J Geophys Res* 116:. <https://doi.org/10.1029/2010jc006908>
- Ehrenberg, C. G. 1853: *Über neue Anschauungen des kleinsten nördlichen Polarlebens. Akad. Wiss., Berlin, Monatsber. 1853. 522.*
- Elliott A (2015) UV-protective compounds in sea ice-associated algae in the Canadian Arctic. *Marine Ecology Progress Series*
- Elliott A, Mundy CJ, Gosselin M, et al (2015) Spring production of mycosporine-like amino acids and other UV-absorbing compounds in sea ice-associated algae communities in the Canadian Arctic. *Mar Ecol Prog Ser* 541:91–104.
<https://doi.org/10.3354/meps11540>

- Fernández J, Pérez-Álvarez JA, Fernández-López JA (1997) Thiobarbituric acid test for monitoring lipid oxidation in meat. *Food Chem* 59:345–353.
[https://doi.org/10.1016/s0308-8146\(96\)00114-8](https://doi.org/10.1016/s0308-8146(96)00114-8)
- Flores H, van Franeker J-A, Cisewski B, et al (2011) Macrofauna under sea ice and in the open surface layer of the Lazarev Sea, Southern Ocean. *Deep Sea Res Part 2 Top Stud Oceanogr* 58:1948–1961. <https://doi.org/10.1016/j.dsr2.2011.01.010>
- Fritsen CH, Wirthlin ED, Momberg DK, et al (2011) Bio-optical properties of Antarctic pack ice in the early austral spring. *Deep Sea Res Part 2 Top Stud Oceanogr* 58:1052–1061. <https://doi.org/10.1016/j.dsr2.2010.10.028>
- Fuhrmann MM, Nygård H, Krapp RH, et al (2011) The adaptive significance of chromatophores in the Arctic under-ice amphipod *Apherusa glacialis*. *Polar Biol* 34:823–832. <https://doi.org/10.1007/s00300-010-0938-1>
- Garcia RR, Randel WJ (2008) Acceleration of the Brewer–Dobson circulation due to increases in greenhouse gases. *J Atmos Sci* 65:2731–2739.
<https://doi.org/10.1175/2008jas2712.1>
- Gradinger R, Bluhm B (2010) Timing of Ice Algal Grazing by the Arctic Nearshore Benthic Amphipod *Onisimus litoralis*. *Arctic* 63:. <https://doi.org/10.14430/arctic1498>
- Gradinger R, Bluhm B (2004) In-situ observations on the distribution and behavior of amphipods and Arctic cod (*Boreogadus saida*) under the sea ice of the High Arctic Canada Basin. *Polar Biol* 27:. <https://doi.org/10.1007/s00300-004-0630-4>
- Gradinger R, Bluhm B, Iken K (2010) Arctic sea-ice ridges—Safe heavens for sea-ice fauna during periods of extreme ice melt? *Deep Sea Res Part 2 Top Stud Oceanogr* 57:86–95. <https://doi.org/10.1016/j.dsr2.2009.08.008>
- Gulliksen B (1984) Under-ice fauna from Svalbard waters. *Sarsia* 69:17–23.
<https://doi.org/10.1080/00364827.1984.10420585>
- Gulliksen B, Lønne OJ (1991) Sea ice macrofauna in the Antarctic and the Arctic. *J Mar Syst* 2:53–61. [https://doi.org/10.1016/0924-7963\(91\)90013-k](https://doi.org/10.1016/0924-7963(91)90013-k)

- Ha S-Y, Kim Y-N, Park M-O, et al (2012) Production of mycosporine-like amino acids of in situ phytoplankton community in Kongsfjorden, Svalbard, Arctic. *J Photochem Photobiol B* 114:1–14. <https://doi.org/10.1016/j.jphotobiol.2012.03.011>
- Ha S-Y, Min J-O, Joo H, et al (2018) Synthesis of mycosporine-like amino acids by a size-fractionated marine phytoplankton community of the arctic beaufort sea. *J Photochem Photobiol B* 188:87–94. <https://doi.org/10.1016/j.jphotobiol.2018.09.008>
- Hall K (2004) Antarctic biology in a global context. Proceedings of the VIIIth SCAR international biology symposium, 27 august–1 September 2001, Vrije Universiteit, Amsterdam, the Netherlands. Edited by ad H L Huiskes, Winfried W C Gieskes, Jelte Rozema, Raymond M L Schorno, Saskia M van der Vies, and Wim J Wolff. Leiden (the Netherlands): ISBN: 90–5782–079–X. 2003. *Q Rev Biol* 79:222–222. <https://doi.org/10.1086/423103>
- Hargreaves BR (2007) Water column optics and penetration of UVR. In: *Comprehensive Series in Photochemical & Photobiological Sciences*. Royal Society of Chemistry, Cambridge, pp 59–106
- Hartmann DL, Wallace JM, Limpasuvan V, et al (2000) Can ozone depletion and global warming interact to produce rapid climate change? *Proc Natl Acad Sci U S A* 97:1412–1417. <https://doi.org/10.1073/pnas.97.4.1412>
- Hidema J, Kang H-S, Kumagai T (1996) Differences in the sensitivity to UVB radiation of two cultivars of rice (*Oryza sativa* L.). *Plant Cell Physiol* 37:742–747. <https://doi.org/10.1093/oxfordjournals.pcp.a029008>
- Hop H, Pavlova O (2008) Distribution and biomass transport of ice amphipods in drifting sea ice around Svalbard. *Deep Sea Res Part 2 Top Stud Oceanogr* 55:2292–2307. <https://doi.org/10.1016/j.dsr2.2008.05.023>
- Hop H, Poltermann M, Lønne OJ, et al (2000) Ice amphipod distribution relative to ice density and under-ice topography in the northern Barents Sea. *Polar Biol* 23:357–367. <https://doi.org/10.1007/s003000050456>
- Horner RA (1985) *Sea Ice Biota*. CRC Press, Boca Raton, FL

- Jain K, Kataria S, Guruprasad KN (2004) Oxyradicals under UV-b stress and their quenching by antioxidants. *Indian J Exp Biol* 42:884–892
- Johnsen S (2012) *Optics of life*. Princeton University Press, Princeton, NJ
- Karentz D (2001) Chemical defenses of marine organisms against solar radiation exposure: UV-absorbing mycosporine-like amino acids and scytonemin. In: *Marine Science*. CRC Press, pp 481–520
- Karentz D (1994) Ultraviolet tolerance mechanisms in Antarctic marine organisms. In: *Ultraviolet Radiation in Antarctica: Measurements and Biological Effects*. American Geophysical Union, Washington, D. C., pp 93–110
- Karentz D, McEuen FS, Land MC, Dunlap WC (1991) Survey of mycosporine-like amino acid compounds in Antarctic marine organisms: Potential protection from ultraviolet exposure. *Mar Biol* 108:157–166. <https://doi.org/10.1007/bf01313484>
- Katlein C, Arndt S, Nicolaus M, et al (2015) Influence of ice thickness and surface properties on light transmission through Arctic sea ice. *J Geophys Res Oceans* 120:5932–5944. <https://doi.org/10.1002/2015JC010914>
- Kauko HM, Taskjelle T, Assmy P, et al (2017) Windows in Arctic sea ice: Light transmission and ice algae in a refrozen lead: Light and Algae in a Refrozen Lead. *J Geophys Res Biogeosci* 122:1486–1505. <https://doi.org/10.1002/2016jg003626>
- Kiko R, Michels J, Mizdalski E, et al (2008) Living conditions, abundance and composition of the metazoan fauna in surface and sub-ice layers in pack ice of the western Weddell Sea during late spring. *Deep Sea Res Part 2 Top Stud Oceanogr* 55:1000–1014. <https://doi.org/10.1016/j.dsr2.2007.12.012>
- Kouwenberg JHM, Browman HI, Cullen JJ, et al (1999a) Biological weighting of ultraviolet (280-400 nm) induced mortality in marine zooplankton and fish. I. Atlantic cod (*Gadus morhua*) eggs. *Mar Biol* 134:269–284. <https://doi.org/10.1007/s002270050545>
- Kouwenberg JHM, Browman HI, Runge JA, et al (1999b) Biological weighting of ultraviolet (280-400 nm) induced mortality in marine zooplankton and fish. II. *Calanus*

- finmarchicus (Copepoda) eggs. *Mar Biol* 134:285–293.
<https://doi.org/10.1007/s002270050546>
- Krapp RH, Berge J, Flores H, et al (2008) Sympagic occurrence of Eusirid and Lysianassoid amphipods under Antarctic pack ice. *Deep Sea Res Part 2 Top Stud Oceanogr* 55:1015–1023. <https://doi.org/10.1016/j.dsr2.2007.12.018>
- Kunisch EH, Bluhm BA, Daase M, et al (2020) Pelagic occurrences of the ice amphipod *Apherusa glacialis* throughout the Arctic. *J Plankton Res* 42:73–86.
<https://doi.org/10.1093/plankt/fbz072>
- Legendre L, Ackley S, Dieckmann G, et al (1992) Ecology of sea ice biota: 2. Global significance. *Polar Biol* 12:. <https://doi.org/10.1007/bf00243114>
- Lesser MP, Barry TM, Lamare MD, Barker MF (2006) Biological weighting functions for DNA damage in sea urchin embryos exposed to ultraviolet radiation. *J Exp Mar Bio Ecol* 328:10–21. <https://doi.org/10.1016/j.jembe.2005.06.010>
- Lesser MP, Lamare MD, Barker MF (2004) Transmission of ultraviolet radiation through the Antarctic annual sea ice and its biological effects on sea urchin embryos. *Limnol Oceanogr* 49:1957–1963. <https://doi.org/10.4319/lo.2004.49.6.1957>
- Little EE, Fabacher D (2007) UVR-induced injuries in freshwater vertebrates. In: *Comprehensive Series in Photochemical & Photobiological Sciences*. Royal Society of Chemistry, Cambridge, pp 431–454
- Lønne OJ, Gulliksen B (1991) On the distribution of sympagic macro-fauna in the seasonally ice covered Barents Sea. *Polar Biol* 11:. <https://doi.org/10.1007/bf00233081>
- Macias-Fauria M, Post E (2018) Effects of sea ice on Arctic biota. *Biol Lett* 14:20180265.
<https://doi.org/10.1098/rsbl.2018.0265>
- Macnaughton MO, Thormar J, Berge J (2007) Sympagic amphipods in the Arctic pack ice: redescrptions of *Eusirus holmii* Hansen, 1887 and *Pleusymtes karstensi* (Barnard, 1959). *Polar Biol* 30:1013–1025. <https://doi.org/10.1007/s00300-007-0260-8>

- Malloy KD, Holman MA, Mitchell D, Detrich HW 3rd (1997) Solar UVB-induced DNA damage and photoenzymatic DNA repair in antarctic zooplankton. *Proc Natl Acad Sci U S A* 94:1258–1263. <https://doi.org/10.1073/pnas.94.4.1258>
- Maslanik JA, Fowler C, Stroeve J, et al (2007) A younger, thinner Arctic ice cover: Increased potential for rapid, extensive sea-ice loss. *Geophys Res Lett* 34:. <https://doi.org/10.1029/2007gl032043>
- Melnikov A (1997) *Arctic Sea Ice Ecosystem*. Taylor & Francis, London, England
- Michalek-Wagner K, Willis BL (2001) Impacts of bleaching on the soft coral *Lobophytum compactum* . I. Fecundity, fertilization and offspring viability. *Coral Reefs* 19:231–239. <https://doi.org/10.1007/s003380170003>
- Mundy CJ, Gosselin M, Ehn JK, et al (2011) Characteristics of two distinct high-light acclimated algal communities during advanced stages of sea ice melt. *Polar Biol* 34:1869–1886. <https://doi.org/10.1007/s00300-011-0998-x>
- Mundy CJ, Gosselin M, Gratton Y, et al (2014) Role of environmental factors on phytoplankton bloom initiation under landfast sea ice in Resolute Passage, Canada. *Mar Ecol Prog Ser* 497:39–49. <https://doi.org/10.3354/meps10587>
- Nairn RS, Morizot DC, Kazianis S, et al (1996) Nonmammalian models for sunlight carcinogenesis: genetic analysis of melanoma formation in *Xiphophorus* hybrid fish. *Photochem Photobiol* 64:440–448. <https://doi.org/10.1111/j.1751-1097.1996.tb03089.x>
- Nansen F (1906) Methods for measuring direction and velocity of currents in the sea. *ICES J Mar Sci* s1:3–32. <https://doi.org/10.1093/icesjms/s1.34.3>
- Nansen. F. 1906: Protozoa on the ice floes of the North Polar Sea. *Sci. Res. Norw. N. Polar Exped.* 5(16), 1.
- Nelson NB, Siegel DA (2002) Chromophoric DOM in the Open Ocean. In: *Biogeochemistry of Marine Dissolved Organic Matter*. Elsevier, pp 547–578

- Nicolaus M, Katlein C (2012) Mapping radiation transfer through sea ice using a remotely operated vehicle (ROV). *cryosph discuss* 6:3613–3646. <https://doi.org/10.5194/tcd-6-3613-2012>
- Notz D, Stroeve J (2016) Observed Arctic sea-ice loss directly follows anthropogenic CO₂ emission. *Science* 354:747–750. <https://doi.org/10.1126/science.aag2345>
- Obermüller B, Karsten U, Abele D (2005) Response of oxidative stress parameters and sunscreens compounds in Arctic amphipods during experimental exposure to maximal natural UVB radiation. *J Exp Mar Bio Ecol* 323:100–117. <https://doi.org/10.1016/j.jembe.2005.03.005>
- Oren A, Gunde-Cimerman N (2007) Mycosporines and mycosporine-like amino acids: UV protectants or multipurpose secondary metabolites? *FEMS Microbiol Lett* 269:1–10. <https://doi.org/10.1111/j.1574-6968.2007.00650.x>
- Parkinson CL (2019) A 40-y record reveals gradual Antarctic sea ice increases followed by decreases at rates far exceeding the rates seen in the Arctic. *Proc Natl Acad Sci U S A* 116:14414–14423. <https://doi.org/10.1073/pnas.1906556116>
- Pavlov AK, Leu E, Hanelt D, et al (2019) The underwater light climate in Kongsfjorden and its ecological implications. In: *The Ecosystem of Kongsfjorden, Svalbard*. Springer International Publishing, Cham, pp 137–170
- Perovich DK, Roesler CS, Pegau WS (1998) Variability in Arctic sea ice optical properties. *J Geophys Res* 103:1193–1208. <https://doi.org/10.1029/97jc01614>
- Piiparinen J, Enberg S, Rintala J-M, et al (2015) The contribution of mycosporine-like amino acids, chromophoric dissolved organic matter and particles to the UV protection of sea-ice organisms in the Baltic Sea. *Photochem Photobiol Sci* 14:1025–1038. <https://doi.org/10.1039/c4pp00342j>
- Poltermann M (2000) Growth, production and productivity of the Arctic sympagic amphipod *Gammarus wilkitzkii*. *Mar Ecol Prog Ser* 193:109–116. <https://doi.org/10.3354/meps193109>

- Poltermann M, Hop H, Falk-Petersen S (2000) Life under Arctic sea ice - reproduction strategies of two sympagic (ice-associated) amphipod species, *Gammarus wilkitzkii* and *Apherusa glacialis*. *Mar Biol* 136:913–920.
<https://doi.org/10.1007/s002270000307>
- Prášil O (2003) Helbling, E.w. zagarese, H. (ed.): UV effects in aquatic organisms and ecosystems. *Photosynthetica* 41:382–382.
<https://doi.org/10.1023/b:phot.0000015525.07495.69>
- Rastogi RP, Sonani RR, Madamwar D (2017) UV photoprotectants from algae—synthesis and bio-functionalities. In: *Algal Green Chemistry*. Elsevier, pp 17–38
- Regoli F, Winston GW (1999) Quantification of total oxidant scavenging capacity of antioxidants for peroxy nitrite, peroxy radicals, and hydroxyl radicals. *Toxicol Appl Pharmacol* 156:96–105. <https://doi.org/10.1006/taap.1999.8637>
- Sakshaug E, Johnsen G, Kovacs K (eds) (2009) *Ecosystem Barents Sea*. Tapir Academic Press, Trondheim, Norway
- Sarangarajan R, Apte SP (2005) Melanin aggregation and polymerization: possible implications in age-related macular degeneration. *Ophthalmic Res* 37:136–141.
<https://doi.org/10.1159/000085533>
- Schnack-Schiel S, Thomas D, Gradinger R, et al (2001) Meiofauna in sea ice of the Weddell Sea (Antarctica). *Polar Biol* 24:724–728. <https://doi.org/10.1007/s003000100273>
- Schnack-Schiel SB (2008) *The Macrobiology of Sea Ice*. In: *Sea Ice*. Blackwell Science Ltd, Oxford, UK, pp 211–239
- Singh SP, Kumari S, Rastogi RP, et al (2008) Mycosporine-like amino acids (MAAs): chemical structure, biosynthesis and significance as UV-absorbing/screening compounds. *Indian J Exp Biol* 46:7–17
- Sommaruga R (2001) The role of solar UV radiation in the ecology of alpine lakes. *J Photochem Photobiol B* 62:35–42. [https://doi.org/10.1016/s1011-1344\(01\)00154-3](https://doi.org/10.1016/s1011-1344(01)00154-3)

- Steer A, Worby A, Heil P (2008) Observed changes in sea-ice floe size distribution during early summer in the western Weddell Sea. *Deep Sea Res Part 2 Top Stud Oceanogr* 55:933–942. <https://doi.org/10.1016/j.dsr2.2007.12.016>
- Stroeve J, Holland MM, Meier W, et al (2007) Arctic sea ice decline: Faster than forecast: ARCTIC ICE LOSS-FASTER THAN FORECAST. *Geophys Res Lett* 34:. <https://doi.org/10.1029/2007gl029703>
- Stroeve J, Notz D (2018) Changing state of Arctic sea ice across all seasons. *Environ Res Lett* 13:103001. <https://doi.org/10.1088/1748-9326/aade56>
- Stroeve JC, Markus T, Boisvert L, et al (2014) Changes in Arctic melt season and implications for sea ice loss. *Geophys Res Lett* 41:1216–1225. <https://doi.org/10.1002/2013gl058951>
- Stroeve JC, Serreze MC, Holland MM, et al (2012) The Arctic’s rapidly shrinking sea ice cover: a research synthesis. *Clim Change* 110:1005–1027. <https://doi.org/10.1007/s10584-011-0101-1>
- Taskjelle T, Hudson SR, Granskog MA, et al (2016) Spectral albedo and transmittance of thin young Arctic sea ice. *J Geophys Res Oceans* 121:540–553. <https://doi.org/10.1002/2015jc011254>
- Thomas DN (ed) (2017) *Sea Ice*, 3rd edn. Wiley-Blackwell, Hoboken, NJ
- Thomas DN, Papadimitriou S, Michel C (2010) Biogeochemistry of Sea Ice. In: *Sea Ice*. Wiley-Blackwell, Oxford, UK, pp 425–467
- Turner J, Hosking JS, Marshall GJ, et al (2016) Antarctic sea ice increase consistent with intrinsic variability of the Amundsen Sea Low. *Clim Dyn* 46:2391–2402. <https://doi.org/10.1007/s00382-015-2708-9>
- United Nations Environment Programme, Environmental Effects Assessment Panel (2017) Environmental effects of ozone depletion and its interactions with climate change: Progress report, 2016. *Photochem Photobiol Sci* 16:107–145. <https://doi.org/10.1039/c7pp90001e>

- Uusikivi J, Vähätalo AV, Granskog MA, Sommaruga R (2010) Contribution of mycosporine-like amino acids and colored dissolved and particulate matter to sea ice optical properties and ultraviolet attenuation. *Limnol Oceanogr* 55:703–713.
<https://doi.org/10.4319/lo.2010.55.2.0703>
- Vershinin A (1999) Functions of carotenoids: diversity and evolution. *Comp Biochem Physiol A Mol Integr Physiol* 124:S113. [https://doi.org/10.1016/s1095-6433\(99\)90448-8](https://doi.org/10.1016/s1095-6433(99)90448-8)
- von der Gathen P, Kivi R, Wohltmann I, et al (2021) Climate change favours large seasonal loss of Arctic ozone. *Nat Commun* 12:3886. <https://doi.org/10.1038/s41467-021-24089-6>
- Weinreb O, Dovrat A (1996) Transglutaminase involvement in UV-A damage to the eye lens. *Exp Eye Res* 63:591–597. <https://doi.org/10.1006/exer.1996.0150>
- Weslawski JM, Ryg M, Smith TG, Oritsland NA (1994) Diet of ringed seals (*Phoca hispida*) in a fjord of west Svalbard. *Arctic* 47:. <https://doi.org/10.14430/arctic1279>
- Winston GW, Regoli F, Dugas AJ Jr, et al (1998) A rapid gas chromatographic assay for determining oxyradical scavenging capacity of antioxidants and biological fluids. *Free Radic Biol Med* 24:480–493. [https://doi.org/10.1016/s0891-5849\(97\)00277-3](https://doi.org/10.1016/s0891-5849(97)00277-3)
- Wright DJ, Smith SC, Joardar V, et al (2005) UV irradiation and desiccation modulate the three-dimensional extracellular matrix of *Nostoc commune* (Cyanobacteria). *J Biol Chem* 280:40271–40281. <https://doi.org/10.1074/jbc.M505961200>
- Yao Z-Y, Qi J-H (2016) Comparison of antioxidant activities of melanin fractions from chestnut shell. *Molecules* 21:487. <https://doi.org/10.3390/molecules21040487>
- Zellmer ID (1995) UV-B-tolerance of alpine and arctic *Daphnia*. *Hydrobiologia* 307:153–159. <https://doi.org/10.1007/bf00032007>
- Zigman S, Reddan J, Schultz JB, McDaniel T (1996) Structural and functional changes in catalase induced by near-UV radiation. *Photochem Photobiol* 63:818–824.
<https://doi.org/10.1111/j.1751-1097.1996.tb09637.x>

List of published articles included and discussed in this synthesis:

- Fuhrmann, M. M., Nygård, H., **Krapp**, R. H., Berge, J., & Werner, I. (2011). The adaptive significance of chromatophores in the Arctic under-ice amphipod *Apherusa glacialis*. *Polar Biology*, *34*(6), 823–832. <https://doi.org/10.1007/s00300-010-0938-1>
- Krapp**, R. H., Berge, J. (in prep). Total content of Mycosporine-like amino acids (MAAs) in the sympagic amphipods *Gammarus wilkitzkii*, *Onisimus nanseni*, *O. glacialis*, and *Apherusa glacialis* under Arctic pack ice during different seasons. *Manuscript in prep*, 1–16.
- Krapp**, R. H., Baussant, T., Berge, J., Pampanin, D. M., & Camus, L. (2009). Antioxidant responses in the polar marine sea-ice amphipod *Gammarus wilkitzkii* to natural and experimentally increased UV levels. *Aquatic Toxicology (Amsterdam, Netherlands)*, *94*(1), 1–7. <https://doi.org/10.1016/j.aquatox.2009.05.005>
- Krapp**, R. H., Berge, J., Flores, H., Gulliksen, B., & Werner, I. (2008). Sympagic occurrence of Eusirid and Lysianassoid amphipods under Antarctic pack ice. *Deep-Sea Research. Part II, Topical Studies in Oceanography*, *55*(8–9), 1015–1023. <https://doi.org/10.1016/j.dsr2.2007.12.018>

Paper 1

Krapp, R.H., Baussant, T., Berge, J., Pampanin, D.M. & Camus, L. (2009).

Antioxidant responses in the polar marine sea-ice amphipod *Gammarus wilkitzkii* to natural and experimentally increased UV levels

Aquatic Toxicology, 94(1), 1-7.



Contents lists available at ScienceDirect

Aquatic Toxicology

journal homepage: www.elsevier.com/locate/aquatox

Antioxidant responses in the polar marine sea-ice amphipod *Gammarus wilkitzkii* to natural and experimentally increased UV levels

Rupert H. Krapp^{a,b,*}, Thievery Bassinet^c, Jørgen Berge^b, Daniela M. Pampanin^c, Lionel Camus^d

^a University of Kiel, Institute for Polar Ecology, Wischhofstr. 1–3, Building 12, 24148 Kiel, Germany

^b University Center in Svalbard, Postbox 156, 9171 Longyearbyen, Norway

^c International Research Institute of Stavanger (IRIS), Mekjarvik 12, N-4070 Randaberg, Norway

^d Akvaplan-niva a/s, Polar Environmental Centre, N-9296 Tromsø, Norway

ARTICLE INFO

Article history:

Received 11 December 2007

Received in revised form 10 May 2009

Accepted 11 May 2009

Keywords:

Arctic

Amphipods

Sea-ice

Under-ice fauna

Sympagic

Oxyradical

TOSC

Malondialdehyde

Ultraviolet radiation

ABSTRACT

Polar marine surface waters are characterized by high levels of dissolved oxygen, seasonally intense UV irradiance and high levels of dissolved organic carbon. Therefore, the Arctic sea-ice habitat is regarded as a strongly pro-oxidant environment, even though its significant ice cover protects the ice-associated (= sympagic) fauna from direct irradiation to a large extent. In order to investigate the level of resistance to oxyradical stress, we sampled the sympagic amphipod species *Gammarus wilkitzkii* during both winter and summer conditions, as well as exposed specimens to simulated levels of near-natural and elevated levels of UV irradiation. Results showed that this amphipod species possessed a much stronger antioxidant capacity during summer than during winter. Also, the experimental UV exposure showed a depletion in antioxidant defences, indicating a negative effect of UV exposure on the total oxyradical scavenging capacity. Another sympagic organism, *Onisimus nansenii*, was sampled during summer conditions. When compared to *G. wilkitzkii*, the species showed even higher antioxidant scavenging capacity.

© 2009 Elsevier B.V. All rights reserved.

1. Introduction

During the last decades, levels of stratospheric ozone have been decreasing over both polar areas (Kerr and McElroy, 1993), allowing an increased amount of ultraviolet radiation (UVR) to reach the Earth's surface (Madronich et al., 1998). Since UVR can penetrate to ecologically important depths in water, a large number of studies on the effects of UVR on aquatic environments have been carried out. UV radiation creates oxidative stress, and causes cellular damage and increased mortality (Browman et al., 2000; Lesser, 2006). The Arctic sea-ice environment is characterized by high dissolved oxygen concentrations, seasonally high levels of dissolved organic carbon (DOC) (Belzile et al., 2000), as well as a seasonally extended photoperiod and high primary productivity. These factors, especially the co-existence of high DOC levels under significant UVR levels (Scully et al., 1996), lead to the production of reactive oxygen species (ROS) (Lesser, 2006; Häder et al., 1998). The deleterious effects of ROS on aquatic organisms have been covered in reviews by Di Giulio et al. (1989) and Winston and Di

Giulio (1991), and include lipid peroxidation, DNA strand breaks, cyclobutane pyrimidine dimers (CPD's), and enzyme inactivation (Livingstone, 2001; Browman et al., 2003; Karentz et al., 2004). To cope with these and other pro-oxidant challenges, aquatic organisms can deploy a number of antioxidant defence mechanisms, which rely on enzymatic as well as nonenzymatic components. These include superoxide dismutase (SOD) (McCord and Fridovich, 1969), catalase (CAT), and glutathione peroxidases as enzymatic defences, while vitamin C (ascorbic acid), glutathione (GSH), vitamin E (tocopherol), carotenoids (Davenport et al., 2004) and several other small-molecule antioxidants like dimethyl sulfide (DMS) and mycosporine-like amino acids (MAA's) function as nonenzymatic antioxidants (Lesser, 2006). Another adaptation to UVR-induced stress is the photoenzymatic repair (PER) mechanism, where the enzyme photolyase breaks down CPD's in the presence of photosynthetically active radiation (PAR, 400–700 nm) and ultraviolet radiation (UVR) in the UVA range (320–400 nm). Grad et al. (2001) and Lacuna and Uye (2001) have published studies on PER in zooplankton which showed that PER can significantly alleviate the UVR-induced stress.

The importance of UVR as a pro-oxidant force in polar surface waters has been recognized by a number of papers, see Belzile et al. (2000) and Browman et al. (2000) for Arctic marine habitats, Karentz and Lutze (1990) and Karentz and Bosch (2001) on

* Corresponding author at: University of Kiel, Institute for Polar Ecology, Wischhofstr. 1–3, Building 12, 24148 Kiel, Germany.

E-mail addresses: rkrapp@ipoe.uni-kiel.de, rupert.krapp@unis.no (R.H. Krapp).

Antarctic marine habitats, Hessen (1996) and Hessen et al. (2002) on Arctic freshwater ponds, and Kepner et al. (2000) and Rocco et al. (2002) on Antarctic freshwater habitats. In order to address the complex issue of oxyradical stress and antioxidant responses, Regoli and Winston (1998) and Winston et al. (1998) developed and proposed the total oxyradical scavenging (TOSC) assay as an integrative approach to the problem of quantifying the level of oxyradical defence in a given tissue or organism sample (Regoli et al., 2002a). Rather than studying one antioxidant component at a time which can be induced through several pathways, this assay quantifies the total antioxidant response to a specific oxyradical challenge. It has since been applied to a number of polar studies (Camus et al., 2003; Corsolini et al., 2001; Regoli et al., 2000, 2002b, 2005) including studies on polar amphipods (Camus and Gulliksen, 2004, 2005; Obermüller et al., 2005).

Lipid peroxidation is a well-known mechanism of cellular injury induced by oxidative stress in cells and tissues. Malondialdehyde (MDA) is a decomposition product of lipid peroxides derived from polyunsaturated fatty acids. This reactive carbonyl compound is the most abundant lipid peroxidation product and therefore widely used as an indicator of lipid peroxidation.

The polar sympagic amphipod *G. wilkitzkii* plays a central role in the ecosystem of Arctic sea-ice-covered waters (Steele and Steele, 1975; Poltermann, 2000; Poltermann et al., 2000), since it consumes sea-ice algae and sympagic fauna (Gulliksen and Lønne, 1989; Scott et al., 2001; Werner, 1997) and thus makes this sympagic biomass available to higher trophic levels (Lønne and Gulliksen, 1989) as well as to the underlying waters (Werner, 2000).

In this study, we measured natural UVR in the sympagic habitat and studied the effects of natural versus artificial UVR exposure on *G. wilkitzkii* to determine whether this species is susceptible to oxyradical stress. As a supplement to the TOSC assay, we also measured the content of malondialdehyde (MDA) as an indicator of lipid peroxidation (Marnett, 1999). We also compared the effects of natural UVR exposure in *G. wilkitzkii* and another sympagic species, *Onisimus nansenii*.

2. Materials and methods

2.1. Fieldwork

2.1.1. Spectral measurements of UVR

Spectral measurements in the field were performed at 78°65' N, 21°25' E during winter and at 81°59' N, 11°50' E during summer, using a TriOS Ramses ACC UV/PAR spectrophotometer (range 280–550 nm, 2.2 nm resolution) which was deployed by scuba-divers under the sea-ice, where it was affixed to the ice underside with a L-shaped arm and ice screws during measurements. Ice thickness in the field ranged from 1.5 to 2 m at the winter station and from 2 to 2.5 m at the summer station, with a snow cover of >1 dm during winter and 2–5 cm during summer. All ice floes in the respective areas were established to be multi-year ice.

2.1.2. Sampling of amphipods

During a winter sampling campaign in March/April 2004, sympagic amphipod samples of *G. wilkitzkii* were collected under consolidated pack ice at 78°65' N, 21°25' E near Heleysundet, on the east coast of the Svalbard Archipelago. More amphipods of this species as well as another sympagic species, *O. nansenii*, were collected during two research cruises to the ice edge north of Svalbard in August and September 2004 at 81°59' N, 11°50' E (compare Fig. 1: study area 1). A battery-driven suction sampler or hand-held dip net, operated by scuba-divers, were used to collect the animals from the sea ice underside. Species, sex and developmental stages

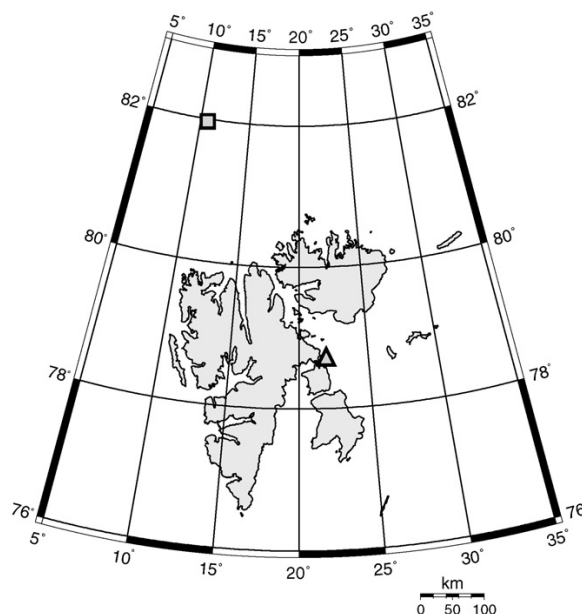


Fig. 1. Sampling areas for winter (March 2004, triangle) and summer (August 2004, square) sea ice stations. Locations were chosen based on their accessibility and sufficient cover of multi-year ice.

as well as total body length were determined immediately with stereomicroscopes. Animals intended for laboratory exposure were kept alive in temperature-controlled aquaria (0 °C) at low white light intensities until transfer to the laboratory. Organisms intended for determination of *in situ*-TOSC and MDA status were frozen immediately in liquid nitrogen and later transferred and stored at –80 °C.

2.2. Laboratory work

2.2.1. Exposure setup

This laboratory exposure was designed to detect whether there was a direct relationship for the sample organisms towards near-natural or increased radiation levels. A daily irradiation period, followed by a recovery period, was programmed to simulate the total radiation received by an organism per day during summer conditions. At the laboratory facilities of IRIS-Akvamiljø, a climate-controlled and light-controlled room was prepared with a controlled sea water supply. Room and water temperatures were set to 0 °C, and were constantly monitored throughout the experimentation period. Five aquaria were setup, of which two were equipped with a high-intensity UVA + B fluorescent lamp array (UVB), another two with a low-intensity UVA fluorescent lamp array (UVA), and the last was kept as control group in near-darkness (DC). All aquaria were supplied from the same climatized water pump with a flow of 1.8–2 l/min. and constant water circulation was maintained by a filtered overflow.

The high-intensity UV fluorescent lamp array consisted of one Q-Panel 340 lamp (40 W tube, 120 cm length) together with two Philips TL-12 lamps (20 W tube, 60 cm length), while the low-intensity UV fluorescent lamp array was composed of only one Q-Panel 340 lamp (40 W tube, 120 cm length) only. The high-intensity array was aimed at modelling Arctic summer sea surface levels of UV radiation (0.7 W m⁻² UV-B, 8.5 W m⁻² UV-A), while the low-intensity array was aimed at modelling typical Arctic under-ice levels of UV radiation (0.2 W m⁻² UV-B, 3.5 W m⁻² UV-A). Lamps were encased in UV-transparent plexi glass tubings to decrease the

warming effect otherwise exerted by fluorescent lamps, as well as protecting the high-voltage switch and contacts from corrosion and short-circuiting in a wet lab environment. The Philips TL-12 lamps were also equipped with a UVC cut-off filter, since these lamps are known to produce a small amount of radiation in the spectral range <280 nm, which as solar radiation is normally not penetrating into the Earth's atmosphere, and was therefore to be excluded in this experiment. Radiation was constantly monitored by a TriOS Ram- ses UV/PAR spectroradiometer, which was attached to the bottom through a hole in one of the aquaria.

Irradiance was limited to 5 days, with a 4 h-period per day, from 10 am to 2 pm, simulating a maximum penetration of UV radiation (UVR) into the sea ice zone during local noon. Outside this irradiance period, ambient light was kept to a minimum (<3 μM). After five irradiance periods, the experiment was terminated and all samples were immediately preserved in liquid nitrogen and then stored at -80°C .

In an additional setup, aquaria without animals were exposed under identical conditions as in the high-intensity UVA+B setup with the identical water supply system, and the overflow from these exposed aquaria was directed into holding tanks containing previously untreated and dark-acclimated amphipods, thus creating a "water-only" exposure where the direct impact of UVR on the animal tissue is removed and only potential oxyradical induction in the sea water was to be determined. Animals were (indirectly) exposed for the identical period and intensity, subsequently sampled and preserved in the same manner as in the previously mentioned setups.

2.2.2. TOSC assay

The method developed by Winston et al. (1998) and the protocol described in Regoli and Winston (1999) was followed, with the only modification that the buffer was adjusted for marine invertebrates. Whole amphipods were homogenized (1:4) in KH_2PO_4 buffer (100 mM, pH 7.4) containing NaCl (2.5%). The homogenate was centrifuged at $100,000 \times g$ for 1 h, and cytosolic fractions were aliquoted and stored at -80°C .

Peroxy radicals were generated by thermal homolysis of 2-2'-azo-bis-(2-methyl-propionamide)-dihydrochloride (ABAP) at 35°C . The iron-ascorbate Fenton reaction was used to generate hydroxyl radicals. The substrate α -keto- γ -methiolbutyric acid (KMBA) can be oxidised by either peroxy or hydroxyl radicals, and the resulting ethylene gas is then measured and quantified by gas-chromatography. Ethylene production was monitored for 96 min with a gas-chromatographic analysis system (Hewlett Packard HP 5890 series II) equipped with a Supelco SPB-1 capillary column and a flame ionization detector (FID). The oven, injection and FID temperatures were 35°C , 160°C , and 220°C , respectively; helium was used as carrier gas (1 ml min^{-1} flow rate) and a split ratio of 20:1 was obtained. Data acquisition was run by Millennium32™ software (Waters). Each analysis consisted of the sequential measurement of a sample (containing substrate and sample fluid) and a control (containing only substrate), which had both been exposed to the same oxyradical simultaneously. In the presence of antioxidants (contained in the sample fluid) the ethylene production was quantitatively reduced, and so higher antioxidant concentrations yielded a longer inhibition of ethylene oxidation and hence a lower total ethylene production for the assay period monitored by the GC system. Samples and controls were serially injected into the GC system with 1-min intervals, and the resulting peaks were analysed for integrated peak area at regular sampling intervals. By plotting the absolute value of the difference between peak areas of sample and control reaction at a series of sampling intervals, it is possible to calculate a kinetic curve for the oxyradical scavenging capacity. The total oxyradical scavenging capacity (TOSC) is then calculated

according to the equation:

$$\text{TOSC} = 100 - \frac{\text{IntSA}}{\text{IntCA}} \times 100 \quad (1)$$

with IntSA and IntCA as the integrated areas from the curve defining the sample and control reactions, respectively.

Final assay conditions were: 0.2 mM α -keto- γ -methiolbutyric acid (KMBA), 20 mM 2-2'-azo-bis-(2-methyl-propionamide)-dihydrochloride (ABAP) in 100 mM potassium phosphate buffer, pH 7.4 for peroxy radicals, and 1.8 μM Fe^{3+} , 3.6 μM ethylene-diamine-tetra-acetic acid (EDTA), 0.2 mM KMBA, 180 μM ascorbic acid in 100 mM potassium phosphate buffer, pH 7.4 for hydroxyl radicals.

TOSC values are expressed in units per mg protein. Total protein content was determined photometrically, using the Bradford assay (Bradford, 1976) with Coomassie Brilliant Blue G-250 as protein dye and bovine serum albumin (BSA) as standard.

2.2.3. MDA assay

The MDA assay used herein is based on the reaction with thiobarbituric acid (TBA), where one molecule of MDA reacts with two molecules of TBA at 80°C , to form a chromophore with peak absorbance at 532 nm (Fernández et al., 1997).

Sample fluid aliquots were mixed with 20% TCA-BHT (trichloroacetic acid with 2% butylated hydroxytoluene) to provide a highly acidic environment as well as an antioxidant to shield the sample from new lipid peroxidation during homogenization. After centrifugation for 15 min at $6000 \times g$, samples were transferred on microplates for incubation for 1 h at 80°C , followed by spectrophotometric analysis at 540 and 595 nm. The MDA concentration was calculated from δ OD using the formula

$$[\text{MDA}] = \frac{(\text{OD}_{540} - \text{OD}_{595}) - b}{a} \times df \quad (2)$$

where $[a]$ and $[b]$ were taken from a standard curve, prepared from tetramethoxypropane (TMOP), and $[df]$ stands for the dilution factor, which was in this case 4.

Final assay conditions were: 500 μl sample + 250 μl TCA-BHT for the initial mix, from which 150 μl sample was added to 30 μl HCl 0.6N and 120 μl Tris-TBA for the incubation and spectrophotometry.

2.3. Statistical analysis

Statistical analysis was carried out using JMP v. 5.0.1a, SAS Institute, Cary, NC, USA. Normal distribution and homogeneity of variances were established before statistical treatment, using \log_n transformation and the Levene and Bartlett tests, respectively. The Student's t -test was applied if variances appeared to be equal, otherwise a Welch ANOVA was performed instead. One-way ANOVA tests were performed for sets with more than two groups, followed by Dunnett's post hoc tests for datasets with control groups. The significance level was set to $P < 0.05$ for all tests.

3. Results

3.1. Field samples

Field TOSC levels towards peroxy and hydroxyl radicals in *G. wilkitzkii* were significantly higher in summer than in winter (see Fig. 2, panels A and B).

MDA levels were also significantly higher during summer than during winter (see Fig. 2, panel C).

In comparison to *G. wilkitzkii*, summer samples of *O. nanseni* showed significantly higher field TOSC levels towards peroxy and hydroxyl radicals (see Fig. 2).

This was also found to be true for the MDA content of *O. nanseni*.

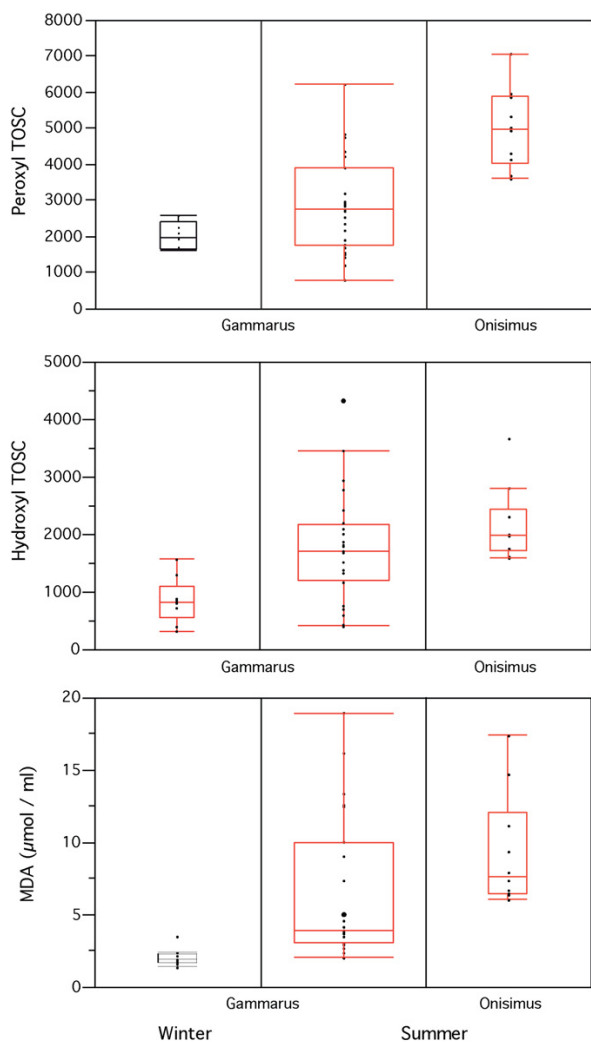


Fig. 2. Quantiles box plot of field TOSC levels for peroxy (panel A) and hydroxyl (panel B), as well as MDA (panel C) by season for *G. wilkitzkii*. The figure also shows the respective TOSC and MDA values of summer (August 2004) samples of *O. nanseni*. The box delimits the 25th and 75th percentile with the 10th and 90th percentile above and below, median in center.

3.2. Lab exposures—direct exposure

TOSC values for both peroxy and hydroxyl radicals were reduced for the two exposure sets as compared to the dark control (DC), but there were no significant differences between animals from high and low UV intensity exposures.

The tests for MDA content showed significantly lower values for the low UV intensity exposure, compared to the dark control (Fig. 3). The differences for the high UV intensity exposure and dark control (DC) or between the two exposures were not significant.

3.3. Lab exposures—indirect exposure

The “water-only” indirect exposure yielded significant differences between the exposed subset and the control subset for peroxy TOSC but not for hydroxyl TOSC, as shown below (Fig. 4).

The values for MDA content were also significantly lower for the “water-only” exposed versus the “control” samples, as shown in Fig. 4.

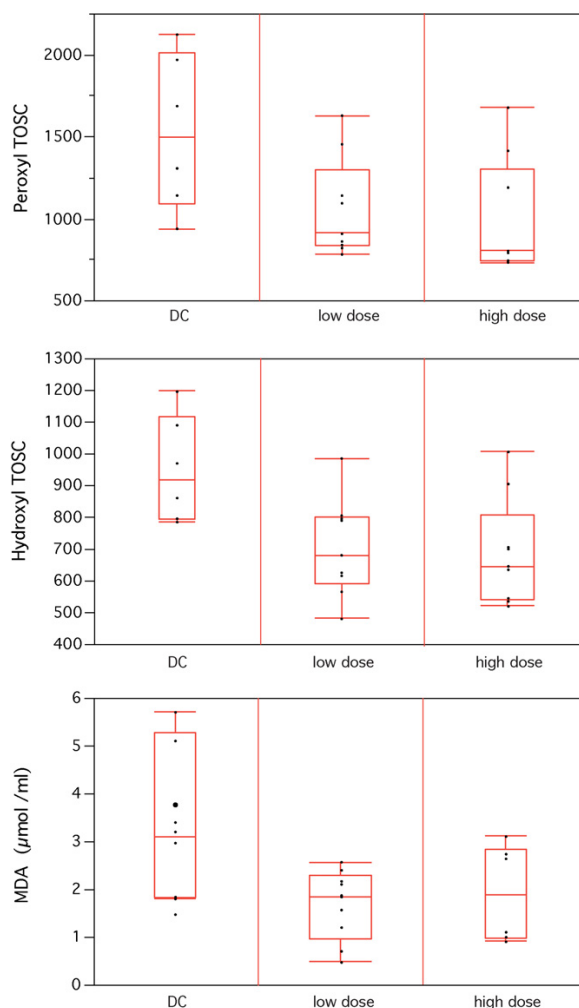


Fig. 3. Quantiles box plot of direct lab exposure TOSC levels for peroxy (panel A) and hydroxyl (panel B), as well as MDA (panel C) for *G. wilkitzkii*. The box delimits the 25th and 75th percentile with the 10th and 90th percentile above and below, median in center.

4. Discussion

4.1. Field UV measurements

Only a limited number of field studies have addressed the *in situ* range and variability of UVR. This is most likely due to the complex nature of optical properties of the sea-ice (Perovich et al., 1998) and to the innate technical challenges posed by the environment and that particular type of radiation measurements (Belzile et al., 2000). In our approach, we aimed at measuring and sampling during typical winter and summer situations at the sea-ice interface. A comparison with an open water scenario reported in Obermüller et al. (2005) yielded similar maximal surface irradiance values for UVB, i.e. 0.7 W^{-2} for our study and 0.8 W^{-2} to 1.2 W^{-2} for their study. Interestingly, we recorded under-ice irradiance values for UVB of up to 0.2 W^{-2} at 2 m and under ice, while they reached only 0.07 to 1.1 W^{-2} at 1 m in open water in a fjordic environment. Due to technical limitations, we could not record attenuation profiles at our ice stations. Therefore, we have to refer to Belzile et al. (2000) for $K_d(\lambda)$ values under similar sea-ice conditions. While Obermüller et al. (2005) calculated $K_d(\lambda)$ values of 0.97 m^{-1} and 0.79 m^{-1} in a fjordic

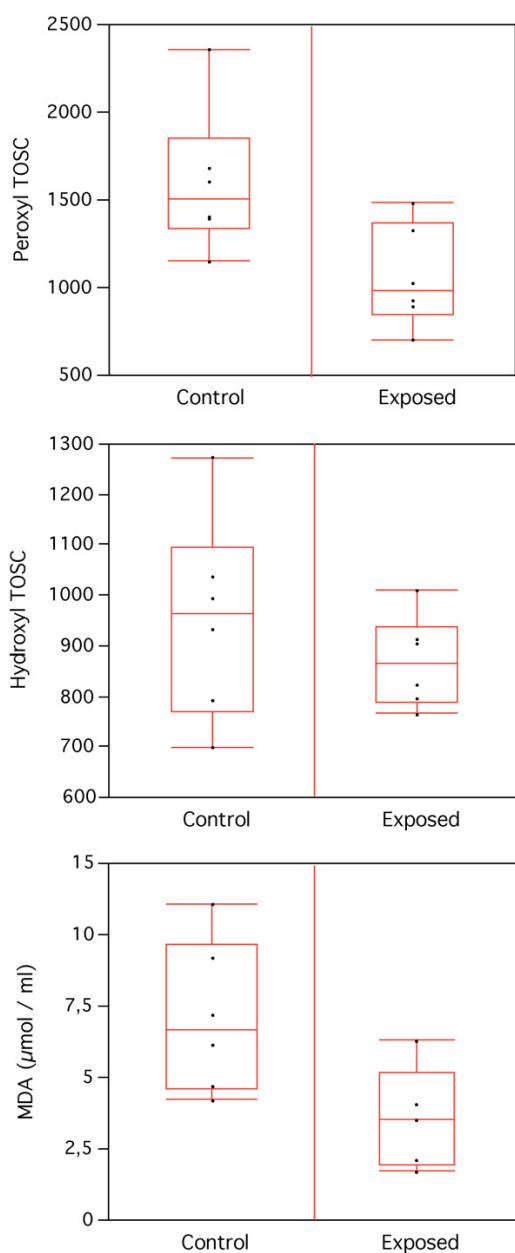


Fig. 4. Quantiles box plot of indirect lab exposure TOSC levels for peroxy (panel A) and hydroxyl (panel B), as well as MDA (panel C) for *G. wilkitzkii*. The box delimits the 25th and 75th percentile with the 10th and 90th percentile above and below, median in center.

environment, Belzile et al. (2000) obtained $K_d(\lambda)$ values between 0.4 m^{-1} to 0.7 m^{-1} under sea-ice. Conversely, the 1% depth for UVB is given as around 4 m in Obermüller et al. (2005) while it varied between 6 m and 12 m in Belzile et al. (2000). This leads us to believe that both our surface and under-ice values for UVR irradiance are reasonable and well in accordance with relevant previous studies.

4.2. Field samples

The summer values for both oxyradical scavenging parameters are on average 1.5 times higher than the winter values, which

may indicate a higher oxidative stress experienced during summer, and therefore a stronger need for antioxidant scavenging capacity (Fig. 2).

The MDA values show the same trend, with summer values significantly higher than winter values (see Fig. 2). This links well with the above mentioned observation and indicates a stronger stress and oxidative damage, expressed as lipid peroxidation, during summer conditions when the sea-ice cover is at its minimum and the impact of UVR is much stronger.

The comparison of the two amphipod species sampled in parallel during summer conditions yielded, not surprisingly, significant differences for all observed factors, as shown in Fig. 2. This is probably explained in the different life styles of the two species, with a carnivorous/herbivorous/detritivorous feeding style attributed to *G. wilkitzkii* (Scott et al., 2001; Werner et al., 2002), while *O. nanseni* is thought to be predominantly detritivorous/necrophagous (Arndt et al., 2005; Poltermann, 2001). Previous studies comparing TOSC assays in several amphipod species have argued similarly, although Camus and Gulliksen (2005) compared a deep-sea species (*Eurythenes gryllus*) and a sublittoral species (*Anonyx nugax*) to the sympagic *G. wilkitzkii* treated in this study. To the extent that the benthic lysianassoid scavenger *A. nugax* can be ecologically compared to the sympagic lysianassoid scavenger *O. nanseni*, the same reasoning could be applied. Also, this study found clearly higher values for both peroxy and hydroxyl TOSC in the lysianassoid *O. nanseni* than in gammarid *G. wilkitzkii*, in accordance to Camus and Gulliksen (2005) who also found a similar pattern in their exposure experiments for both control and exposed individuals, with *Anonyx* TOSC > *Gammarus* TOSC and peroxy > hydroxyl TOSC.

Interestingly, these authors hypothesized the presence of an adaptive mechanism in *G. wilkitzkii* that either prevents the diffusion of external H_2O_2 or facilitates the excretion of internal H_2O_2 . This might explain why *G. wilkitzkii* shows lower MDA values than *O. nanseni* while displaying lower field values of peroxy and hydroxyl TOSC, as demonstrated in Fig. 2.

4.3. Lab experiments—direct exposure

In the setup presented here, significantly lower levels were observed for the peroxy and hydroxyl TOSC in low- and high-intensity exposures, compared to the dark control (Fig. 3). This indicates that the exposed individuals experienced a significantly higher oxyradical stress than the control individuals. This observation fits well with previous studies where exposure to stressors resulted in significant reduction of TOSC values (Camus et al., 2004; Pampanin et al., 2005). The authors argued that such a decline in TOSC values was indicative of either a depletion of low molecular weight scavengers as shown by Regoli (2000), or alternatively an inhibition of antioxidant enzyme activities, demonstrated in Regoli and Principato (1995).

We found a significantly decreased MDA content (see Fig. 3) in samples from low-intensity experiments, while the levels from high-intensity experiments also were lower than the control, but not significantly. We assume that our control samples used in these lab exposures were comparable to the summer field samples in terms of MDA content, as they were sampled almost simultaneously, and indeed the values group in a similar range, with medians of about $3\text{--}5 \text{ } \mu\text{mol ml}^{-1}$. It appears that some factor in our laboratory experiments triggered a further decrease of MDA content in the exposed organisms. In a controlled UVR exposure study on benthic amphipods, Obermüller et al. (2005) found that the enzyme activity of superoxide dismutase (SOD) was significantly increased by short-term laboratory exposure in both *Gammarus homari* and *A. nugax*, while the enzyme activity of catalase (CAT) was significantly reduced, assumedly through photo-inhibition. On the other hand, MDA concentrations after 7 days of exposure (in that study

labelled “TBARS”) were in most cases lower in exposed than in control organisms, thus showing a similar trend as in our study of 5 days of exposure.

In order to address these observations, one has to allow that although some studies have found a good correlation between oxyradical stress levels, antioxidant enzymes or total scavenging capacity, and MDA content, these parameters are not directly linked. In most cases, there are other parameters affecting the outcome, as well as feedback mechanisms, for example between MDA and antioxidant enzymes, leading to more complex interactions. Also, there is a third factor that belongs into the equation of oxyradical “defence” (here measured as TOSC) and “damage” (here quantified as MDA), and that is “repair”. Our experiment was designed with UVR- and PAR-exposed amphipods, while the control animals were kept in near-darkness. The absence of irradiation might well have led to the absence of photoenzymatic repair (PER), while the irradiated individuals received both a stress from the shorter wavelengths of UVR, especially the UVB part (280–320 nm), but also activation of PER, in the UVA (320–400 nm) and PAR (400–700 nm) part of the experimental irradiance. So as the only obvious difference between control and UVR-exposed amphipods was the irradiation, the observed increase in MDA content would have to be attributed to some other stress, i.e. the absence of PER-inducing irradiation. However, since PER is effective towards cyclobutane pyrimidine dimers, a form of UVR-induced DNA damage where a pair of thymine or cytosine bases on the same DNA strand bind together, this does not directly relate to lipid peroxidation. Starvation as a stress factor affecting control individuals can be ruled out, since all animals were sampled, transferred and held in the experimental setup in an identical fashion and for an identical time span, which was well below starvation limits previously recorded in this species, which range in months (Werner et al., 2002).

4.4. Lab experiments—indirect exposure

One further intention of our lab exposure was to elucidate whether the UV radiation acts on the organisms themselves, inducing tissue damage as an internal process, or alternatively, whether the UV radiation acts on the sea water, inducing oxyradical formation which then act on the organisms contained in that water, thereby inducing tissue damage as an external process. This was addressed by the “water-only” exposure, where two sets of holding tanks were setup, of which the upper was without animals and the lower contained animals. The upper set of tanks was supplied by a constant flow of temperature-controlled sea water (set point 0 °C) with an overflow leading into the lower set of holding tanks. The upper set was then again exposed to high-intensity UV radiation, using the identical lamp array as previously in the direct exposures.

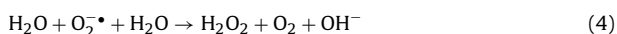
The “water-only” samples were again tested for significant differences in the two TOSC factors as well as in MDA content. Here a significantly lower peroxy TOSC could be detected in the exposed samples, but although the values for hydroxyl TOSC also appeared lower than those of the control samples, this difference was not significant (Fig. 4).

We consider these results as possible evidence for an exogenous production of ROS through UVR exposure of the sea water in the holding tanks. As Scully et al. (1995, 1996) showed, this is possible through the activation of dissolved organic carbon which reacts with molecular oxygen according to the simplified formula (after Cooper et al., 1994 in Scully et al., 1996):



where DOC^* represents activated dissolved organic carbon, $\text{DOC}^{*\bullet}$ represents peroxy radicals, and $\text{O}_2^{\bullet-}$ represents superoxide anions. Also the interaction of water molecules with superoxide anions can generate both hydroxyl (OH^\bullet) and hydrogen peroxide (H_2O_2) as in

Eq. 4:



A comparison of MDA content in control and exposed organisms again yielded a significant difference, with the values for the control significantly higher than those measured from the exposed samples (Fig. 4).

4.5. Methodological constraints

For the laboratory irradiance, we chose fluorescent tubes as a light source with a limited photoperiod of 4 h daily. Obviously, such a “on/off” simulation is very crude and inaccurate compared to the highly dynamic diurnal variation in light intensity, cloud cover, albedo, and spectral absorbance and transmission in sea water at different azimuth angles. Also, the sea-ice habitat in itself modifies the ambient light regime by its percentage of ice cover, ice thickness, snow cover on top of ice floes, released sediment and plankton particles, which together create a complex system acting on the under-ice light field. A further technical limitation was set by the radiation source, which was in this case chosen to consist of fluorescent lamps, since they have a near-natural output of UV radiation in both intensity and spectral distribution. However, this is only true in the UVB and UVA range of their output, while the emission in the PAR range is very low in comparison to the natural spectrum.

Due to the limited amount of samples, we were not able to perform analyses of other parameters like SOD or CAT. We are therefore not in a position to discuss the contribution of these individual enzymes to the end result. It would also have been desirable to take more samples at several time intervals, p.e. after each exposure day, in order to gain a better temporal resolution of the dynamics of antioxidant capacity and MDA content. However, due to the limited availability of sample organism, this was impossible in the present study.

Finally, the motility of the organisms in their complex and three-dimensional natural environment further complicates an accurate simulation of total radiation levels experienced by a sympagic amphipod during the diurnal cycle.

Another thing to be taken into consideration was the light regime for the dark control groups for both direct and indirect exposures. We chose near-darkness for these organisms, which was also identical to the “ground state” for the exposed organisms outside their daily 4 h-exposure period. This background level of PAR intensity could have been regulated in a way to supply a stronger PAR dosage, which might have avoided the “dark stress” problem that apparently dominates the trend in MDA levels.

5. Conclusion

We showed clear differences between summer and winter in TOSC and MDA values for the sympagic gammarid amphipod *G. wilkitzkii*, with significantly higher values for the summer situation, where presumably the oxidative stress levels are much higher than during winter, when UVR is completely absent from the habitat. We also presented a first set of baseline data for the sympagic lysianasoid amphipod *O. nanseni*, which shows a significantly higher level of TOSC than *G. wilkitzkii*. A series of UVR exposure experiments showed clear oxyradical scavenging depletion effects under both direct and indirect UVR exposure of *G. wilkitzkii*.

Acknowledgements

We would like to thank the UNIS logistics department as well as the captain and crew of R/V Jan Mayen for their excellent technical

support of our fieldwork in the sea-ice around Svalbard. Also, we owe thanks to Steinar Sanni and Kjell-Birger Øysæd for their relentless support during laboratory analyses at IRIS-Akvamiljø. The first author was fully supported by grants no. WE 2536/6-1 to . . . /6-3 of the Deutsche Forschungsgemeinschaft (DFG) for this work.

References

- Arndt, C., Berge, J., Brandt, A., 2005. Mouthpart-atlas of Arctic sympagic amphipods – trophic niche separation based on mouthpart morphology and feeding ecology. *J. Crust. Biol.* 25, 401–412.
- Belzile, C., Johannessen, S., Gosselin, M., Demers, S., Miller, W., 2000. Ultraviolet attenuation by dissolved and particulate constituents of first-year ice during late spring in an Arctic polynya. *Limnol. Oceanogr.* 45, 1265–1273.
- Bradford, M.M., 1976. Rapid and sensitive method for quantitation of microgram quantities of protein utilizing principle of protein-dye binding. *Anal. Biochem.* 72, 248.
- Browman, H., Rodriguez, C., Beland, F., Cullen, J., Davis, R., Kouwenberg, J., Kuhn, P., McArthur, B., Runge, J., St-Pierre, J.-F., Vetter, R., 2000. Impact of ultraviolet radiation on marine crustacean zooplankton and ichthyoplankton: a synthesis of results from the estuary and gulf of St. Lawrence, Canada. *Mar. Ecol. Prog. Ser.* 199, 293–311.
- Browman, H., Vetter, R., Rodriguez, C., Cullen, J., Davis, R., Lynn, E., St. Pierre, J., 2003. Ultraviolet (280–400 nm)-induced DNA damage in the eggs and larvae of *Calanus finmarchicus* G. (Copepoda) and Atlantic Cod (*Gadus morhua*). *Photochem. Photobiol.* 77, 397–404.
- Camus, L., Birkely, S., Jones, M., Børseth, J., Grøsvik, B., Gulliksen, B., Lønne, O., Regoli, F., Depledge, M., 2003. Biomarker responses and PAH uptake in *Mya truncata* following exposure to oil-contaminated sediment in an Arctic fjord (Svalbard). *Sci. Total Environ.* 308, 221–234.
- Camus, L., Gulliksen, B., 2004. Total oxyradical scavenging capacity of the deep-sea amphipod *Eurythenes gryllus*. *Mar. Environ. Res.* 58, 615–618.
- Camus, L., Gulliksen, B., 2005. Antioxidant defense properties of Arctic amphipods: comparison between deep-, sublittoral and surface-water species. *Mar. Biol.* 146, 355–362.
- Camus, L., Pampanin, D., Volpato, E., Delaney, E., Sanni, S., Nasci, C., 2004. Total oxyradical scavenging capacity responses in *Mytilus galloprovincialis* transplanted into the Venice lagoon (Italy) to measure the biological impact of anthropogenic activities. *Mar. Pollut. Bull.* 49, 801–808.
- Cooper, W.J., Shao, C., Lean, D.R.S., Gordon, A.S., Scully Jr., F.E., 1994. Factors affecting the distribution of H₂O₂ in surface waters. *Adv. Chem. Ser. vol. 237 pp.* 391–422.
- Corsolini, S., Nigro, M., Olmastroni, S., Focardi, S., Regoli, F., 2001. Susceptibility to oxidative stress in Adélie and emperor penguin. *Polar Biol.* 24, 365–368.
- Davenport, J., Healy, A., Casey, N., Heffron, J., 2004. Diet-dependent UVAR and UVBR resistance in the high shore harpacticoid copepod *Tigriopus brevicornis*. *Mar. Ecol. Prog. Ser.* 276, 299–303.
- Di Giulio, R., Washburn, P., Wenning, R., 1989. Biochemical responses in aquatic animals: a review of determinants of oxidative stress. *Environ. Toxicol. Chem.* 8, 1103–1123.
- Fernández, J., Pérez-Álvarez, J., Fernández-López, J., 1997. Thiobarbituric acid test for monitoring lipid oxidation in meat. *Food Chem.* 59, 345–353.
- Grad, G., Williamson, C., Karapelou, D., 2001. Zooplankton survival and reproduction responses to damaging UV radiation: a test of reciprocity and photoenzymatic repair. *Limnol. Oceanogr.* 46, 584–591.
- Gulliksen, B., Lønne, O., 1989. Distribution, abundance, and ecological importance of marine sympagic fauna in the Arctic. *Rapp. P-V Reun. Cons. Int. Explor. Mer.* 188, 133–138.
- Häder, D., Kumar, H., Smith, R., Worrest, R., 1998. Effects on aquatic ecosystems. *J. Photochem. Photobiol. B: Biol.* 46, 53–68.
- Hessen, D., 1996. Competitive trade-off strategies in arctic *Daphnia* linked to melanism and uv-b stress. *Polar Biol.* 16, 573–579.
- Hessen, D., Borgeraas, J., Ørbæk, J., 2002. Responses in pigmentation and anti-oxidant expression in arctic *Daphnia* along gradients of doc and uv exposure. *J. Plankton Res.* 24, 1009–1017.
- Karentz, D., Bosch, I., 2001. Influence of ozone-related increases in ultraviolet radiation on antarctic marine organisms. *Am. Zool.* 41, 3–16.
- Karentz, D., Bosch, I., Mitchell, D., 2004. Limited effects of Antarctic ozone depletion on sea urchin development. *Mar. Biol.* 145, 277–292.
- Karentz, D., Lutze, L., 1990. Evaluation of biologically harmful ultraviolet radiation in antarctica with a biological dosimeter designed for aquatic environments. *Limnol. Oceanogr.* 35, 549–561.
- Kepner, R., Wharton, R., Collier, R., Cockell, C., Jeffrey, W., 2000. UV radiation and potential biological effects beneath the perennial ice cover of an antarctic lake. *Hydrobiologia* 427, 155–165.
- Kerr, J., McElroy, C., 1993. Evidence for large upward trends of ultraviolet-B radiation linked to ozone depletion. *Science* 262, 1032–1034.
- Lacuna, D., Uye, S.-I., 2001. Influence of mid-ultraviolet (UVB) radiation on the physiology of the marine planktonic copepod *Acartia omorii* and the potential role of photoreactivation. *J. Plankton Res.* 23, 143–155.
- Lesser, M., 2006. Oxidative stress in marine environments: biochemistry and physiological ecology. *Annu. Rev. Physiol.* 68, 253–278.
- Livingstone, D., 2001. Contaminant-stimulated reactive oxygen species production and oxidative damage in aquatic organisms. *Mar. Pollut. Bull.* 42, 656–666.
- Lønne, O., Gulliksen, B., 1989. Size, age and diet of polar cod, *Boreogadus saida* (Lep-echin 1773), in ice covered waters. *Polar Biol.* 9, 187–191.
- Madronich, S., McKenzie, R., Björn, L., Caldwell, M., 1998. Changes in biologically active ultraviolet radiation reaching the Earth's surface. *J. Photochem. Photobiol. B: Biol.* 46, 5–19.
- Marnett, L., 1999. Lipid peroxidation – DNA damage by malondialdehyde. *Mutat. Res.* 424, 83–95.
- McCord, J., Fridovich, I., 1969. Superoxide dismutase – an enzymatic function for erythrocyte (hemocuprein). *J. Biol. Chem.* 244, 6049–6055.
- Obermüller, B., Karsten, U., Abele, D., 2005. Response of oxidative stress parameters and sunscreens compounds in arctic amphipods during experimental exposure to maximal natural uvb radiation. *J. Exp. Mar. Biol. Ecol.* 323, 100–117.
- Pampanin, D., Camus, L., Gomiero, A., Maragon, I., Volpato, E., Nasci, C., 2005. Susceptibility to oxidative stress of mussels (*Mytilus galloprovincialis*) in the Venice Lagoon (Italy). *Mar. Pollut. Bull.* 50, 1548–1557.
- Perovich, D., Roesler, C., Pegau, W., 1998. Variability in arctic sea ice optical properties. *J. Geophys. Res.* 103, 1193–1208.
- Poltermann, M., 2000. Growth, production and productivity of the Arctic sympagic amphipod *Gammarus wilkitzkii*. *Mar. Ecol. Prog. Ser.* 193, 109–116.
- Poltermann, M., 2001. Arctic sea ice as feeding ground for amphipods – food sources and strategies. *Polar Biol.* 24, 89–96.
- Poltermann, M., Hop, H., Falk-Petersen, S., 2000. Life under Arctic sea ice – reproduction strategies of two sympagic (ice-associated) amphipod species, *Gammarus wilkitzkii* and *Apherusa glacialis*. *Mar. Biol.* 136, 913–920.
- Regoli, F., 2000. Total oxyradical scavenging capacity (tosc) in polluted and translocated mussels: a predictive biomarker of oxidative stress. *Aquat. Toxicol.* 50, 351–361.
- Regoli, F., Gorbi, S., Frenzilli, G., Nigro, M., Corsi, I., Focardi, S., Winston, G., 2002a. Oxidative stress in ecotoxicology: from the analysis of individual antioxidants to a more integrated approach. *Mar. Environ. Res.* 54, 419–423.
- Regoli, F., Nigro, M., Benedetti, M., Fattorini, D., Gorbi, S., 2005. Antioxidant efficiency in early life stages of the Antarctic silverfish, *Pleuragramma antarcticum*: responsiveness to pro-oxidant conditions of platelet ice and chemical exposure. *Aquat. Toxicol.* 75, 43–52.
- Regoli, F., Nigro, M., Bompadre, S., Winston, G., 2000. Total oxidant scavenging capacity (TOSC) of microsomal and cytosolic fractions from Antarctic, Arctic and Mediterranean scallops: differentiation between three potent oxidants. *Aquat. Toxicol.* 49, 13–25.
- Regoli, F., Nigro, M., Chiantore, M., Winston, G., 2002b. Seasonal variations of susceptibility to oxidative stress in *Adamussium colbecki*, a key bioindicator species for the Antarctic marine environment. *Sci. Total Environ.* 289, 205–211.
- Regoli, F., Principato, G., 1995. Glutathione, glutathione-dependent and antioxidant enzymes in mussel, *Mytilus galloprovincialis*, exposed to metals under field and laboratory conditions: implications for the use of biochemical biomarkers. *Aquat. Toxicol.* 31, 143–164.
- Regoli, F., Winston, G., 1998. Applications of a new method for measuring the total oxyradical scavenging capacity in marine invertebrates. *Mar. Environ. Res.* 46, 439–442.
- Regoli, F., Winston, G., 1999. Quantification of total oxidant scavenging capacity of antioxidants for peroxynitrite, peroxy radicals, and hydroxyl radicals. *Toxicol. Appl. Pharmacol.* 156, 96–105.
- Rocco, V., Oppezzo, O., Pizarro, R., Sommaruga, R., Ferraro, M., Zagarese, H., 2002. Ultraviolet damage and counteracting mechanisms in the freshwater copepod *Boeckella poppei* from the antarctic peninsula. *Limnol. Oceanogr.* 47, 829–836.
- Scott, C., Falk-Petersen, S., Gulliksen, B., Lønne, O.-J., Sargent, J., 2001. Lipid indicators of the diet of the sympagic amphipod *Gammarus wilkitzkii* in the marginal ice zone and in open waters of Svalbard (Arctic). *Polar Biol.* 24, 572–576.
- Scully, N., Lean, D., McQueen, D., Cooper, W., 1995. Photochemical formation of hydrogen peroxide in lakes: effects of dissolved organic carbon and ultraviolet radiation. *Can. J. Fish. Aquat. Sci.* 52, 2675–2681.
- Scully, N., McQueen, D., Cooper, W., Lean, D., 1996. Hydrogen peroxide formation: the interaction of ultraviolet radiation and dissolved organic carbon in lake waters along a 43–75 degree N gradient. *Limnol. Oceanogr.* 41, 540–548.
- Steele, D., Steele, V., 1975. The biology of *Gammarus* (Crustacea, Amphipoda) in the northwestern Atlantic. ix. *Gammarus wilkitzkii* Birula, *Gammarus stoerensis* Reid, and *Gammarus mucronatus* Say. *Can. J. Zool.* 53, 1105–1109.
- Werner, I., 1997. Grazing of Arctic under-ice amphipods on sea-ice algae. *Mar. Ecol. Prog. Ser.* 160, 93–99.
- Werner, I., 2000. Faecal pellet production by Arctic under-ice amphipods – transfer of organic matter through the ice/water interface. *Hydrobiologia* 426, 89–96.
- Werner, I., Auel, H., Friedrich, C., 2002. Carnivorous feeding and respiration of the Arctic under-ice amphipod *Gammarus wilkitzkii*. *Polar Biol.* 25, 523–530.
- Winston, G., Di Giulio, R., 1991. Prooxidant and antioxidant mechanisms in aquatic organisms. *Aquat. Toxicol.* 19, 137–161.
- Winston, G., Regoli, F., Dugas, A., Fong, J., Blanchard Jr., K., 1998. A rapid gas chromatographic assay for determining oxyradical scavenging capacity of antioxidants and biological fluids. *Free Radic. Biol. Med.* 24, 480–493.

Paper 2

Fuhrmann, M.M., Nygård, H., Krapp, R.H., Berge, J. & Werner, I. (2011).

The adaptive significance of chromatophores in the Arctic under-ice amphipod *Apherusa glacialis*

Polar Biology, 34, 823–832.

The adaptive significance of chromatophores in the Arctic under-ice amphipod *Apherusa glacialis*

Mona M. Fuhrmann · Henrik Nygård ·
Rupert H. Krapp · Jørgen Berge · Iris Werner

Received: 28 September 2010 / Revised: 24 November 2010 / Accepted: 29 November 2010
© The Author(s) 2010. This article is published with open access at Springerlink.com

Abstract Solar radiation is a crucial factor governing biological processes in polar habitats. Containing harmful ultraviolet radiation (UVR), it can pose a threat for organisms inhabiting surface waters of polar oceans. The present study investigated the physiological color change in the obligate sympagic amphipod *Apherusa glacialis* mediated by red-brown chromatophores, which cover the body and internal organs of the species. Short-term experimental exposure to photosynthetic active radiation (PAR) led to pigment dispersal in the chromatophores, resulting in darkening of the animal. Irradiation in the PAR range (400–700 nm) was identified as the main trigger with high light intensities evoking marked responses within 15 min. After exposure to high PAR, darkness led to a slow aggregation of pigments in the cell center after 24 h. Experiments revealed no statistically significant change in coloration of the animal when exposed to different background colors nor UV radiation. Our results point to a dose- and time-dependent photoprotective role of chromatophores in the amphipod, presuming a shielding effect from harmful radiation in a dispersed state. The reversible nature

of the physiological color change enables the species to adapt dynamically to prevailing light conditions and thereby minimize the cost of increased conspicuousness toward visually hunting predators.

Keywords Photoprotection · Ultraviolet radiation · Color change · Sympagic · *Apherusa glacialis* · Chromatophores · Sea ice fauna · Svalbard · Arctic

Introduction

Chromatophores are pigment cells, through which a relatively fast physiological color change of the organism can take place. Crustacean chromatophores are generally regarded to serve one or more of the following functions: photoprotection, crypsis, or thermoregulation. In photoprotection, the chromatophores are used as shields protecting the animal or sensitive organs against harmful radiation (Miner et al. 2000; Auerswald et al. 2008), such as ultraviolet radiation (UVR), that can damage biological macromolecules like DNA (Malloy et al. 1997). Crypsis is a type of camouflage, where blending into the background reduces the risk of being detected by predators. This is achieved by matching the body color to the background color or using disruptive coloration patterns that break up the body outline and create false boundaries (Stevens and Merilaita 2009). Thermoregulation is mainly occurring among semiterrestrial species inhabiting the tidal zone where diurnal and seasonal changes in the temperature regime are significant (Willmer et al. 1989; Noël and Chassard-Bouchaud 2004). As darker color absorbs more light, and thus heat, the dispersion or contraction of pigments in the chromatophores can help animals control their body temperature. The role of chromatophores as

M. M. Fuhrmann · H. Nygård (✉) · R. H. Krapp · J. Berge
University Centre in Svalbard, 9171 Longyearbyen,
Norway
e-mail: henrik.nygard@unis.no

M. M. Fuhrmann · R. H. Krapp · I. Werner
Institute for Polar Ecology, University of Kiel,
24148 Kiel, Germany

M. M. Fuhrmann · H. Nygård
Faculty of Biosciences, Fisheries and Economics,
University of Tromsø, 9037 Tromsø, Norway

J. Berge
Akvaplan-niva, 9296 Tromsø, Norway

thermoregulator is not considered as probable for purely aquatic species (Nöel and Chassard-Bouchaud 2004).

The Arctic amphipod *Apherusa glacialis* is autochthonous to the sympagic habitat fulfilling the life cycle there (Lønne and Gulliksen 1991; Poltermann et al. 2000). The ability of the species to cope with the seasonality and the extreme environmental conditions on the underside of the ice enables it to thrive there during all seasons (Werner 2006; Kiko et al. 2009). It prefers smooth, flat ice and is aggregated at places with high algal biomass such as ice edges and thin ice (Lønne and Gulliksen 1991; Hop et al. 2000). During a cruise to the pack ice north of Svalbard, Norway in 2007, we noted a high variation in the color appearance of sampled *A. glacialis*, and that their color changed after some time. The color change was found to be caused by a dispersion (resulting in darker appearance) or aggregation (resulting in lighter appearance) of pigments in the chromatophores arranged along the body of the amphipod. Based on in situ observations by divers (Berge 2007), the amphipods had a dark appearance on the edges of ice floes, whereas most had a lighter appearance further in under the ice floe (Fig. 1).

In the sea ice environment, conditions are highly variable on both temporal and spatial scales, which make the ability to adapt thereafter advantageous. Chromatophores offer a possibility to adapt to environmental variation with a short response-time. Functions that seem plausible as triggers of the color change in *A. glacialis* are photoprotection and crypsis, since the stable temperature regime in the ice–water interface is unlikely to evoke any compensation for physiological thermoregulation mediated through the chromatophores. Solar radiation is highly seasonal in polar environments, and during the polar summer, the animals are exposed to continuous light (of varying intensity) for a period of up to 6 months. Due to depletion of ozone in polar areas (Kerr and McElroy 1993; Müller et al. 1997), the incoming UVR reaches biologically harmful levels (Madronich et al. 1998) that can penetrate

down to 20–30 water depth (Karentz and Lutze 1990). Harmful effects of UVR have been documented for various organisms, including polar crustaceans (Malloy et al. 1997; Obermüller et al. 2005; Ban et al. 2007; Krapp et al. 2009). Even though factors like low sun angle, clouds, snow and ice cover and thickness, and particles incorporated in the ice reduce the light intensity penetrating to the underside of the ice, harmful levels of UVR have been recorded under the ice. For example, Lesser et al. (2004) linked mortality and DNA damage in sea urchin larvae in the water below 2- to 3-m-thick first-year ice (FYI) to UVB transmittance through the ice. Thus, it seems realistic to propose photoprotection as a reason for the physiological color change in *A. glacialis*, which thrives under FYI and close to ice floe edges.

Background adaptation has been found in several crustacean species (Fingerman 1965, 1970; Johnson 1974; Willmer et al. 1989) and represents one of the most common methods of crypsis (Endler 2006; Stevens 2007). During the bloom of ice algae and at locations where detritus has aggregated or sediments are incorporated in the ice, the underside of the ice is patchy in color (Werner and Lindemann 1997). An ability to adapt to the different background shades could prevent detection by visual predators such as polar cod (*Boreogadus saida*), making crypsis an advantageous reason for color change in *A. glacialis*.

The aim of this study was to investigate the role and use of chromatophores in *A. glacialis*. Hence, we designed an experimental setup to examine the above-described predictions. Based upon our field observations, we hypothesize that physiological color change is an adaptive trait in this species. In the experiments, the following questions were addressed: (1) Are the animals responding differently to light exposures with different intensities or wavelengths? A stronger response to higher intensity or UVR could indicate photoprotection. (2) Are the animals responding to different background shades? An adjustment of the body coloration depending on the background shade



Fig. 1 Under-ice photographs taken in September 2009 at the edge of an ice floe (a) and at 15-m distance from the edge underneath the ice (b). Note the different color shade of the animals due to a difference

dispersion of pigments within the chromatophores. Size of animals approximately 7 mm. Photographed by Erling Svensen

could indicate crypsis. (3) Can thermoregulation be excluded as a reason for the color change? The temperature variations are rather small in the ice–water interface, and therefore a thermoregulatory function of the chromatophores is regarded unlikely, but if present, thermoregulation should result in aggregation of pigments at elevated temperature.

Materials and methods

Experimental animals

The experimental animals were sampled September 1–2, 2008, and September 3, 2009, during cruises with RV *Jan Mayen* to the pack ice north of Svalbard, Arctic Ocean (station coordinates: 81.05°N, 14.54°E; 81.15°N, 13.12°E). The animals were collected by SCUBA divers using both hand-held nets (0.5-mm mesh) and an electric suction pump (Lønne 1988). *Apherusa glacialis* were immediately separated from other amphipods and maintained in a climate chamber on-board the ship where they were reared in aquaria until arrival in Longyearbyen, Svalbard 7 days later. In Longyearbyen, the animals were transferred to The University Centre in Svalbard (UNIS), where they were reared in a cold cabinet at a temperature of $0 \pm 1^\circ\text{C}$. Water was exchanged once a week during the rearing. Food was provided 2–3 times per week and consisted of cultivated ice algae (monoculture of *Thalassiosira gravida* or field extractions of ice algae) frozen into small ice blocks. Molting was observed occasionally, evidenced by exuviae found in the tanks. Animals for the experiments were picked out randomly. The mean size of the experimental animals was 6.5 mm (range 4.0–13.2 mm) and consisted of two cohorts. No sex determination was done. All experiments took place at UNIS during daytime, and all animals used in the study ($n = 64$) were adapted to darkness for a minimum of 24 h prior to the experiments.

Chromatophore index (CI)

In order to document the color change, digital images were taken before and after the treatments, and, depending on

treatment, also during the exposures. For the photographing, animals were placed in a drop of sea water on a pre-cooled petri dish under a Leica MZ 9.5 stereomicroscope equipped with a Sony HDR-HC7R video camera with still photo recording mode, or a Nikon D300 equipped with a Tamron 90 mm/f2.8 macro lens was used. The whole procedure was limited to a few seconds, after which the animals were placed back in the experimental jar. No change in CI was detected during this procedure.

To quantify the chromatophoric response from the pictures, a chromatophore index (CI) was established based on Hogben and Slome (1931), on a scale from 1 (pigment maximally concentrated) to 5 (pigment maximally dispersed; Fig. 2). For the picture analyses, three chromatophores, located on the first, second, and third segment of the pleon, were chosen. The reasons for choosing these were as follows: (1) they were almost always present, (2) the contrast between the chromatophore and the body tissue was good, and (3) adjacent chromatophores did not merge when expanded and therefore could be analyzed individually. If different stages were observed in the three chromatophores, the mean value was given as the CI of the individual.

Experiments

PAR exposure

Experimental irradiation in the PAR range was provided by a 14-W fluorescent tube (Philips Master TL5 HE). Light intensity was measured using a cosine-corrected flathead sensor (LICOR Quantum Li190SA), measuring the photosynthetic photon flux density (PPFD) in the range of PAR (400–700 nm). Measures were recorded in air, and the light intensity was regulated by adjusting the height of the lamp to the experimental jars. Two exposure treatments were established, being low PPFD ($33\text{--}34 \mu\text{mol m}^{-2} \text{s}^{-1}$; 35-cm distance) and high PPFD ($300\text{--}400 \mu\text{mol m}^{-2} \text{s}^{-1}$; 15-cm distance), respectively. In the experimental setup, specimens of *A. glacialis* were put in small glass jars (5 cm in diameter, 60 ml seawater) placed on an ice bath to keep the temperature low. Two individuals, which could be distinguished by different size, were put in each jar. Exposure

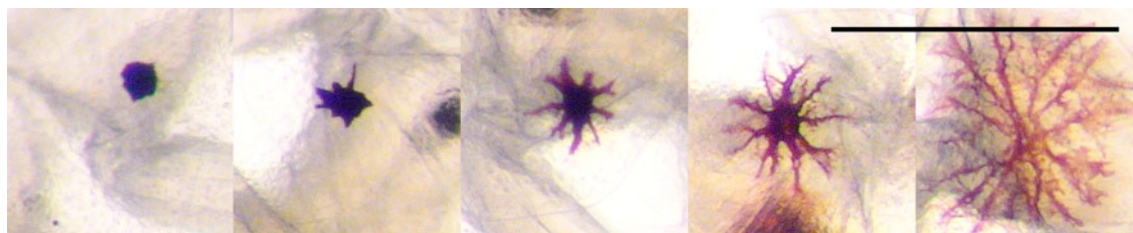


Fig. 2 Chromatophore index (CI) from 1 to 5 of representatively selected pigment cells from the pleon of *Apherusa glacialis*. Scale bar = 1 mm

time was set to 60 min (low PPFD treatment) and 45 min (high PPFD treatment), respectively. Chromatophore response was recorded before the start of exposure and at intervals of 15 min thereafter.

To test the reversibility of the response, amphipods were exposed to $350\text{--}500\ \mu\text{mol m}^{-2}\ \text{s}^{-1}$ for 180 min and then put into darkness for 24 h. The chromatophoric response was recorded before and after exposure and in intervals during the darkness treatment.

UVR exposure

Irradiation in the UVR range was provided by a 400-W high-pressure lamp (Osram, HQI-BT), with an emission spectrum close to sun light, containing wavelengths in the UV spectrum (280–380 nm) as well as in the PAR range (with a peak at 540 nm). At a distance of 70 cm, the lamp emitted $114 \pm 2\ \mu\text{mol m}^{-2}\ \text{s}^{-1}$ in the PAR range and $2\text{--}3\ \text{W m}^{-2}$ in the UV range. This intensity can be expected under thin ice where *A. glacialis* is most commonly found (Hop et al. 2000), as Hanelt et al. (2001) measured atmospheric intensities of UVR up to $16.8\ \text{W m}^{-2}$ in Kongsfjorden, Svalbard, and Belzile et al. (2000) report a transmittance of 5–19% UVA and 2–13% UVB through 0.5- to 1.3-m-thick FYI. Additionally, in situ measurements of UVR under multi-year sea ice in September 2005, at a similar latitude as where the experimental animals were sampled, show intensities up to $0.18\ \text{W m}^{-2}$ (Fig. 3). UVR was measured using a UV-meter (UV-IR-Technology, 250–410 nm). Two amphipods, distinguished by size, were put in plastic aquaria (6 l volume) filled with seawater up to 10 cm. A control

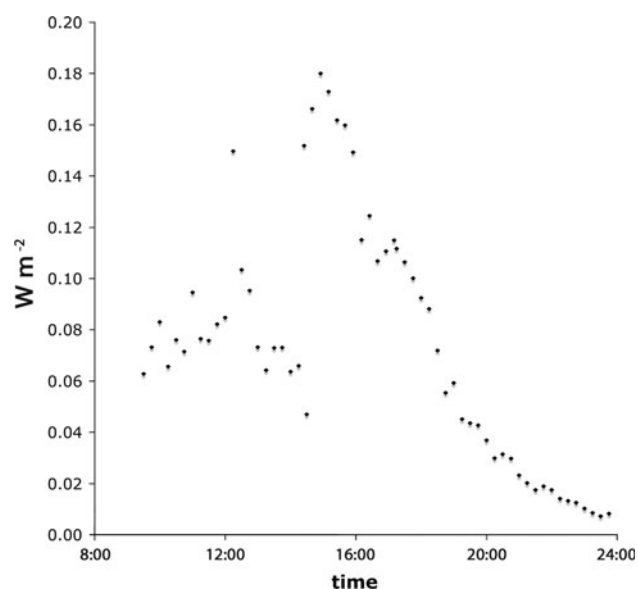


Fig. 3 Diurnal variation in UVR measured under multi-year sea ice in September 2005

was performed by placing a polycarbonate sheet (Lexan) over the aquaria to cut off the UV wavelengths. The aquaria were placed 70 cm under the UV-lamp and exposed for 30 min. The polycarbonate sheet slightly altered the intensity in the PAR range from 114 ± 2 to $107 \pm 2\ \mu\text{mol m}^{-2}\ \text{s}^{-1}$ PPFD.

Background experiments

In order to study the influence of different backgrounds on the chromatophores, a setup with light and dark backgrounds was established. Specimens of *A. glacialis* were kept in 200-ml plastic jars containing seawater in a cooling cabinet (0°C). The jars were covered with white or black plastic from the outside leaving the top open. Control specimens were collected by covering the jars with aluminum foil shielding them from any light. Illumination in the cooling cabinet was provided from the inbuilt fluorescent tube, with an intensity varying between 30 and $35\ \mu\text{mol m}^{-2}\ \text{s}^{-1}$ PPFD. Chromatophore response was recorded at start, after 24, and 48 h.

Temperature experiments

The influence of temperature on chromatophores was investigated by exposing experimental animals to increasing temperatures from 0 to 8°C for various intervals in glass jars (200 ml) containing seawater. This was achieved by leaving the experimental jars at room temperature and allowing the water to heat up slowly. Pictures of the animals were taken at 0 , 2 , 4 , 6 , and 8°C (accuracy $\pm 0.5^{\circ}\text{C}$) under the stereomicroscope. All experiments were carried out in darkness (apart from short interruptions in order to take photographs) by covering the jars with aluminum foil. Water temperature was monitored using a core thermometer (Ebro TFX 410).

Statistical analyses

Statistical analyses were carried out using the software package Statistica 7. Nonparametric tests (Mann–Whitney U test and Kruskal–Wallis test for independent samples; Wilcoxon Signed-Rank tests and Friedman’s tests for dependent samples) were applied, since the sample size was low and requirements for a normal distribution were not met in most cases. Statistical significance was accepted at $P < 0.05$. Multiple comparisons following a Friedman’s test were corrected using the Bonferroni–Holm adjustment for multiple P -levels. Results are expressed as means with the standard deviation or medians with standard errors. Change in the CI was calculated by subtracting the initial stage from the observed stage after each interval of exposure.

Results

Arrangement of chromatophores

Chromatophores were present in various body regions of *A. glacialis*. The chromatophores on the pleon used in the analyses were arranged superficially, one on each side on all three segments. On the pereon, profound chromatophores were arranged in lateral rows on each side (usually one cell per segment), covering internal organs laterally, but leaving a gap on the dorsal side (Fig. 1). Assemblages of chromatophores around the brain were present in most specimens and mouthparts seemed to carry chromatophores too. Occasionally, chromatophores were also found on the appendages or other body parts.

Experiments

PAR exposure

A. glacialis responded to visible light in the PAR range by dispersing pigments within the chromatophores, depending on light intensity and exposure time. Figure 4 shows the dispersion of pleon chromatophores of an experimental

animal exposed to the high-light treatment from CI 1 to stage 4 after 45 min. Chromatophores on the rest of the body generally responded in the same way to the light treatment.

High-intensity light treatments evoked a significant increase in the CI of experimental animals after only 15 min of exposure (Paired Wilcoxon Signed-Rank test, $P < 0.01$). After 30 min, all animals had a CI higher than 2, and after 45 min, the mean increase in CI was 1.7. The low-intensity light treatment did not result in significant change of the CI (Fig. 5) even after an exposure time of 60 min. Multiple Mann–Whitney U tests using the Bonferroni–Holm adjustment showed significant differences in the change of CI between low- and high-light treatment for each time interval (15, 30, 45 min; $P < 0.01$).

In the experiment, to study the reversibility of the response, a significant increase in CI (Wilcoxon Signed-Rank test, $P = 0.01$), from 1.6 initially to 3.6 after 180-min exposure to PAR, was observed. The subsequent dark adaptation caused aggregation of the pigments (Fig. 6), but at 240 and 360 min (60 and 180 min after put into darkness), the CI still differed significantly from the starting value. After 24 h in darkness, the CI had decreased to 2.8, which was insignificant to the initially recorded CI of 1.6

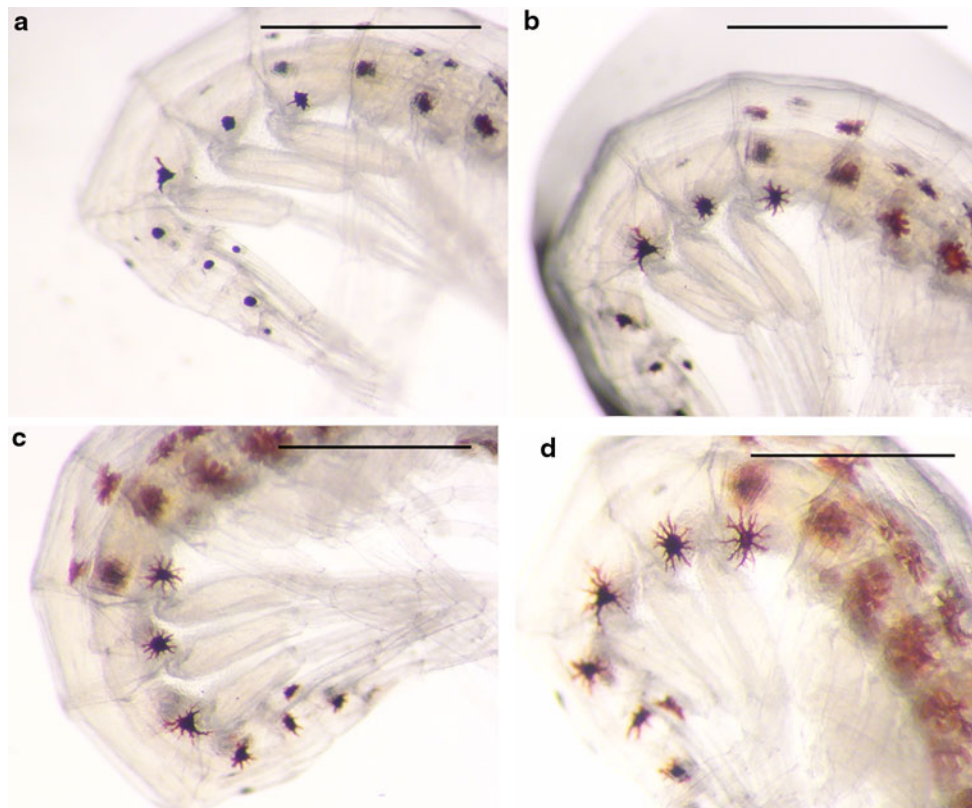


Fig. 4 Pigment dispersion in chromatophores of *Apherusa glacialis* before (a) and after exposure to PAR ($300\text{--}400\ \mu\text{mol m}^{-2}\ \text{s}^{-1}$) for 15 min (b), 30 min (c), and 45 min (d). Scale bars = 1 mm

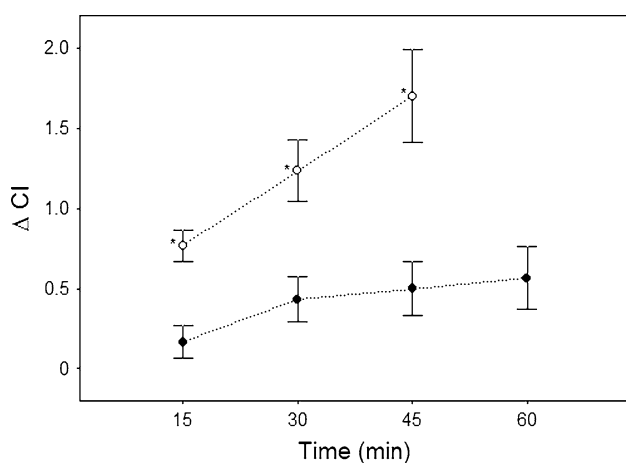


Fig. 5 Time course of the change in the chromatophore index (CI) after exposure to a high and low light intensity: *open circles*, 300–400 $\mu\text{mol m}^{-2} \text{s}^{-1}$; *filled circles*, 33–34 $\mu\text{mol m}^{-2} \text{s}^{-1}$. Data expressed as means \pm SE ($n = 10$). *Significantly different from the low-light treatment ($P < 0.01$, Multiple Mann–Whitney U tests using Bonferroni–Holm adjustment)

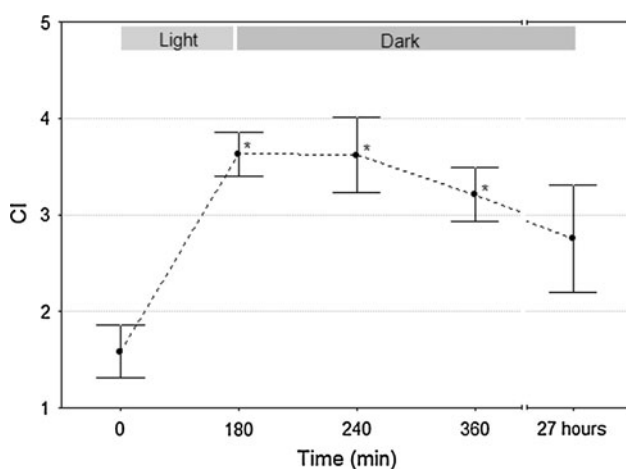


Fig. 6 Development of the chromatophore index (CI) after experimental animals were exposed to high light intensities (350–500 $\mu\text{mol m}^{-2} \text{s}^{-1}$) for 180 min and then put back in darkness. Values are means, *error bars* denote the SE ($n = 8$). *Statistically different compared to initial CI (0 min) ($P < 0.05$, Wilcoxon Signed-Rank tests)

(Wilcoxon Signed-Rank test, $P = 0.13$). Thus, pigment aggregation in the chromatophores occurred clearly more slowly than had dispersion at high light intensities.

UVR exposure

The exposure to UV wavelengths in addition to PAR also caused pigment dispersion in chromatophores in *A. glacialis*. The change in CI after 30 min was greater in the UVR treatment (0.9) than in the control (0.5), but no

statistical difference was observed (Mann–Whitney U test, $P = 0.08$; see Table 1). Note that the sample size in the control group was smaller ($n = 10$) than in the UVR treatment group ($n = 16$).

Background and temperature experiments

A. glacialis did not show any background matching behavior mediated by chromatophores. Both on white and black backgrounds, the CI increased slightly (0.4 and 0.3, respectively, after 24 h), but no difference was found between the treatments (Mann–Whitney U tests, $P = 0.46$). Only in the treatment with white background, a significant change in CI, compared to the control, was observed after 24 h (Wilcoxon Signed-Rank test, $P = 0.04$; see Table 1).

Higher temperatures led to a slight dispersal of pigments in chromatophores in *A. glacialis*. An increase in the mean CI of 0.6 ± 0.3 was recorded when temperature increased from 0 to 8°C (data not shown). A Friedman's test showed this to be a significant increase, but multiple comparisons (Wilcoxon Signed-Rank tests using Bonferroni–Holm adjustment) were unable to detect differences between the initial CI and the individual temperature intervals. Elevation of the temperature to 10°C was tolerated by the amphipods.

Discussion

The present study describes for the first time the physiological color change of the Arctic under-ice amphipod *A. glacialis*, a process that is mediated by chromatophores. Based on our findings, the chromatophores appear to have a photoprotective function and provide an adaptation to short-term changes in solar irradiation.

Photoprotection

The experiments show that the physiological color change mediated through pigment dispersal in chromatophores is most likely triggered by changes in light conditions. In order to evoke a fast response, relatively high intensity of PAR was needed, but intensities likely to occur under sea ice also caused a response (UV-experiment control). Pigment dispersal due to exposure to visible light (PAR) is a common phenomenon and has been shown to occur in various crustacean species, mostly decapods (Perkins 1928; Brown and Sandeen 1948; Pautsch 1953; Rao 1966; Barnwell 1968; Coohill et al. 1970; Johnson 1974; Miner et al. 2000; Auerswald et al. 2008). *Apherusa glacialis* showed an increase in the CI following both higher light intensities and longer exposure times. It is therefore likely

Table 1 Experimental treatments conducted under different light conditions regarding the effect of solar radiation (in the UV and PAR range), background shade and temperature on the chromatophore index (CI)

	Number of experimental animals (<i>n</i>)	Light	Experimental irradiation	Exposure time	Water temperature (°C)	Background	CI	ΔCI
UVR experiments	16	UVR PAR	2–3 mW cm ⁻² 114 ± 2 μmol m ⁻² s ⁻¹	30 min	0 ± 1	–	4.0* ± 0.2	0.9 ± 0.1
	10	Control (PAR only)	107 ± 2 μmol m ⁻² s ⁻¹	30 min	0 ± 1	–	3.5* ± 0.4	0.5 ± 0.2
Background experiments	11	PAR	30–35 μmol m ⁻² s ⁻¹	24 h	0 ± 1	White	4.6* ± 0.2	0.4 ± 0.1
	10	PAR	30–35 μmol m ⁻² s ⁻¹	24 h	0 ± 1	Black	5.0 ± 0.0	0.3 ± 0.1
	9	Dark control	–	24 h	0 ± 1	Non	4.3 ± 0.4	–0.4 ± 0.4
Temperature experiments	7	Darkness	–	39 ± 3 min	0–8	–	3.7 ± 0.5	0.6 ± 0.3

CI and ΔCI values are means ± SE. Temperature experiments performed in intervals of 2°C

* Significantly different to initial CI (Wilcoxon signed-ranks tests, $P < 0.05$)

that *A. glacialis* is able to adapt individually to specific levels of irradiation, rather than responding to a threshold light intensity in an “all-or-nothing” type of response.

The physiological color change in *A. glacialis* is reversible, as pigments aggregated when animals were put back in darkness after exposure to PAR. Adaptation to darkness takes longer (up to 24 h to reach the initial stage of dark-adapted animals) than adaptation to high light intensities, which could ensure a fast protection against harmful radiation in a rapidly changing photic environment. Furthermore, the reversibility of the process demonstrates that pigment dispersion within the chromatophores is not due to damage of cells.

Assuming a photoprotective role of the chromatophores, this is most likely to be a shielding against UVR (e.g. Auerswald et al. 2008), although a direct harmful effect of blue light (450 nm) has been detected for the copepod species *Diaptomus nevadensis* (Hairston 1976). Documented harmful effects of PAR are otherwise rare, although high PAR intensity is known to inhibit photosynthesis in plants (Krause 1988), while UVR commonly known to have harmful effects (Browman et al. 2000; Lesser et al. 2004; Ban et al. 2007; Bancroft et al. 2007). However, the UVR treatment contra the control did not prove any difference in the response of the animals, suggesting that *A. glacialis* is not able to specifically detect UVR. Since UVR probably never occurs without accompanying PAR in nature, there is probably a low selectivity for a specific detection of UVR. The mechanism of light perception, which leads to the cascade of chromatophore response, is unclear and may not involve wavelengths in the UV range. However, since the ratio of UVR to PAR can vary due to different attenuation in sea ice (Belzile et al. 2000) or selective increase in UVR due to ozone depletion

(Kerr and McElroy 1993), it might be of vital importance for organisms to detect these wavelengths (Hessen 2002).

The arrangement of chromatophores in the amphipod points to the purpose of shielding the animal against incident irradiation from above. Whereas chromatophores in Antarctic krill are mainly located dorsally (Auerswald et al. 2008), pigment cells in *A. glacialis* are located at the ventral and lateral body side, a finding that might be related to the upside-down position the organisms take under the ice. Chromatophores are a unique feature of *A. glacialis* among the other sympagic amphipods, enabling the species to thrive at lit flow edges, remain in near-surface waters and even survive in melt ponds (Hop et al. 2000; Kiko et al. 2009). As an exclusive herbivore/detritivore species, the amphipod depends on the high primary production at these localities (Werner and Gradinger 2002).

Crypsis and thermoregulation

No indication of adapting the color appearance to background shade was seen in *A. glacialis*, excluding a cryptic function of chromatophores. Transparency can be regarded as the preferred appearance in the sea ice environment in avoidance of being detected by visual predators, but in patches where ice algae and detritus are aggregated, a dark-colored amphipod could have better camouflage. The arrangement of chromatophores is also not supporting crypsis, since they are basically aligned in a repetitive, rather than a cryptic, pattern on each body segment, as has been suggested for example in the isopod *Idothea baltica* (Merilaita 1998).

Acclimatization to a temperature of 8°C resulted in pigment dispersal in the chromatophores in some specimens of *A. glacialis*. The opposite response (contraction of

pigments) would have been expected if the animal was trying to prevent a build-up of heat in the body. A possible explanation for this phenomenon could be that increased metabolic stress leads to dispersion of pigments. Based on our results, we can exclude a thermoregulatory role of the chromatophores in *A. glacialis*.

As an additional note, *A. glacialis* seems to have considerable tolerance for elevated temperatures. Temperatures exceeding the normal variability in the natural habitat were tolerated for exposure times of more than 30 min. These findings correspond to those of Aarset (1991), who reported that short-term exposure to 10°C was not lethal in *A. glacialis*.

Photoprotection versus crypsis—a trade-off

Assuming that chromatophores with dispersed pigments absorb harmful radiation (most likely UVR) and are advantageous at high light intensities, there must be a fitness cost having dispersed chromatophores at low light intensities; otherwise, dispersed chromatophores would be preferred continuously. By dispersing pigments in the chromatophores, the animals appear darker, thus losing transparency. As transparency is regarded to be a successful camouflage in well-illuminated epipelagic layers (McFall Ngai 1990; Johnsen 2001), *A. glacialis* will become easier to detect by predators such as polar cod, which is a visual predator (e.g. Benoit et al. 2010). This is an inevitable risk to gain photoprotection, and *A. glacialis* seems to be able to regulate the pigment dispersion in chromatophores depending on light intensity to minimize the loss of transparency. This kind of compromise between photoprotection by pigments and crypsis has been suggested for various other crustaceans (Morgan and Christy 1996; Auerswald et al. 2008). For instance, Hansson (2000) and Hansson et al. (2007) showed that specimens of Arctic *Daphnia* spp. were more pigmented in lakes without predatory fish and that pigment levels can be adjusted to the prevailing conditions in a matter of days. Antarctic krill, *Euphausia superba*, has lower number of chromatophores and lower pigment concentration in winter than in summer, showing an ability to adapt to seasonal differences in the light conditions (Auerswald et al. 2008).

Color change by chromatophores provides a solution to the conflicting demands of camouflage and photoprotection. However, there are limits to the color change that can be achieved, which will affect the ability of the animal to express an optimal phenotype in a given situation. Such fitness costs are the associated physiological costs, as pigment movement is energy demanding (Miner et al. 2000; Boyle and McNamara 2008). The only indication regarding such costs in *A. glacialis* was that animals tended to aggregate the

pigments in their chromatophores when showing obvious signs of decreased activity or shortly before death, probably due to physiological stress. This could be a simple side effect of a general decrease in metabolism or part of an effort to reduce all energy-requiring processes.

Conclusions

Organisms inhabiting polar marine surface waters may be regarded as particularly exposed to high levels of dissolved oxygen, seasonally intense UV irradiance, and high levels of dissolved organic carbon (Krapp et al. 2009). In order to comply with these and other pro-oxidant challenges, aquatic organisms are known to have developed a number of antioxidant defense mechanisms, including superoxide dismutase (SOD) (McCord and Fridovich 1969), carotenoids (Davenport et al. 2004) as well as other small-molecule antioxidants like dimethyl sulfide (DMS), and mycosporine-like amino acids (MAA's) function as non-enzymatic antioxidants (Lesser 2006). In this study, we have examined the change in coloration of the ice amphipod *Apherusa glacialis* as a response to PAR and UV radiation as well as a potential cryptic effect. Pending further studies into the nature and chemophysical shielding effects of the pigments, we conclude that dispersion of pigments in the chromatophores plays a photoprotective role in *A. glacialis*, the response being triggered by light in the PAR spectrum. A similar response has been described (Auerswald et al. 2008) in the Antarctic krill (*Euphausia superba*), which responds to PAR in order to avoid harmful UV radiation. Specific detection of wavelengths in the UV range was not supported in this study, but it is likely that pigments in *A. glacialis* mainly serve to shield the animals from solar radiation, which is most harmful in the UV range. The dispersion of pigments in the chromatophores is a reversible process, causing aggregation of pigments in darkness. Therefore, the chromatophores enable the sympagic amphipod to react to different levels of solar radiation, balancing photoprotection against conspicuousness for visually hunting predators. Our study shows that *A. glacialis* is equipped to inhabit areas with high solar irradiation such as floe edges and areas of thin ice and can take advantage of the higher primary production there.

Acknowledgments We would like to thank the captain and crew of RV *Jan Mayen* for their technical support during the cruises. We also want to thank Erling Svensen for the underwater photographs and Bjørn Gulliksen, Geir Johnsen, and Daniel Vogedes for help with collecting amphipods for our experiments. Robert Dumbleby is acknowledged for comments and language corrections on the manuscript. The study was financed by the University Centre in Svalbard, the University foundation of the Christian-Albrechts-Universität zu Kiel, the Nordic Network on Sea-ice Research (NetICE) and Statoil through the StatoilHydro-ARCTOS Arctic Research Programme.

Open Access This article is distributed under the terms of the Creative Commons Attribution Noncommercial License which permits any noncommercial use, distribution, and reproduction in any medium, provided the original author(s) and source are credited.

References

- Aarset AV (1991) The ecophysiology of under-ice fauna. *Polar Res* 10:309–324
- Auerswald L, Freier U, Lopata A, Meyer M (2008) Physiological and morphological colour change in Antarctic krill, *Euphausia superba*: a field study in the Lazarev Sea. *J Exp Biol* 211:3850–3858
- Ban S, Ohi N, Leong SCY, Takahashi KT, Wexels Riser C, Taguchi S (2007) Effect of solar ultraviolet radiation on survival of krill larvae and copepods in Antarctic Ocean. *Polar Biol* 30:1295–1302
- Bancroft BA, Baker NJ, Blaustein AR (2007) Effects of UVB radiation on marine and freshwater organisms: a synthesis through meta-analysis. *Ecol Lett* 10:332–345
- Barnwell FH (1968) Comparative aspects of the chromatophoric response to light and temperature in fiddle crabs of the genus *Uca*. *Biol Bull* 134:221–234
- Belzile C, Johannessen SC, Gosselin M, Demers S, Miller WL (2000) Ultraviolet attenuation by dissolved and particulate constituents of first-year ice during late spring in an Arctic polynya. *Limnol Oceanogr* 45:1265–1273
- Benoit D, Simard Y, Gagne J, Geoffroy M, Fortier L (2010) From polar night to midnight sun: photoperiod, seal predation, and the diel vertical migration of polar cod (*Beoreogadus saida*) under landfast ice in the Arctic Ocean. *Polar Biol*. doi:10.1007/s00300-010-0840-x
- Boyle RT, McNamara JC (2008) A spring-matrix model for pigment translocation in the red ovarian chromatophores of the freshwater shrimp *Macrobrachium olfersi* (Crustacea, Decapoda). *Biol Bull* 214:111–121
- Browman H, Rodriguez C, Beland F, Cullen J, Davis R, Kouwenberg J, Kuhn P, McArthur B, Runge J, St-Pierre J-F, Vetter R (2000) Impact of ultraviolet radiation on marine crustacean zooplankton and ichthyoplankton: a synthesis of results from the estuary and gulf St. Lawrence, Canada. *Mar Ecol Prog Ser* 199:293–311
- Brown FA, Sandeen MI (1948) Responses of the chromatophores of the fiddler crab, *Uca*, to light and temperature. *Physiol Zool* 21:361–371
- Coohill TP, Bartell CK, Fingerman M (1970) Relative effectiveness of ultraviolet and visible light in eliciting pigment dispersion directly in melanophores of the fiddler crab, *Uca pugnator*. *Physiol Zool* 43:232–239
- Davenport J, Healy A, Casey N, Heffron J (2004) Diet-dependent UVAR and UVBR resistance in the high shore harpacticoid copepod *Tigriopus brevicornis*. *Mar Ecol Prog Ser* 276:299–303
- Endler JA (2006) Disruptive and cryptic coloration. *Proc R Soc Lond B* 273:2425–2426
- Fingerman M (1965) Chromatophores. *Physiol Rev* 45:296–339
- Fingerman M (1970) Comparative physiology: chromatophores. *Annu Rev Physiol* 32:345–372
- Hairston NG (1976) Photoprotection by carotenoid pigments in the copepod *Diaptomus nevadensis*. *Proc Nat Acad Sci U S A* 73(3):971–974
- Hanelt D, Tüg H, Bishop K, Groß C, Lippert H, Sawall T, Wiencke C (2001) Light regime in an Arctic fjord: a study related to stratospheric ozone depletion as a basis for determination of UV effects on algal growth. *Mar Biol* 138:649–658
- Hansson LA (2000) Induced pigmentation in zooplankton: a trade-off between threats from predation and ultraviolet radiation. *Proc R Soc Lond B* 267:2327–2331
- Hansson LA, Hylander S, Sommaruga R (2007) Escape from UV threats in zooplankton: a cocktail of behavior and photoprotective pigmentation. *Ecology* 88:1932–1939
- Hessen DO (2002) UV radiation and Arctic freshwater zooplankton. In: Hessen DO (ed) UV radiation and arctic ecosystems. *Ecological Studies* 153. Springer, Berlin, pp 157–180
- Hogben L, Slome D (1931) The pigmentary effector system. VI. The dual character of endocrine coordination in amphibian colour change. *Proc R Soc Lond B* 108:10–53
- Hop H, Poltermann M, Lønne OJ, Falk-Petersen S, Korsnes R, Budgell WP (2000) Ice amphipod distribution relative to ice density and under-ice topography in the northern Barents Sea. *Polar Biol* 23:357–367
- Johnsen S (2001) Hidden in plain sight: the ecology and physiology of organismal transparency. *Biol Bull* 201:301–318
- Johnson DF (1974) The development of the chromatophore response to light in the larvae of the crab, *Uca pugnator*. *Chesap Sci* 15:165–167
- Karentz D, Lutze LH (1990) Evaluation of biological harmful ultraviolet radiation in Antarctica with a biological dosimeter designed for aquatic environments. *Limnol Oceanogr* 35:549–561
- Kerr J, McElroy C (1993) Evidence for large upward trends of ultraviolet-B radiation linked to ozone depletion. *Science* 262:1032–1034
- Kiko R, Werner I, Wittmann A (2009) Osmotic and ionic regulation in response to salinity variations and cold resistance in the Arctic under-ice amphipod *Apherusa glacialis*. *Polar Biol* 32:393–398
- Krapp RH, Bassinet T, Berge J, Pampanin DM, Camus L (2009) Antioxidant responses in the polar marine sea-ice amphipod *Gammarus wilkitzkii* to natural and experimentally increased UV levels. *Aquat Toxicol* 94:1–7
- Krause HG (1988) Photoinhibition of photosynthesis. An evaluation of damaging and photoprotective mechanisms. *Physiol Plant* 74:566–574
- Lesser M (2006) Oxidative stress in marine environments: biochemistry and physiological ecology. *Annu Rev Physiol* 68:253–278
- Lesser MP, Lamare MD, Barker F (2004) Transmission of ultraviolet radiation through the Antarctic annual sea ice and its biological effects on sea urchin embryos. *Limnol Oceanogr* 46:1957–1963
- Lønne OJ (1988) A diver-operated electric suction sampler for sympagic (=under-ice) invertebrates. *Polar Res* 6:135–136
- Lønne OJ, Gulliksen B (1991) On the distribution of sympagic macrofauna in the seasonally ice covered Barents Sea. *Polar Biol* 11:457–469
- Madronich S, McKenzie R, Björn L, Caldwell M (1998) Changes in biologically active ultraviolet radiation reaching the Earth's surface. *J Photochem Photobiol B* 46:5–19
- Malloy KD, Holman MA, Mitchell D, Detrich HW (1997) Solar UVB-induced DNA damage and photoenzymatic DNA repair in Antarctic zooplankton. *Proc Natl Acad Sci USA* 94:1258–1263
- McCord J, Fridovich I (1969) Superoxide dismutase—an enzymatic function for erythrocyte hemocuprein (hemocuprein). *J Biol Chem* 244:6049–6055
- McFall Ngai MJ (1990) Cypsis in the pelagic environment. *Am Zool* 30:175–188
- Merilaita S (1998) Cypsis through disruptive coloration in an isopod. *Proc R Soc Lond B* 265:1059–1064
- Miner BG, Morgan SG, Hoffman JR (2000) Postlarval chromatophores as an adaptation to ultraviolet radiation. *J Exp Mar Biol Ecol* 249:235–248
- Morgan SG, Christy JH (1996) Survival of marine larvae under the countervailing selective pressures of photodamage and predation. *Limnol Oceanogr* 41:498–504

- Müller R, Crutzen PJ, Grooß J-U, Bürhl C, Russell JM, Gernandt H, McKenna DS, Tuck AF (1997) Severe chemical ozone loss in the Arctic during the winter of 1995–96. *Nature* 389:709–712
- Nöel PY, Chassard-Bouchaud C (2004) Chromatophores and pigmentation. In: Forest J, von Vaupel Klein JC (eds) *The crustacea* I. Leiden, Brill, pp 145–160
- Obermüller B, Karsten U, Abele D (2005) Response of oxidative stress parameters and sunscreens compounds in Arctic amphipods during experimental exposure to maximal natural UVB radiation. *J Exp Mar Biol Ecol* 323:100–117
- Pautsch F (1953) The colour change of the zoea of the shrimp, *Crangon crangon*. *Experientia* 9:274–276
- Perkins EB (1928) Colour changes in crustaceans, especially in *Palaemonetes*. *J Exp Zool* 50:71–105
- Poltermann M, Hop H, Falk-Petersen S (2000) Life under Arctic sea ice—reproduction strategies of two sympatric (ice-associated) amphipod species, *Gammarus wilkitzkii* and *Apherusa glacialis*. *Mar Biol* 136:913–920
- Rao KR (1966) Responses of crustacean larval chromatophores to light and endocrines. *Experientia* 23:231–232
- Stevens M (2007) Predator perception and the interrelation between different forms of protective coloration. *Proc R Soc Lond B* 274:1457–1464
- Stevens M, Merilaita S (2009) Animal camouflage: current issues and new perspectives. *Philos Trans R Soc Lond B* 364:423–427
- Werner I (2006) Seasonal dynamics, cryo-pelagic interactions and metabolic rates of Arctic pack-ice and under-ice fauna. A review. *Polarforschung* 75:1–19
- Werner I, Gradinger R (2002) Under-ice amphipods in the Greenland Sea and Fram Strait (Arctic): environmental controls and seasonal patterns below the pack ice. *Mar Biol* 140:317–326
- Werner I, Lindemann F (1997) Video observations of the underside of arctic sea ice—features and morphology on medium and small scales. *Polar Res* 16:27–36
- Willmer PG, Baylis M, Simpson CL (1989) The roles of colour change and behaviour in the hygrothermal balance of a littoral isopod, *Ligia oceanica*. *Oecologia* 78:349–356

Paper 3

Krapp, R.H. & Berge, J.

Total content of Mycosporine-like amino acids (MAAs) in the sympagic amphipods *Gammarus wilkitzkii*, *Onisimus nansenii*, *O. glacialis*, and *Apherusa glacialis* under Arctic pack ice during different seasons

Manuscript.

Total content of Mycosporine-like amino acids (MAAs) in the sympagic amphipods *Gammarus wilkitzkii*, *Onisimus nanseni*, *O. glacialis*, and *Apherusa glacialis* under Arctic pack ice during different seasons

Rupert H. Krapp^{a,b,*}, Jørgen Berge^b

^aNorwegian Polar Institute, Fram Centre, PO Box 6606, N-9296, Tromsø, Norway

^bThe Arctic University of Norway, Department of Arctic and Marine Biology, 9019 Tromsø, Norway

Abstract

Mycosporine-like amino acids have been shown to be present in a range of taxa, from phytoplankton and zooplankton to macroalgae, invertebrates and even fish. Their capacity to absorb and thus offer protection from UV radiation has made them an attractive group of natural “sunscreen” components also for human medical and pharmaceutical applications.

This study aimed to determine whether they could also be present in that function in sympagic amphipods, and whether there could be a seasonal trend in the concentrations present in these organisms. This was of particular interest as these species of amphipods had been found to be exposed to considerable levels of UV radiation, despite the fact that they are living on the underside of sea ice.

Our results showed that there seemed to be substances present in all four species which appear to have similar signatures as mycosporine-like amino acids. Technical difficulties with the analytical standards available prevented us from determining and quantifying the exact composition of the UV-absorbing components found in our samples. The material presented in this paper provides a baseline on the presumed presence of these important components.

KEY WORDS: Arctic, amphipods, sea ice, under-ice fauna, mycosporine-like amino acids

* Corresponding author.

Email address: rupert.krapp@npolar.no (Rupert H. Krapp).

The first author was fully supported by grants no. WE 2536/6-1 to .../6-3 of the Deutsche Forschungsgemeinschaft (DFG) for this work.

Introduction

The denominating component of mycosporine-amino acids is an aromatic chromatophore, mycosporine, which was first isolated from fungi, hence the name, and its production in fungi apparently coincides with UV-stimulated reproduction (Dionisio-Sese, 2010). Their ability of as natural defenses against exposure to ultraviolet radiation in other organisms has been investigated in tropical coral reefs and in the Antarctic marine environments at least since the 1980's, and has probably to a large part been motivated by the emerging research focus on seasonal ozone depletion, also known as the "Ozone Hole" in the Antarctic. Relevant surveys by Karentz et al (1990, 1991, 1994) and McClintock and Karentz (1997) provided a lot of the relevant groundwork for Antarctic marine biota. Their presence in Arctic marine biota has only come into the focus more recently, possibly due to the increasing awareness that also in the Arctic, seasonal ozone depletion events have been known to occur when suitable atmospheric conditions were present to facilitate activation of CFC's and similar ozone-depleting substances (ODP's), although to a smaller extent, mainly due to less pronounced and less stable polar vortex conditions (Hannigan et al, 2012; McFarlane, 2008; Solomon et al, 2014).

Mycosporine-like amino acids (MAAs) can be found in marine organisms from the poles to the tropics, ranging from bacteria to vertebrates (Karentz et al. 1991, Karentz 2001, Dunlap & Shick 1998). MAAs are derivatives of mycosporines, compounds identified in the mycelia of fungi. More than 30 different types of MAAs have been identified (Singh et al, 2008), and they are commonly perceived as "microbial sunscreen", although their intracellular functions may also include antioxidant properties, and have been found to help with cellular resistance to desiccation (Wright et al, 2005), osmotic stress (Oren & Gunde-Cimerman, 2007) and heat stress (Michalek-Wagner & Willis, 2001).

Elliot et al (2015) and Ha (2012) have documented MAA's in Arctic sea ice and Svalbard fjords, respectively, but to our knowledge, the only study into MAA's in Arctic amphipods was done on benthic amphipods so far (Obermüller et al, 2005).

Material and Methods

Collection of animals for analysis

Four species of Arctic sympagic (=under-ice dwelling) amphipods were collected during this study: *Gammarus wilkitzkii*, *Onisimus nanseni*, *O. glacialis* and *Apherusa glacialis*. The gammarid *G. wilkitzkii* has been described as an omnivorous/carnivorous/detritivorous species, while the two lysianassoid species *O. nanseni* and *O. glacialis* have been described to be predominantly necrophagous in the former and herbivorous/detritivorous in the latter case. The eusirid *A. glacialis* is a herbivorous/detritivorous species. All organisms were collected by divers operating hand-held suction pumps or dip nets directly under the sea ice. Collections took place in March/April (HE-04 expedition), May (OTI-III expedition), August (AB-202 expedition) and September (AB- 320 expedition) of 2004. Animals were directly preserved in liquid nitrogen and later stored at -80 C, until final analysis.

Analysis of mycosporine-like amino acid content in animals

Extraction and analysis was carried out according to the following protocol: animals were freeze-dried for 48h and 10-50 mg whole animal dry weight of either individual or pooled samples were extracted in 1 ml of 25% methanol for 2.5h at 45 C in screw-capped centrifuge vials filled with 1 mL 25% aqueous methanol (v/v) and incubated in a waterbath at 45 C.

After centrifugation at 6000 g for 6 min, 600 mL of the supernatants were evaporated to dryness under vacuum (Speed Vac Konzentrator SPD 111V, Thermo Quest Scientific Equipment Group, Egelsbach, Germany). Dried extracts were redissolved in 600 mL 100% methanol and vortexed for 30 s.

After passing through a 0.2-mm membrane filter, samples were analyzed with an Agilent HPLC (Waldbronn, Germany) system according to the method of Karsten et al. (1998c), modified as follows. The MAAs were separated on a stainless-steel Phenomenex Spherclone RP-8 column (5 mm, 250 4 mm I.D.) protected with an RP-8 guard cartridge (20 4 mm I.D.) (Phenomenex, Aschaffenburg, Germany). The mobile phase was 2.5% aqueous methanol (v/v) plus 0.1% acetonitrile (v/v) in water, run isocratically at a flow rate of 0.7 mL min⁻¹. The MAAs were detected online with a photodiode array detector at 330 nm, and absorption spectra (290–400 nm) were recorded each second directly on the HPLC-separated peaks.

Identification by spectra was attempted by comparing retention time, and co-chromatography with standards extracted from the marine green macroalga *Prasiola crispa* ssp. *antarctica* (Hoyer et al. 2001), the red macroalgae *Chondrus crispus* Stackhouse (Karsten et al. 1998a), and *Porphyra umbilicalis* (L.) Kützing, the lichen *Lichina* sp., as well as from ocular lenses of the coral trout *Plectropomus leopardus* (Lacepède, 1802), provided by Dr. David Bellwood (James Cook University, Townsville, Australia).

Concentrations are expressed in $\mu\text{g ml}^{-1}$ and $\mu\text{g g}^{-1}$ DM (dry mass).

Results

Preliminary HPLC absorption characteristics in the UV range

As a first step, we analyzed a set of pooled amphipod samples collected during August and September 2004 by the methodology described above, to determine whether they contained substances that absorbed in the UVR range in a way that is typical for mycosporine-like amino acids. We found that the absorption spectra of *G. wilkitzkii* and *O. nanseni* both appeared to have two distinctive peaks, around 270-280 and 320-330nm, respectively.

On the other hand, the absorption spectra of *O. glacialis* and *A. glacialis* did not show such distinctive “peaks” but showed strongest absorption in the range <280nm. However, the absorption profile for *A. glacialis* displays a distinctive “shoulder” around 300-330nm.

Ideally, these samples should have been compared by co-chromatography with the above-mentioned standards, both for identification and quantification purposes. Based on such co-chromatography, one could have re-diluted and re-analyzed the original samples in order to achieve better separation. We were unable to perform those steps due to technical issues with the available standards.

Going forward we therefore had to refer to the results of these analyses as “total content of MAAs” rather than addressing the individual types of MAAs, and we thus also were only able to determine the total MAA content per gram dry weight (g DW) instead of specific content per g DW.

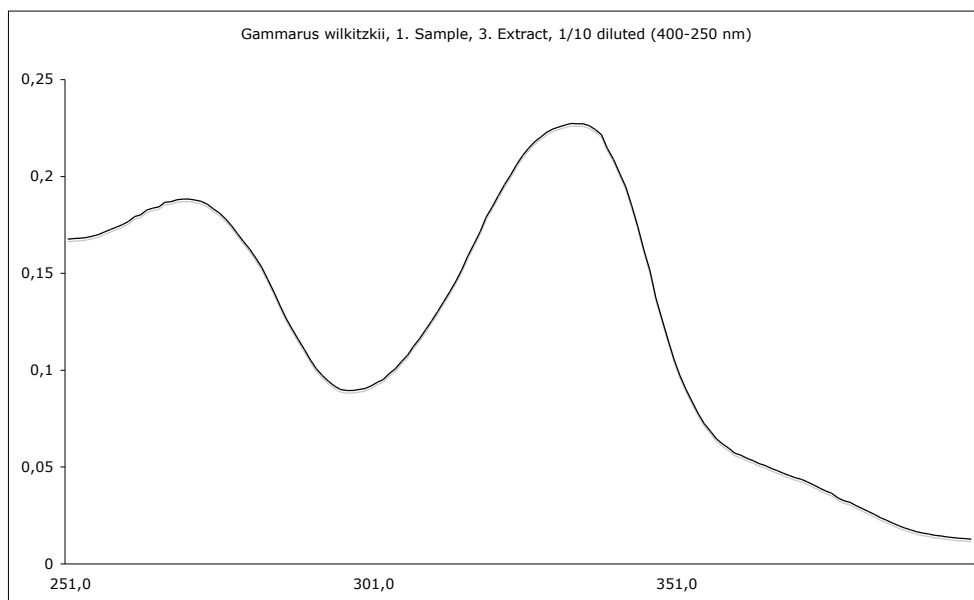


Fig. 1: HPLC absorption profile for pooled sample of *G. wilkitzkii*, 400 – 250 nm

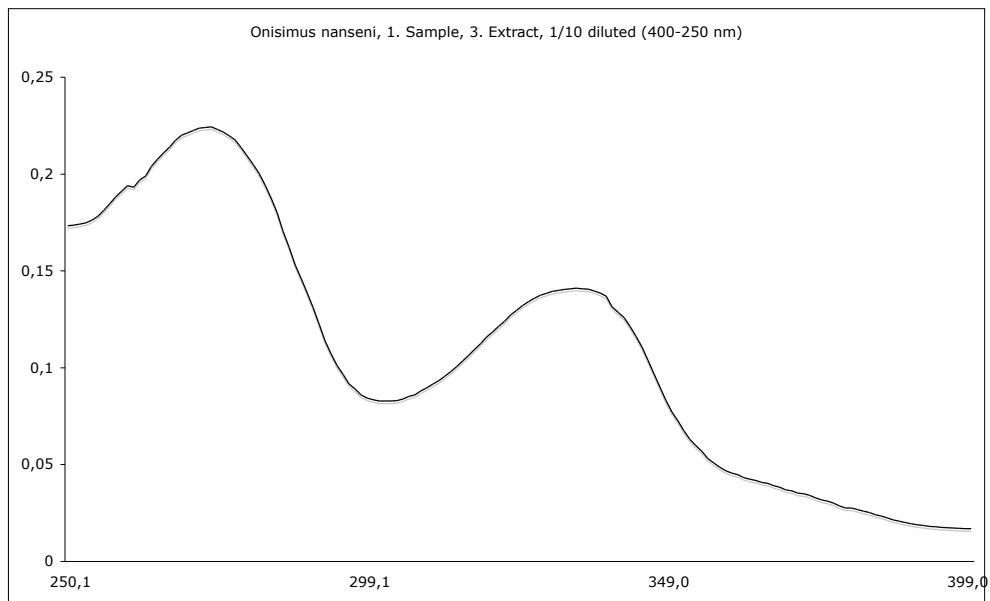


Fig. 2: HPLC absorption profile for pooled sample of *O. nanseni*, 400 – 250 nm

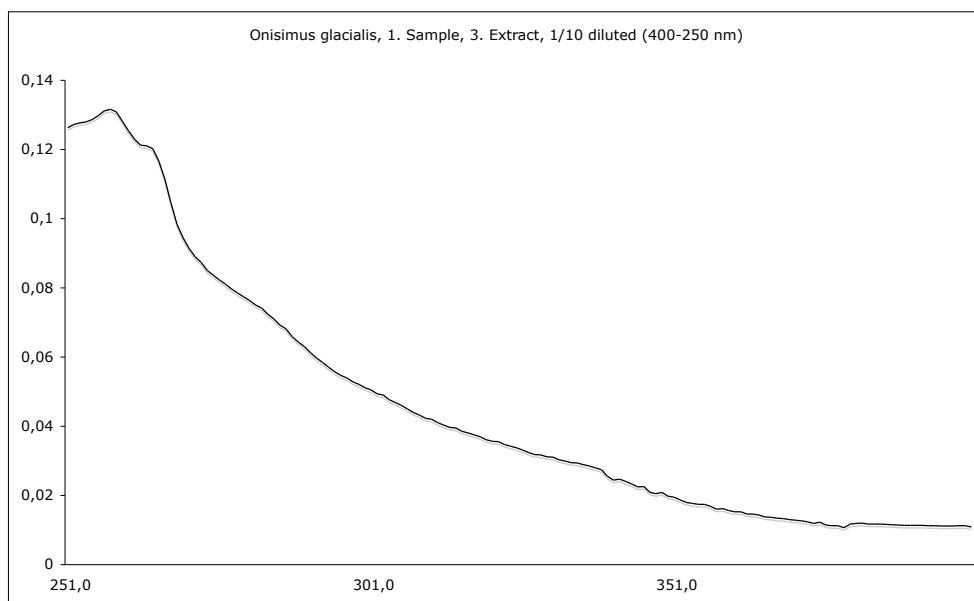


Fig. 3: HPLC absorption profile for pooled sample of *O. glacialis*, 400 – 250 nm

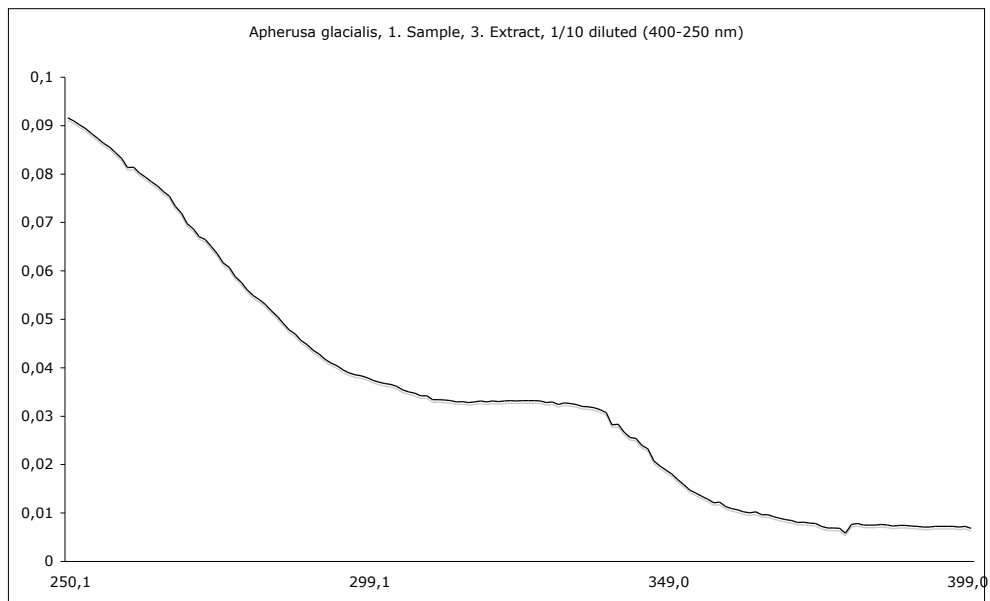


Fig. 4: HPLC absorption profile for pooled sample of *A. glacialis*, 400 – 250 nm

Comparison of total MAA per species

A statistical analysis of total content of MAAs per dry weight of pooled samples from both August and September expeditions showed that the species *Apherusa glacialis* showed significantly higher content than *Gammarus wilkitzkii*, and both showed significantly higher content than the two other species, *Onisimus glacialis* and *O. nanseni*.

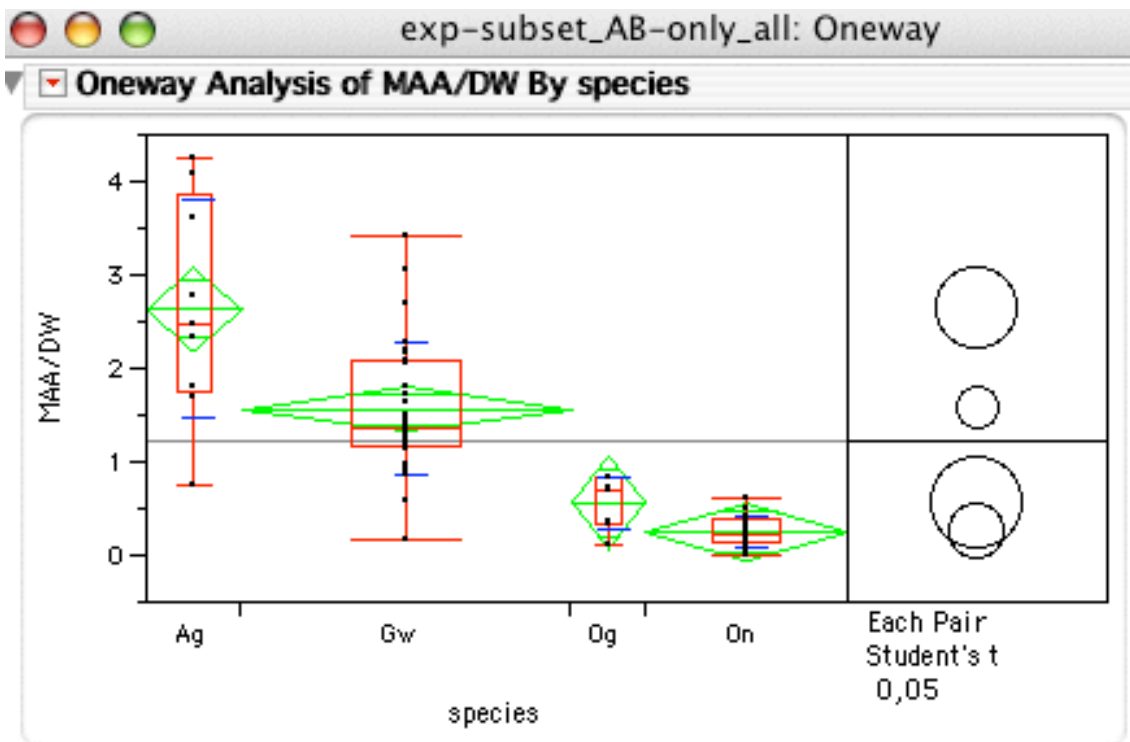


Fig. 5: Student's T test of total MAA content per dry weight (samples pooled per species, taken in August and September 2004). Ag = *Apherusa glacialis*, Gw = *Gammarus wilkitzkii*, Og = *Onisimus glacialis* and On = *Onisimus nanseni*.

Comparison of total MAA per season

We also performed similar statistical tests to determine whether samples taken from different seasons were significantly different in total MAA content. Due to technical constraints with the required amount of sampling material, we could not perform this on all species, since we were not able to collect the required amount of biomass in all four species investigated here.

But while not the most numerous, the large size and therefore also biomass of *G. wilkitzkii* allowed for a comparison between pooled samples of the August and September expeditions in comparison to samples from the winter expedition (HE-04, march-april 2004) and the spring expedition (OTI-III, may 2004). The test performed on these samples showed a clear difference between the summer/autumn samples and the winter/spring samples (see fig 6).

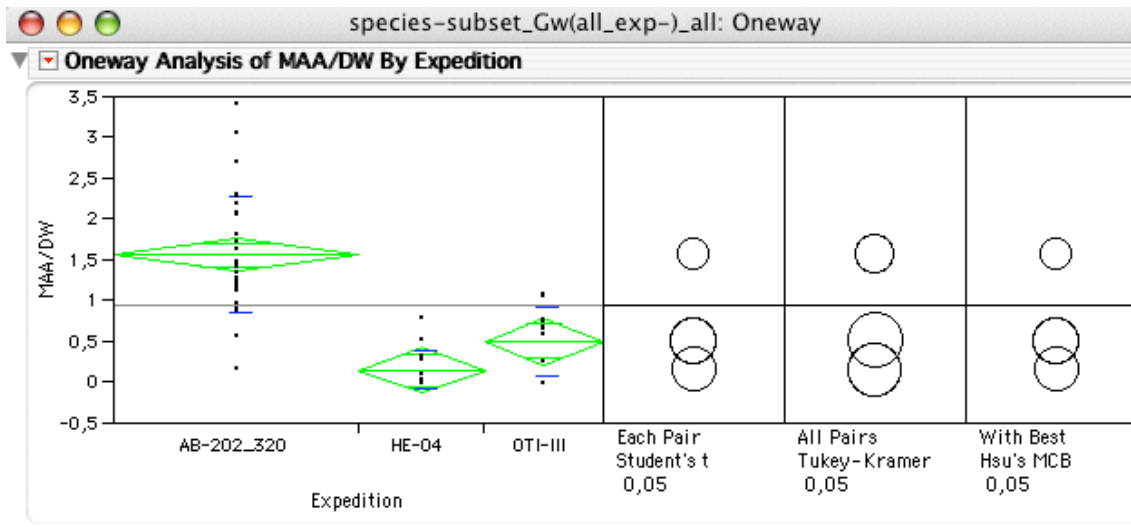


Fig. 6: Student's T test of total MAA content per dry weight during different parts of the year: AB-202_320 = August and September 2004; HE-04 = March/April 2004; OTI-III = May 2004). All samples were taken of *G. wilkitzkii*.

The species *Onisimus glacialis* had also been collected to a sufficient amount to allow these samples to be pooled for the two summer / autumn expeditions (AB-202_320) and compare these with one of the earlier expeditions, performed during spring (May 2004). And again, a clear difference could be determined by all tests (see fig. 7).

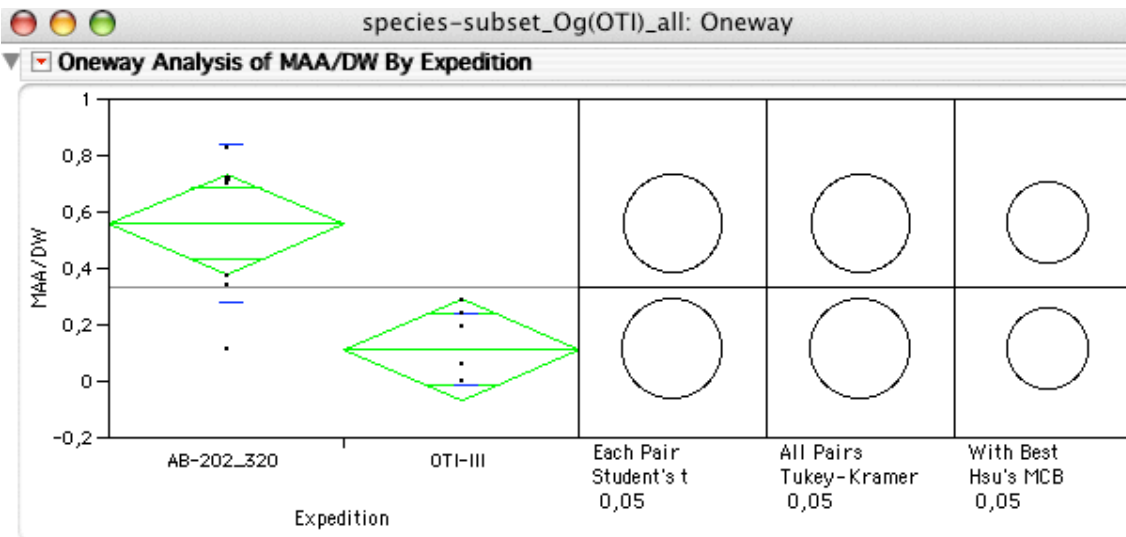


Fig. 7: Student's T test of total MAA content per dry weight during different parts of the year: AB-202_320 = August and September 2004; HE-04 = March/April 2004; OTI-III = May 2004). All samples were taken of *Onisimus glacialis*.

In summary, our samples show that there is a significant increase of MAA content found in several species, as can be seen in the following figure (fig. 8).

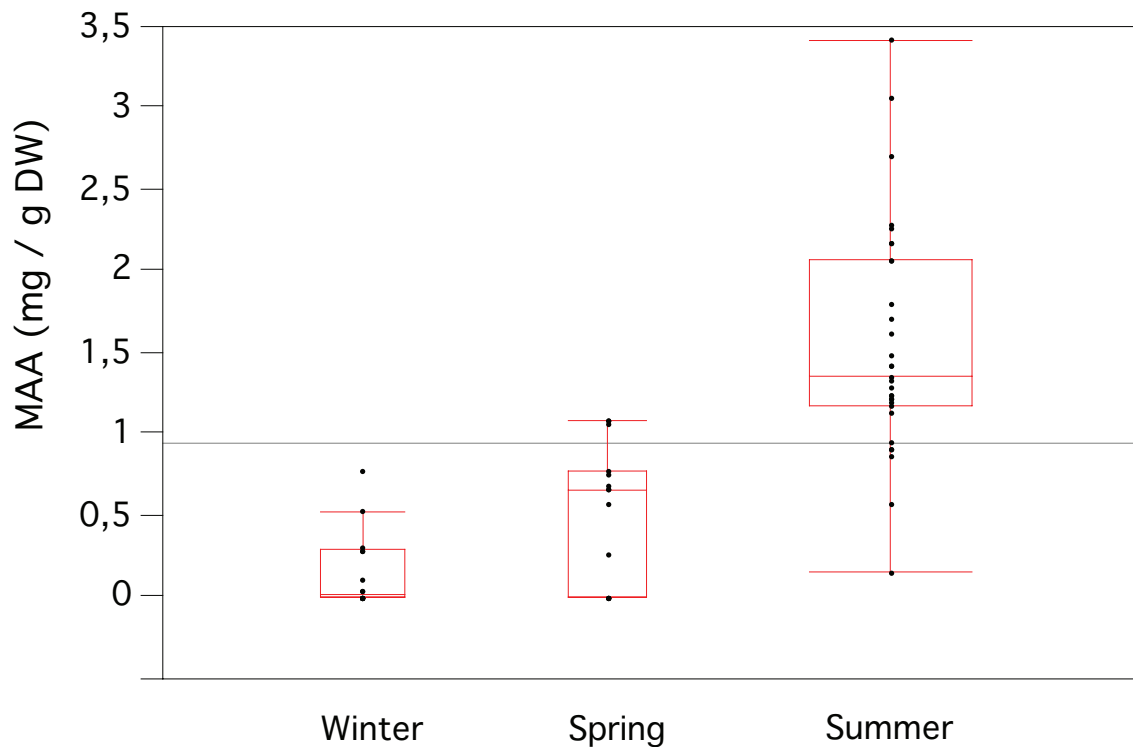


Fig. 8: Total MAA content per dry weight during different parts of the year: Winter = HE-04 (March/April 2004); Spring = OTI-III (May 2004). Summer = AB-202_320 (August and September 2004); All samples were taken of *G. wilkitzkii*.

We also tried to discern whether there is a noticeable difference in such pigment accumulation in different parts of the amphipod bodies of *Gammarus wilkitzkii*. We used pooled samples of individuals of this species as that was the only species sampled in sufficient quantities to allow for sufficient amounts of pooled biomass to be separated in such a way. We separated the “heads” and “appendages” from the main “body” of these amphipods by fine tweezers and processed the resulting pooled samples in a similar manner as with previous samples.

The following figure (Fig. 9) shows that the body (=pereon & pleon) parts of the amphipods contained by far the highest amount of MAAs per dry weight sampled.

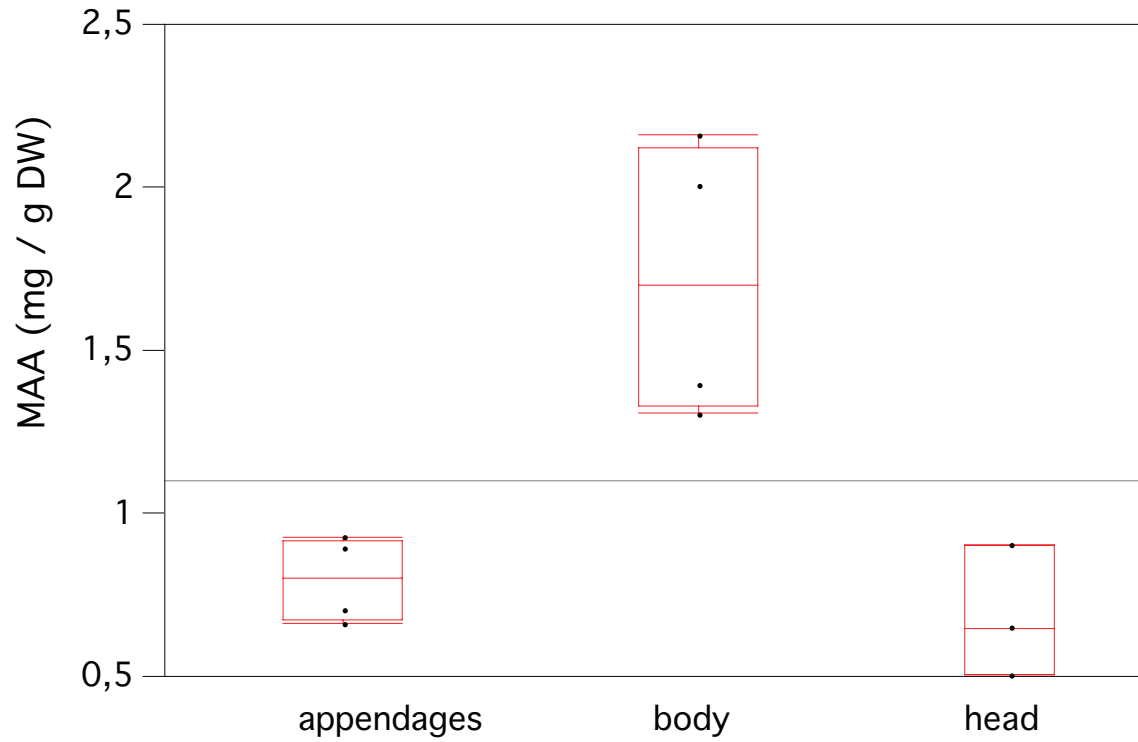


Fig. 9: Total MAA content per dry weight found in different body parts of the amphipod *Gammarus wilkitzkii*: appendages (antennae, gnathopods, pereopods, pleopods), body (pereon & pleon) and head (caput, eye & rostrum).

Discussion

Photo-protective screening compounds, which typically are being acquired through dietary uptake and then retained, have been found in different amphipod species in various extent and forms, and can be found as carapace pigmentation, chromophores, and pigmentation of soft tissue within the carapace structure.

In crustaceans, at least 10 different MAAs and the chemical precursor gadusol have been identified so far, with shinorine, porphyra 334, mycosporine- glycine, palythenic acid and palythine being the most dominant substances. UV-protection by MAAs in animals is clearly shown, though stimulation of uptake and accumulation still varies from species to species and results are sometimes contradictory (Banaszak et al, 2006).

These UV-protective substances are known to have an important photoprotective role as they efficiently absorb potentially harmful UV radiation, as well as act in a strong antioxidant role (Rastogi et al, 2017). They have previously been described mainly from a variety of Antarctic invertebrate species, notably including krill, but also echinoderms, crustaceans, and even fish (Karentz, 1994). In the Arctic, there are to date only a few studies on MAAs in sea ice environments, notably the Baltic Sea (Uusikivi et al., 2010; Piiparinen et al., 2015), the Canadian Arctic (Elliott et al., 2015) and the southern Nansen Basin north of Svalbard (Kauko et al, 2017). Ha et al (2012) documented several MAAs in phytoplankton samples collected in and around Kongsfjorden, Svalbard, and Ha et al (2018) documented MAA synthesis and size-dependent contents from the Beaufort Sea as well.

MAA-like signatures have also been documented in particle absorption samples from sea ice (Uusikivi et al., 2010; Fritsen et al., 2011; Mundy et al., 2011; Piiparinen et al., 2015; Taskjelle et al., 2016).

Their role has been well-studied in Arctic macro-algae and in certain benthic amphipod species grazing on these algae, which due to such a relatively shallow benthic lifestyle also are exposed to potentially harmful UV radiation (Obermüller et al, 2005). These and earlier studies found that the grazers were gaining a clear benefit from ingesting and retaining these pigments for the photoprotection against harmful levels of UV radiation.

It is reasonable to assume that such photoprotective pigments are important not only for the sea ice algal community, but also for the sea ice amphipod community, as members of the latter live in close connection with the former. And while amphipods are mobile and thereby able to reduce exposure to some extent by moving to less exposed sites, their ice-associated lifestyle prevents them from escaping potential exposure altogether.

Conclusions

Our results indicate that the UV-protective substances belonging to the class of mycosporine-like amino acids (MAAs) are likely also present and appear to play a role also in Arctic amphipods.

Our preliminary findings indicate that sea ice algae grazers likely benefit from the ingestion and retention of such MAA's. There is also a marked seasonal trend in the MAA content in such sea ice algal grazers, which fits well with the onset of the spring phytoplankton bloom.

When comparing typical algal grazers with omnivore/grazers and scavengers, the algal grazers contained the highest relative concentration of MAAs.

Unfortunately, technical difficulties in chemical resolution of our sample contents prevented us from identifying the contributing MAA types, and lack of supporting data on the MAA producing sea ice algae prevented us from identifying the nutritional sources and types.

This material in prep provides a baseline on the total MAA content in Arctic sea ice amphipods.

Acknowledgements

We would like to thank Deneb Karentz for invaluable advice on the sampling and analysis of MAAs in invertebrates, as well as our scientific diving partners, notably Bjørn Gulliksen, Geir Johnsen, Haakon Hop and Daniel Vogedes, for their assistance during the collection of this material. Ulf Karsten and Sebastian Lembcke of the University of Rostock provided us with technical support and access to their pigment lab infrastructure, and interpretation and analysis of the HPLC results. The study was financially supported by the University Centre in Svalbard, the University of Tromsø, and the Christian-Albrechts-Universität zu Kiel.

The first author (RK) was fully supported by grants no. WE 2536/6-1, 6-2 and 6-3 of the Deutsche Forschungsgemeinschaft (DFG) for this work.

Literature

- Banaszak AT, Barba Santos MG, LaJeunesse TC, Lesser MP (2006) The distribution of mycosporine-like amino acids (MAAs) and the phylogenetic identity of symbiotic dinoflagellates in cnidarian hosts from the Mexican Caribbean. *J Exp Mar Bio Ecol* 337:131–146. <https://doi.org/10.1016/j.jembe.2006.06.014>
- Carefoot TH, Karentz D, Pennings SC, Young CL (2000) Distribution of mycosporine-like amino acids in the sea hare *Aplysia dactylomela*: effect of diet on amounts and types sequestered over time in tissues and spawn. *Comp Biochem Physiol C* 126:91–104. [https://doi.org/10.1016/S0742-8413\(00\)00098-0](https://doi.org/10.1016/S0742-8413(00)00098-0)
- Carreto JJ, Carignan MO, Daleo G, Marco SGD (1990) Occurrence of mycosporine-like amino acids in the red-tide dinoflagellate *Alexandrium excavatum*: UV-photoprotective compounds? *J Plankton Res* 12:909–921. <https://doi.org/10.1093/plankt/12.5.909>
- Dionisio-Sese ML (2010) Aquatic Microalgae As Potential Sources Of Uv-Screening Compounds. *Philippine Journal of Science* Vol. 139 No. 1, June 2010 5–16
- Dunlap WC, Shick JM (1998) Review-ultraviolet radiation-absorbing mycosporine-like amino acids in coral reef organisms: A biochemical and environmental perspective. *J Phycol* 34:418–430. <https://doi.org/10.1046/j.1529-8817.1998.340418.x>
- Elliott A, Mundy CJ, Gosselin M, et al (2015) Spring production of mycosporine-like amino acids and other UV-absorbing compounds in sea ice-associated algae communities in the Canadian Arctic. *Mar Ecol Prog Ser* 541:91–104. <https://doi.org/10.3354/meps11540>
- Fritsen CH, Wirthlin ED, Momberg DK, et al (2011) Bio-optical properties of Antarctic pack ice in the early austral spring. *Deep Sea Res Part 2 Top Stud Oceanogr* 58:1052–1061. <https://doi.org/10.1016/j.dsr2.2010.10.028>
- Geraldes V, Pinto E (2021) Mycosporine-like amino acids (MAAs): Biology, chemistry and identification features. *Pharmaceuticals (Basel)* 14:63. <https://doi.org/10.3390/ph14010063>
- Ha S-Y, Kim Y-N, Park M-O, et al (2012) Production of mycosporine-like amino acids of in situ phytoplankton community in Kongsfjorden, Svalbard, Arctic. *J Photochem Photobiol B* 114:1–14. <https://doi.org/10.1016/j.jphotobiol.2012.03.011>
- Ha S-Y, Min J-O, Joo H, et al (2018) Synthesis of mycosporine-like amino acids by a size-fractionated marine phytoplankton community of the arctic beaufort sea. *J Photochem Photobiol B* 188:87–94. <https://doi.org/10.1016/j.jphotobiol.2018.09.008>

- Hannigan JW, Batchelor RL, Coffey MT (2012) Intense arctic ozone depletion in the spring of 2011. *Arctic* 65:. <https://doi.org/10.14430/arctic4221>
- Karentz D (2001) Chemical defenses of marine organisms against solar radiation exposure: UV-absorbing mycosporine-like amino acids and scytonemin. In: *Marine Science*. CRC Press, pp 481–520
- Karentz D (1994) Ultraviolet tolerance mechanisms in Antarctic marine organisms. In: *Ultraviolet Radiation in Antarctica: Measurements and Biological Effects*. American Geophysical Union, Washington, D. C., pp 93–110
- Karentz D (1991) Ecological considerations of Antarctic ozone depletion. *Antarct Sci* 3:3–11. <https://doi.org/10.1017/s0954102091000032>
- Karentz D, McEuen FS, Land MC, Dunlap WC (1991) Survey of mycosporine-like amino acid compounds in Antarctic marine organisms: Potential protection from ultraviolet exposure. *Mar Biol* 108:157–166. <https://doi.org/10.1007/bf01313484>
- McClintock JB, Karentz D (1997) Mycosporine-like amino acids in 38 species of subtidal marine organisms from McMurdo Sound, Antarctica. *Antarct Sci* 9:392–398. <https://doi.org/10.1017/s0954102097000503>
- McFarlane N (2008) Connections between stratospheric ozone and climate: Radiative forcing, climate variability, and change. *Atmosphere-Ocean* 46:139–158. <https://doi.org/10.3137/ao.460107>
- Michalek-Wagner K, Willis BL (2001) Impacts of bleaching on the soft coral *Lobophytum compactum* . I. Fecundity, fertilization and offspring viability. *Coral Reefs* 19:231–239. <https://doi.org/10.1007/s003380170003>
- Moisan TA, Mitchell BG (2001) UV absorption by mycosporine-like amino acids in *Phaeocystis antarctica* Karsten induced by photosynthetically available radiation. *Mar Biol* 138:217–227. <https://doi.org/10.1007/s002270000424>
- Mundy CJ, Gosselin M, Ehn JK, et al (2011) Characteristics of two distinct high-light acclimated algal communities during advanced stages of sea ice melt. *Polar Biol* 34:1869–1886. <https://doi.org/10.1007/s00300-011-0998-x>
- Newman SJ, Dunlap WC, Nicol S, Ritz D (2000) Antarctic krill (*Euphausia superba*) acquire a UV-absorbing mycosporine-like amino acid from dietary algae. *J Exp Mar Bio Ecol* 255:93–110. [https://doi.org/10.1016/s0022-0981\(00\)00293-8](https://doi.org/10.1016/s0022-0981(00)00293-8)
- Obermüller B, Karsten U, Abele D (2005) Response of oxidative stress parameters and sunscreens compounds in Arctic amphipods during experimental exposure to maximal natural UVB radiation. *J Exp Mar Bio Ecol* 323:100–117. <https://doi.org/10.1016/j.jembe.2005.03.005>

- Oren A, Gunde-Cimerman N (2007) Mycosporines and mycosporine-like amino acids: UV protectants or multipurpose secondary metabolites? *FEMS Microbiol Lett* 269:1–10. <https://doi.org/10.1111/j.1574-6968.2007.00650.x>
- Piiparinen J, Enberg S, Rintala J-M, et al (2015) The contribution of mycosporine-like amino acids, chromophoric dissolved organic matter and particles to the UV protection of sea-ice organisms in the Baltic Sea. *Photochem Photobiol Sci* 14:1025–1038. <https://doi.org/10.1039/c4pp00342j>
- Raj S, Kuniyil AM, Sreenikethanam A, et al (2021) Microalgae as a source of mycosporine-like amino acids (MAAs); Advances and future prospects. *Int J Environ Res Public Health* 18:12402. <https://doi.org/10.3390/ijerph182312402>
- Rastogi RP, Sonani RR, Madamwar D (2017) UV photoprotectants from algae—synthesis and bio-functionalities. In: *Algal Green Chemistry*. Elsevier, pp 17–38
- Ryan KG, McMinn A, Mitchell KA, Trenerry L (2002) Mycosporine-like amino acids in Antarctic sea ice algae, and their response to UVB radiation. *Z Naturforsch C* 57:471–477. <https://doi.org/10.1515/znc-2002-5-612>
- Singh A, Čížková M, Bišová K, Vítová M (2021) Exploring mycosporine-like amino acids (MAAs) as safe and natural protective agents against UV-induced skin damage. *Antioxidants (Basel)* 10:. <https://doi.org/10.3390/antiox10050683>
- Singh SP, Kumari S, Rastogi RP, et al (2008) Mycosporine-like amino acids (MAAs): chemical structure, biosynthesis and significance as UV-absorbing/screening compounds. *Indian J Exp Biol* 46:7–17
- Solomon S, Haskins J, Ivy DJ, Min F (2014) Fundamental differences between Arctic and Antarctic ozone depletion. *Proc Natl Acad Sci U S A* 111:6220–6225. <https://doi.org/10.1073/pnas.1319307111>
- Taskjelle T, Hudson SR, Granskog MA, et al (2016) Spectral albedo and transmittance of thin young Arctic sea ice. *J Geophys Res Oceans* 121:540–553. <https://doi.org/10.1002/2015jc011254>
- Uusikivi J, Vähätalo AV, Granskog MA, Sommaruga R (2010) Contribution of mycosporine-like amino acids and colored dissolved and particulate matter to sea ice optical properties and ultraviolet attenuation. *Limnol Oceanogr* 55:703–713. <https://doi.org/10.4319/l.2010.55.2.0703>
- Vega J, Schneider G, Moreira BR, et al (2021) Mycosporine-like amino acids from red macroalgae: UV-photoprotectors with potential cosmeceutical applications. *Appl Sci (Basel)* 11:5112. <https://doi.org/10.3390/app11115112>
- Whitehead, Karentz, Hedges (2001) Mycosporine-like amino acids (MAAs) in phytoplankton, a herbivorous pteropod (*Limacina helicina*), and its pteropod

predator (*Clione antarctica*) in McMurdo Bay, Antarctica. *Mar Biol* 139:1013–1019. <https://doi.org/10.1007/s002270100654>

Whittock AL, Auckloo N, Cowden AM, et al (2021) Exploring the blueprint of photoprotection in mycosporine-like amino acids. *J Phys Chem Lett* 12:3641–3646. <https://doi.org/10.1021/acs.jpcllett.1c00728>

Wright DJ, Smith SC, Joardar V, et al (2005) UV irradiation and desiccation modulate the three-dimensional extracellular matrix of *Nostoc commune* (Cyanobacteria). *J Biol Chem* 280:40271–40281. <https://doi.org/10.1074/jbc.M505961200>

Paper 4

Krapp, R.H., Berge, J., Flores, H., Gulliksen, B. & Werner, I. (2008).

Sympagic occurrence of Eusirid and Lysianassoid amphipods under Antarctic pack ice

Deep-Sea Research II, 55, 1015-1023.

Sympagic occurrence of Eusirid and Lysianassoid amphipods under Antarctic pack ice

Rupert H. Krapp^{a,b,*,1}, Jørgen Berge^b, Hauke Flores^{c,d}, Bjørn Gulliksen^{b,e}, Iris Werner^a

^aInstitute for Polar Ecology, University of Kiel, Wischhofstr. 1-3, Building 12, 24148 Kiel, Germany

^bUniversity Center in Svalbard, P.O. Box 156, 9171 Longyearbyen, Norway

^cIMARES Wageningen, P.O. Box 167, 1790 AD Den Burg, The Netherlands

^dCenter for Ecological and Evolutionary Studies, Groningen University, P.O. Box 14, 9750 AA Haren, The Netherlands

^eNorwegian College of Fishery Sciences, University of Tromsø, 9037 Tromsø, Norway

Accepted 24 December 2007

Available online 5 May 2008

Abstract

During three Antarctic expeditions (2004, ANT XXI-4 and XXII-2; 2006, ANT XXIII-6) with the German research icebreaker R/V *Polarstern*, six different amphipod species were recorded under the pack ice of the Weddell Sea and the Lazarev Sea. These cruises covered Austral autumn (April), summer (December) and winter (August) situations, respectively. Five of the amphipod species recorded here belong to the family Eusiridae (*Eusirus antarcticus*, *E. laticarpus*, *E. microps*, *E. perdentatus* and *E. tridentatus*), while the last belongs to the Lysianassidea, genus *Cheirimedon* (cf. *femoratus*). Sampling was performed by a specially designed under-ice trawl in the Lazarev Sea, whereas in the Weddell Sea sampling was done by scuba divers and deployment of baited traps. In the Weddell Sea, individuals of *E. antarcticus* and *E. tridentatus* were repeatedly observed *in situ* during under-ice dives, and single individuals were even found in the infiltration layer. Also in aquarium observations, individuals of *E. antarcticus* and *E. tridentatus* attached themselves readily to sea ice. Feeding experiments on *E. antarcticus* and *E. tridentatus* indicated a carnivorous diet. Individuals of the Lysianassoid *Cheirimedon* were only collected in baited traps there. Repeated conventional zooplankton hauls performed in parallel to this study did not record any of these amphipods from the water column. In the Lazarev Sea, *E. microps*, *E. perdentatus* and *E. laticarpus* were regularly found in under-ice trawls. We discuss the origin and possible sympagic life style of these amphipods.

© 2008 Elsevier Ltd. All rights reserved.

Keywords: Antarctic; Amphipods; Under-ice fauna; Sympagic; Weddell Sea; Lazarev Sea

1. Introduction

The lower boundary layer of polar sea ice is inhabited by several allochthonous and autochthonous species, of which amphipods have been described as the most conspicuous macrofaunal elements in the Arctic, while euphausiids are the dominant group in the Antarctic (Lønne and Gulliksen, 1991; Gulliksen and Lønne, 1991). Copepods are common in the sea-ice habitats of both regions. Unlike in the Arctic

sea-ice zone, where amphipods have been commonly recorded both under coastal fast ice as well as under offshore pack ice, Antarctic sympagic amphipods have mostly been described for the coastal fast-ice zone (Arndt and Swadling, 2006). In this habitat, species like *Paramoera walkeri*, *Cheirimedon fougneri* and *Pontogeneia antarctica* seem to originate from the benthos and occur under the sea ice only seasonally and in relatively shallow water depths (Sagar, 1980; Gulliksen and Lønne, 1991; Garrison, 1991). Comparatively little is known about the distribution of Antarctic amphipods in sea ice above greater water depths, although several reports of amphipods in the sub-ice or even under-ice habitat have been published recently (Kaufmann et al., 1993, 1995; Fisher et al., 2004). This could be due to the relative inaccessibility of these areas, as

*Corresponding author at: Institute for Polar Ecology, University of Kiel, Wischhofstr. 1-3, Building 12, 24148 Kiel, Germany.

E-mail address: rkrapp@ipoe.uni-kiel.de (R.H. Krapp).

¹The first author was fully supported by Grant nos. WE 2536/6-1 to .../6-3 of the Deutsche Forschungsgemeinschaft (DFG) for this work.

well as the higher frequency and greater feasibility of studies based on land stations. Also, the distribution of these highly motile under-ice organisms at the ice under-surface is often very patchy (Hop et al., 2000), and the effective observation and collection require the use of divers or ROVs (remotely operated vehicles), while core-hole based methods like under-ice pumping or video camera systems cover only a very limited sampling area surrounding the hole (Werner and Lindemann, 1997).

Ainley et al. (1986) discovered the amphipod *Eurythenes gryllus* along with the decapod *Pasiphaea longispina* and the ostracod *Gygantocypris mulleri* in sea bird stomachs collected in pack ice of the Southern Ocean. All three species were otherwise believed to be mesopelagic, but since the sea bird species examined (Antarctic petrel, *Thalassoica antarctica*) was known to dive no deeper than 5 m, it was concluded that these crustacean plankton species must have migrated to the immediate sub-ice habitat. Another report by Kaufmann et al. (1995) mentions the Lysianasoid *Abyssorchomene rossi* in large numbers from baited traps deployed directly under pack ice of the northwestern Weddell Sea, while deeper traps did not catch any of these amphipods.

During the three Antarctic research cruises reported here, six amphipod taxa were sampled directly from the underside of sea-ice floes by various methods, in what we believe to be the first recorded observation and collection of these species from Antarctic pack ice.

The aims of this paper are: (1) to present findings of new sympagic occurrences of Eusirid and Lysianassoid amphipods; (2) to record feeding behaviour observed in some of these taxa; (3) to compare these findings with other reports of Antarctic amphipods found in association with sea ice.

2. Material and methods

2.1. Study area

This study is based on three Antarctic cruises with the German research icebreaker R/V *Polarstern*. The two expeditions into the Lazarev Sea (ANT XXI-4, March–May 2004 and ANT XIII-6, June–August 2006) were part of the multiyear study LAzarev Sea KRill Survey (LAKRIS). The goal of the expedition into the Weddell Sea (ANT XXII-2, November 2004 to January 2005) was to carry out the Ice Station POLarstern experiment (ISPOL), see Hellmer et al. (2008). For the purpose of this paper, the three expeditions will be referred to by these acronyms: LAKRIS 2004, ISPOL and LAKRIS 2006 (see Fig. 1, Tables 1 and 2 for details).

2.2. ISPOL—sampling

The ISPOL drift station was set up in an area where sea-ice cover contained both first-year and multi-year ice, with ice cover of 8–9/10. The vessel was moored to a large ice floe and drifted with it for the period of November 29, 2004

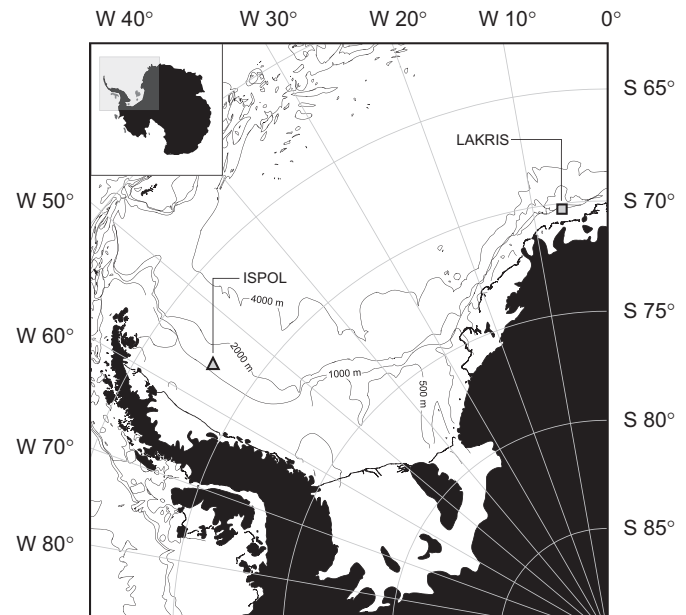


Fig. 1. Map of the study area indicating the sampling areas of the ISPOL drift station and the LAKRIS 2004 and 2006 cruises. For details on positions, ice cover and depth, refer to tables.

to January 02, 2005, between positions 68°2.7'S 54°51.1'W and 67°21.2'S 55°24.3'W, while sounded depths ranged from 1030 to 2075 m. An introduction and overview of the ISPOL experiment is given by Hellmer et al. (2008).

During the course of the ISPOL experiment, ice under-side and under-ice temperatures, salinity and chlorophyll *a* values were measured from ice cores as well as under-ice water samples at regular intervals. Ice-core salinity and chlorophyll *a* content were measured from sampled core segments, melted at 4 °C in the dark. Chlorophyll *a* content also was determined from melted core segments that were filtered and extracted from a detailed time-series study of these parameters in the ISPOL floe (Steffens & Dieckmann, unpublished data). Under-ice water and zooplankton samples were obtained from an under-ice pumping system, deployed simultaneously to the time-series core sampling events, and results of this are presented in detail in Kiko et al. (2008).

Under-ice fauna was sampled by scuba diving as well as by deployment of baited traps (see Table 1). Scuba divers used a hand-net with 25 × 25-cm frame opening and 500- μ m mesh size, which was scraped along the underside of the ice. Sampling by scuba diving was done on five different dates and positions (see Table 1), while baited traps were checked every other day from initial deployment on December 07, 2004 until final retrieval on January 2, 2005.

Traps deployed along the floe edge as well as through core holes were plastic tubes with 102.5 mm inside diameter, 150 mm tube length, with a funnel opening to the inside on one end and a 100- μ m aluminium mesh on the other end. The opening of the funnel was 12 mm wide, and traps were suspended in the water column in such a way

Table 1
Sampling stations during the ISPOL drift station

	Sampling method	Location	Date	Latitude	Longitude	Depth (m)	Ice thickness (m)
Weddell Sea							
ISPOL	SCUBA	2	December 01, 2004	68°10.4'S	54°53.4'W	1896	0.9
	SCUBA	3	December 03, 2004	68°7.9'S	55°13.8'W	1576	0.9
	SCUBA	4	December 11, 2004	67°59.7'S	55°19.0'W	1471	0.9
	SCUBA	5	December 15, 2004	67°46.6'S	55°29.2'W	1274	0.9
	SCUBA	6	December 18, 2004	67°45.9'S	55°18.1'W	1504	0.9
	Baited traps	7	From December 07, 2004	67°25.6'S	55°24.2'W	1494	0.8
			To January 02, 2005	67°21.2'S	55°24.3'W	1382	1.0
	Slush sample	8	January 01, 2005	67°22.6'S	55°25.8'W	1398	1.0

Table 2
Sampling stations during the LAKRIS cruises

	Sampling method	Location	Date	Latitude	Longitude	Depth (m)	Ice thickness (m)
Lazarev Sea							
LAKRIS 2004	SUIT	1	April 10, 2004	70°18.5'S	6°1.1'W	240	n.a.
LAKRIS 2006	SUIT	9	July 05, 2006	67°26.1'S	2°53.2'E	4564	0.2–0.6
	SUIT	10	July 06, 2006	68°32.6'S	2°51.4'E	4130	0.4–0.6
	SUIT	11	July 07, 2006	69°31.1'S	3°12.7'E	3765	0.9–1.0
	SUIT	12	July 12, 2006	67°31.2'S	0°3.5'W	4499	0.3–0.5
	SUIT	13	July 19, 2006	66°8.0'S	0°11.0'W	3840	0.2–0.7
	SUIT	14	July 19, 2006	66°7.7'S	0°10.5'W	3840	0.4–0.6
	SUIT	15	July 29, 2006	69°22.8'S	2°43.7'W	3312	0.2–1.0
	SUIT	16	July 30, 2006	68°0.3'S	2°54.3'W	4090	0.2–0.8
	SUIT	17	August 03, 2006	66°3.5'S	3°3.8'W	4760	0.4
	SUIT	18	August 04, 2006	65°5.3'S	2°51.2'W	no data	0.2–0.6

that the two openings were aligned horizontally. Traps were deployed just off the floe edge and through core holes at 1, 5 and 10 m from the edge, and were positioned directly at the ice–water interface (ice depth), 5, 10, 15, 20 and 35 m below the ice. Bait consisted of fish and shrimp meat enriched with fish oil.

Sampling from the infiltration layer was performed either by picking up individuals from the slush with small hand-sieves of 500 µm mesh size, or by collecting slush with a bucket and pouring the content through a larger sieve of the same mesh size.

Parallel to these sampling efforts, zooplankton sampling was performed at regular intervals and with conventional zooplankton gear, i.e. multinet and bongo net hauls (see Table 5).

2.2.1. ISPOL—feeding experiments

Amphipods were separated by species and size and kept in aquaria at 0 °C in a climate-controlled room. Every other day, a small piece of artificial sea ice was added to each aquarium to provide a substrate, and to ensure that the water temperature remained constant. Sea-ice blocks were produced using pre-filtered water which was frozen in zip-loc bags at –20 °C.

A subsample ($n = 15$) of the species *Eusirus antarcticus* was fed with ice algal concentrates that were frozen into

these artificial sea-ice blocks, while a control group (also $n = 15$) was provided with “pure” Sea-ice blocks, therefore regarded as unfed. All organisms were kept in aquaria for at least 10 days to allow evacuation of the digestive tract of the unfed animals, whereas the algal-fed group was regularly offered frozen algal concentrates during that period. Mortality was noted on a daily basis, and dead animals, animal parts and exuviae were removed and preserved in 70% ethanol for taxonomic analysis. After the end of the experiment, all remaining animals were immediately frozen in liquid nitrogen and stored at –80 °C for later chlorophyll extraction. Extracts were then analysed using spectrophotometry.

A second feeding experiment with both *E. tridentatus* ($n = 2$) as well as *E. antarcticus* ($n = 3$) was performed, using two known copepod species as live prey. Single amphipods of both species were kept in separate aquaria and were offered an abundance of prey items of either *Metridia gerlachei* or *Calanoides acutus*. Daily control counts yielded the number of consumed prey items (see Table 4).

2.3. LAKRIS—sampling

During the LAKRIS 2004 and 2006 cruises, the sea-ice undersurface was sampled using a “Surface and Under Ice

Trawl” (SUIT) (see Table 2). In contrast to conventional trawls, the SUIT was towed sideways of the ship, allowing to sample under undisturbed ice, at a distance of approximately 150 m from the water channel produced by the towing vessel. The upper side of the net frame was equipped with drivers to provide permanent close contact of the net with the undersurface of the ice. The net had a frame with an opening of 2.25×2.25 m and was equipped with a 7-mm mesh shrimp net. Towing speed was 1.0–1.5 knots. During LAKRIS 2004 a plankton net with a 50-cm diameter (mesh size 0.3 mm) was attached inside the rear end of the shrimp net in a centred position. Towing speed was approximately 2.5 knots. In total, 24 stations were sampled covering an area between 0°W to 6°W in longitude and 61°S to 70°S in latitude. Further details on the LAKRIS 2006 expedition are provided in Smetacek et al. (2005). During LAKRIS 2006, the rear end of the net was entirely lined with 0.3 mm gaze. In total, 30 stations were sampled covering an area between 3°E to 3°W in longitude and 57°S to 70°S in latitude. On both expeditions, the catch was immediately sorted by taxon. The size of amphipods was measured as the length from the frontal edge of the eye to the tip of the telson. They were either preserved on 4% buffered formaldehyde–seawater solution or directly frozen at -20 or -80°C .

2.4. Species identification

Identification of all Eusirid species treated herein follows Andres et al. (2002), where a key to the *Eusirus* species from Antarctica is given.

3. Results

3.1. Environmental parameters—ISPOL station

Temperature values ranged from -2.2 to -1.4°C for the lowermost centimetres of the ice and -1.8 to -1.9°C for the under-ice water down to 8 m below the ice. Salinity values ranged from 5 to 11.6 for the lowermost centimetres and 34.2 to 34.7 for the under-ice water down to 8 m below the ice, while chlorophyll *a* values ranged from 57.64 to 261.69 $\mu\text{g l}^{-1}$ and from 0.07 to 0.35 $\mu\text{g l}^{-1}$, respectively.

Table 3
Amphipod species observed under Antarctic pack ice

Expedition	Species	Location	Total number	Size range (mm)
LAKRIS 2004	<i>Eusirus perdentatus</i>	1	1	49
	<i>Eusirus microps</i>	1	1	42
ISPOL	<i>Eusirus antarcticus</i>	2, 3, 4, 6, 7, 8	60	9–15
	<i>Eusirus tridentatus</i>	2, 5, 8	3	18–24
	<i>Cheirimeidon</i> (cf. <i>femoratus</i>)	7	8	8–10
LAKRIS 2006	<i>Eusirus laticarpus</i>	9, 10, 12, 13, 14, 15, 16, 17, 18	24	6–19
	<i>Eusirus microps</i>	9, 12, 15, 16, 18	7	12–38

3.2. Under-ice amphipods of the ISPOL station

Two species of the five Eusirid amphipod species reported here, *E. tridentatus* and *E. antarcticus*, were found at several sampling sites at the underside of the pack ice, in the infiltration layer as well as in baited traps deployed at the ice–water interface (see Table 3). Another amphipod species, *Cheirimedon* cf. *femoratus*, was found exclusively in those baited traps deployed directly at the ice–water interface (see Table 3). No amphipods were collected by any of the baited traps deployed below the ice–water interface.

3.2.1. Lysianassoid amphipods

Material examined: Eight specimens, including one immature female and one immature male, both 10 mm in length. All specimens were collected with baited traps, from Weddell Sea.

Identification: The specimens collected during this study could not be identified to species level with certainty, as the studied specimens possess morphological affinities with both of the two species *C. femoratus* and *C. fougneri*. These are both very common shallow benthic species in the Southern Ocean. The main discrepancies between the sampled material and *C. femoratus* and *C. fougneri* are as follows:

- our material differs from *C. fougneri* in having two relatively short antennae, (*C. fougneri*: two long antennae), antenna 1 stout with broad peduncle 1;
- eyes longer and more droplet shaped;
- our material shows a rounded epimeral plate 3 (*C. femoratus* has a produced epimeral plate 3);
- our material: coxa 1 anteriorly expanded (as in *C. femoratus*).

Based upon these morphological discrepancies, and as we did not have any adult individuals at our disposal from the Weddell Sea, we will herein refer to the material as *C. cf. femoratus*, as it shares the distinct shape of the coxa 1 with this species, although the shape of the epimeral plate 3 is different.

3.3. Under-ice amphipods of the LAKRIS cruises

Two individual amphipods were collected at one station of the LAKRIS 2004 autumn expedition. They were

Table 4
Feeding experiment of *Eusirus tridentatus* and *Eusirus antarcticus* with calanoid copepods

	Day 1	Day 2	Day 3	Day 4	Day 5	Day 6	Day 7
<i>E. tridentatus</i>	3 M.g.	3 M.g.	1 M.g.	0 C.a.	1 C.a.	0 C.a.	0 C.a.
<i>E. antarcticus</i>	1 C.a.	1 C.a.	1 C.a.	0 C.a.	0 C.a.	1 C.a.	0 C.a.

Numbers indicate individual prey items devoured by one amphipod d⁻¹. E. = *Eusirus*, M.g. = *Metridia gerlachei*, C.a. = *Calanoides acutus*.

identified as *E. microps* and *E. perdentatus*. The sizes of both specimens were at the higher end of the size ranges of these species (Table 2). On the winter expedition LAKRIS 2006, another Eusirid species was obtained from SUIT catches. This was *E. laticarpus*, which occurred at 9 of the 30 stations sampled, covering a broad size range. *E. microps* was found only at 5 stations (Table 3). Specimens of this species kept in an aquarium with sea ice actively sought the ice and stayed attached to it. All amphipods collected on the LAKRIS 2006 expeditions occurred in the part of the sampling area south of 64°S.

3.4. Feeding experiments—ISPOL station

Selected individuals of *E. tridentatus* and *E. antarcticus* were observed repeatedly to predate both on smaller *E. antarcticus* as well as on copepods of the species *Metridia gerlachei* and *Calanoides acutus*, which were offered in controlled feeding experiments (Table 4).

The other feeding experiment performed with *E. antarcticus*, offering ice algae frozen into artificial ice blocks was analysed for chl *a* content. Methanolic extracts of both fed and unfed amphipods did not show any significant difference in their chlorophyll signatures, which were both below the detection limit.

3.5. Collection of zooplankton samples under pack ice

Sampling of zooplankton with conventional net hauls did not yield any of the aforementioned amphipod species collected from the pack ice underside. Instead, other amphipod taxa, both Hyperiididae and Scinidae, as well as some isopods, were routinely sampled in multinet hauls, alongside with copepods, for which results will be presented in detail in Schnack-Schiel et al. (2008). A single Eusirid amphipod was recorded from a bongo net haul (December 23, 2004, 200–0 m) but was determined to belong to a different genus than *Eusirus*.

4. Discussion

This paper presents data from under-ice amphipods found in the pack ice of the Weddell Sea and the Lazarev Sea. While many authors have previously described amphipods living attached to sea ice close to shore and over relatively shallow water depths, such recordings so far

have only been reported occasionally from sea ice over deep water and further offshore in the Antarctic (Gulliksen and Lønne, 1991; Kaufmann et al., 1995). We discuss the possible origin and the degree of sympagic adaptation in these species, based on direct observations and feeding experiments.

4.1. Origin of Eusirid species found under Antarctic pack ice

Our samples of the species *E. antarcticus*, *E. laticarpus*, *E. microps*, *E. perdentatus* and *E. tridentatus* reported here fit well with previous records of these species from ice-covered Antarctic waters, although in most cases methodological constraints prohibit a statement about their exact origin. For example, Foster (1987) reports the Eusirid *E. antarcticus* for his zooplankton collections done through holes in the land-fast ice of the McMurdo Sound, but his study sampled integrated depth intervals of 100–0 and 300–0 m. In another study of the zooplankton of McMurdo Sound, Hopkins (1987) also reports the Eusirids *E. tridentatus* and *E. propeperdentatus* among his plankton net samples, as well as the Lysianassoid amphipods *Abyssorhomene plebs* and *A. rossi*. The samples described in this study were performed by oblique sweeps of the upper 800 m with a Tucker trawl. The Eusirid species *E. antarcticus* and *E. microps* also have been recorded from epipelagic (0–50, 50–100 m) MOCNESS trawl samples in the NW Weddell Sea performed at pack-ice covered stations (Fisher et al., 2004). A switch from a pelagic to a sympagic mode of life as soon as ice becomes available is supported by low pelagic catches of *E. microps* and *E. antarcticus* when sea ice was present compared to significantly higher catches in ice-free waters reported by Fisher et al. (2004). Reports on *E. laticarpus* are scarcer and further complicated by the fact that this species was often included in *E. antarcticus* in the past, before the species was re-established by De Broyer and Jazdzewski (1993).

E. perdentatus was caught only once at a shelf station of the LAKRIS 2004 expedition and due to its relatively shallow depth (see Table 2) it is conceivable that it had actively sought the under-ice habitat because potential prey, especially euphausiid larvae, were abundant under the ice at that time (Flores, unpublished data). However, it is possible but unlikely that the specimen originated from a shallower area and subsequently drifted to the location of capture with the sea ice. Klages (1993) and Klages and Gutt (1990) cover the distribution and feeding patterns of *E. perdentatus*, which had been sampled from meso- and epipelagic stations by various gear. However, recent re-analysis of the material used for the former publication by Andres et al. (2002) revealed a new species, *E. giganteus*, which had mistakenly been regarded as *E. perdentatus*, so these results should be treated with caution. It also should be noted that *E. tridentatus* Bellan-Santini and Ledoyer (1974), and *E. microps* Walker (1906) have been described as separate species by Barnard and Karaman (1991), but

synonymized by De Broyer and Jazdzewski (1993). Therefore, reports of *E. microps* will also have to be treated with some caution, depending on whose species definition they were based on. The same is also true about the other Eusirids found by this study: De Broyer (1983) treated *E. antarcticus* and *E. laticarpus* as separate species. While Barnard and Karaman (1991) treated them as synonyms. We follow the most recent key to Antarctic Eusirids by Andres et al. (2002) who clearly distinguishes and maintains all above mentioned species and names.

Due to the range of gears and depths, we regard all these above mentioned records as epipelagic to mesopelagic. To our knowledge, direct under-ice observation and sampling of any of the above mentioned species has not been reported from the Antarctic pack ice zone (Arndt and Swadling, 2006). Based on these reports and our own observations and samples, we conclude that the pelagic realm is the most likely origin for these Eusirids. Since our samples also cover a considerable temporal and spatial range, it seems safe to say that there is evidence for a pelago-sympagic coupling, i.e. Eusirid amphipods seem to be able to utilize the under-ice habitat during their life cycle.

This hypothesis is supported by our *in situ* observations as well as aquarium observations. Both *E. tridentatus* and *E. antarcticus* were observed by divers to swim very close to the underside of the ice and attach themselves for periods of time to it, as well as sometimes to enter cracks and holes in the ice. Single individuals were even found in slush sampled from the infiltration layer (see Table 3). Also, whenever a small piece of artificially produced sea ice was put in their aquarium, individuals of *E. antarcticus*, *E. microps* and *E. tridentatus* immediately started to swim towards it and then attached themselves to its surfaces (see Figs. 2 and 3).

However, the water column had been sampled extensively and regularly during the month-long ISPOL drift station, not one Eusirid amphipod of the species recorded under the ice was found in those zooplankton net samples (see Table 5). As mentioned above, all of these species have otherwise been reported from zooplankton samples with various gear and depth ranges, so it seems strange that none were collected by our zooplankton sampling efforts. This seems even more surprising given the fact that those samples regularly recorded Hyperiididae and Scinidae of similar size ranges, proving that animals of such size and shape could be found in our samples after all.

4.2. Origin of Lysianassoid species found under Antarctic pack ice

We were not able to directly observe any specimen of *Cheirimedon* in or around the ice, but only recorded them in two neighbouring traps immediately after their first retrieval (see Table 3). The animals showed limited swimming activities in holding tanks, and were not observed to seek contact with sea ice when offered.



Fig. 2. *Eusirus antarcticus* attached to artificial sea ice, image©Ingo Arndt.



Fig. 3. *Eusirus tridentatus* attached to artificial sea ice, image©Ingo Arndt.

Lysianassoids have previously been reported by Kaufmann et al. (1993) who found hundreds of large specimens of *A. rossi* from baited traps deployed just under the pack ice, while similarly deployed traps in open water remained empty. The authors argued that this observation suggests that these amphipods may be present in large numbers just beneath the ice surface, and established this as the first record of these scavenging amphipods in the microhabitat of the Antarctic pack ice, where water depths in excess of 1000 m were recorded. This was confirmed by Tucker trawl hauls from the same cruise, published by the same authors in Kaufmann et al. (1995), where *A. rossi* also was found in shallow trawl samples (10–35, 50–85 m) taken at night in partly ice-covered waters. Fisher et al. (2004) also list *A. rossi* from MOCNESS trawls at depth intervals 100–50 and 50–0 m in that area. Stockton (1982) collected what probably was the same species (using its previous genus name, *Orchomene rossi*) also in baited trap samples taken from under the Ross Ice Shelf, 400 km from the shelf edge at a depth of 600 m, so one must assume that this species is flexible in its habitat use.

Table 5
Amphipods and isopods caught by multinet hauls during ISPOL station, see Schnack-Schiel et al. (2008)

Date	Depth range (m)	Scinidae	Hyperiididae	Isopoda
December 01, 2004	1000–500	1		
December 06, 2004	100–50	1		
December 06, 2004	500–200	1	3	
December 06, 2004	1000–500	1		
December 09, 2004	500–200	3		
December 09, 2004	1000–500	4		
December 13, 2004	500–200		1	
December 13, 2004	1000–500	1		1
December 17, 2004	200–100		1	
December 17, 2004	500–200	1	3	
December 21, 2004	1000–500	2		
December 21, 2004	500–200	1		
December 21, 2004	1000–500	3		1
December 26, 2004	500–200	2		
December 26, 2004	1000–500	2		
December 29, 2004	500–200	2		
December 29, 2004	1000–500	1	1	
January 02, 2005	100–50		1	
January 02, 2005	200–100			1
January 02, 2005	500–200		4	
January 02, 2005	1000–500	3		

Although we were not able to determine the species of the Lysianassoids found on the ISPOL drift station, a very different picture can be gained from the literature for the most similar to those found in this study. No source known to us has listed either *C. femoratus* or *C. fougneri* from a pelagic sampling station. Instead, Bregazzi (1972a,b, 1973) described *C. femoratus* to be bottom-dwelling types with limited swimming capabilities which inhabit the top layer of sandy-gravelly subtidal zones around Antarctica (Jazdzewski et al., 2000).

Gulliksen and Lønne (1991) describe *C. fougneri* from sampling efforts in McMurdo Station, where amphipods were only recorded in significant amounts under sea ice above relatively shallow water, i.e. in the tens of metres. Interestingly, they also noticed a broadcast event of *C. fougneri* for the period November–December, based on observations of a rapid increase of free-swimming juveniles between two sampling dates, while adults were still observed with unreleased juveniles in their marsupia on the first sampling event (Gulliksen, pers. comm.). From that, one can assume that this species annually utilizes the sea ice underside both as adult and juvenile stages for part of their life span.

In other cases where shallow benthic Lysianassoid amphipods were unexpectedly found under pack ice, Werner et al. (2004) and Nygård (2005) described *Anonyx sarsi* under Arctic pack ice, but their stations were also at much shallower water depths than in the present study. Therefore, the authors argued that their findings could be explained by benthic–sympagic coupling. In our case, it seems safe to say that any benthic–sympagic coupling

based on active migration is unlikely, since water depths exceeded 1000 m.

Also, since our findings are exclusively of small and juvenile specimens, which we estimate to be no older than one year, one has to assume that they have either been advected to the ice since their hatching, or that they indeed were hatched in the vicinity of the ice. Still, the basic question remains as to how they got to the ice station where we found it in our baited traps. If active migration is ruled out, then advection or other passive transport seems to be the only possible alternative. The most likely transport medium would be the ice itself, as it cannot be ruled out that some of the ice present in the area of our ISPOL study had originally formed over shallower depths.

Since the ISPOL drift station was set up in an area with a variety of ice types and probably ages and origins, it seems futile to speculate about when and where the colonization or advection of benthic amphipods might have taken place. Still, the relatively small size and inferred young age of the *C. cf femoratus* points to the hypothesis that these animals had been hatched under the ice and had been developing there since.

Aerial transport could be mentioned as another—though rather improbable—possibility for advection. There are a few published reports, p.e. Segerstråle (1946, 1954), where the author proves experimentally how the freshwater amphipod *Gammarus lacustris* was able to cling to bird feathers and even showed tolerance exposure of up to 2 h. One could alternatively also speculate that penguins might have acted as vectors, but we regard both possibilities as highly unlikely in this case.

4.3. Feeding types in Antarctic sympagic amphipods

The feeding experiments indicate that *E. antarcticus* and *E. tridentatus* are predatory and carnivorous species. The initially observed cannibalism cannot be excluded to be an artificially induced behaviour in captivity.

Since investigations covering the ice-algal biomass found within the ice as well as the under-ice water had shown ice algae to be there, and the succession of these concentrations even indicated some melting out of ice algae into the underlying water (see Kiko et al., 2008), one could have assumed that this would serve as a food source for the amphipods found under the ice, in a similar fashion as it had been established for krill earlier (Marschall, 1988). However, we were not able to prove ice algal uptake by means of methanolic extractions. Preferably, the feeding experiment should have been performed following the procedure described in Werner (1997), where algal concentrations before and after introduction of grazers were determined.

In a paper by Klages and Gutt (1990), a macropredatory carnivorous feeding type is documented for *E. perdentatus* from aquaria observations. This has been confirmed by Graeve et al. (2001), who present lipid, fatty acid and digestive tract content analyses, and by Dauby et al. (2001),

who describe the relative proportions (in %) of food items for various amphipods and found that *E. perdentatus* contained a broader range of food items, all of which could well originate from predation as well as scavenging. Unfortunately, due to the sampling gear used, we cannot report any observed feeding behaviour for this species, but concurrent sampling of zooplankton yielded an abundance of copepods and krill larvae under the ice.

We did not directly record any feeding behaviour for *C. cf femoratus*. Richardson and Whitaker (1979) describe the closest species, i.e. *C. femoratus* as predator and *Pontogeneia antarctica* as algal grazer in a scuba-based observational and sampling study off Signy Island. Both species were recorded in the immediate vicinity of sea ice by them, where *C. femoratus* was observed actively preying on the newly released young of *Pontogeneia antarctica*. Bregazzi (1972b) reports algal material for juveniles of *C. femoratus*, while adult specimens contained a large variety of food items ranging from algae to copepods and euphausiid larvae. In the same study, trap experiments recorded a strong response from these amphipods as well. These reports fit well with our results from baited trap samples, which suggest a possible scavenging behaviour for *C. cf femoratus*. However, due caution should be applied when comparing these results, since our material very likely belongs to another species than either *C. femoratus* or *C. fougneri*.

5. Conclusion

The results from this study suggest that the underside of Antarctic pack ice serves at least temporarily as a habitat for Eusirid amphipods. Although this could not be determined with certainty, we believe that their origin for the reported oceanic occurrences is most probably the pelagic habitat, from which they can colonize the sea ice during favourable conditions. It is thus puzzling that none of these amphipods were found in any of the extensive concurrent zooplankton sampling efforts, which did record a number of isopods, as well as scinid and hyperiid amphipods of similar size classes. One explanation might be that the transition to a sympagic life style had been initiated prior to our sampling period.

For the Lysianassoid *Cheirimedon cf. femoratus*, which also were found by this study, such a pelagic origin seems less likely, but since the species determination is still uncertain for the sampled material, it cannot be completely ruled out.

In conclusion, we recommend that further studies of the under-ice fauna of Antarctic pack ice should be undertaken to gain more insight into the biology, distribution and significance of amphipods in this habitat. One aspect that should deserve special attention is the possible interaction of amphipods with other under-ice and zooplankton organisms like krill and copepods, where possible predatory interaction can be assumed. Also, their potential role and availability as food for higher trophic levels like fish and sea birds should be investigated.

Acknowledgements

We thank the captain and crew of the R/V *Polarstern* for excellent support during both ANT XXI-4 (LAKRIS 2004), ANT XXII-2 (ISPOL) and ANT XXIII-6 (LAKRIS 2006) cruises. Also, we would like to express our deepest gratitude to the cruise leader and the organizers of the “Ice Station POLarstern” (ISPOL) field experiment, which provided a unique opportunity to work in the Antarctic pack ice environment for such an extended period. Ingo Arndt, the expedition photographer of ANT XXII-2, skillfully produced the excellent images of live amphipods. Sigi Schiel generously shared both the multinet amphipod samples as well as live copepods for the predation experiments with us, and both Angelika Brandt and Wim Vader provided insightful and constructive comments as reviewers.

References

- Ainley, D., Fraser, W., Sullivan, C., Torres, J., Hopkins, T., Smith, W., 1986. Antarctic mesopelagic micronekton: evidence from seabirds that pack ice affects community structure. *Science* 232, 847–849.
- Andres, H., Lörz, A., Brandt, A., 2002. A common, but undescribed huge species of *Eusirus* KRØYER, 1845 (Crustacea, Amphipoda, Eusiridae) from Antarctica. *Mitteilungen aus dem Hamburgischen Zoologischen Museum und Institut* 99, 109–126.
- Arndt, C., Swadling, K., 2006. Crustacea in Arctic and Antarctic sea ice: distribution, diet and life history strategies. *Advances in Marine Biology* 51, 197–315.
- Barnard, J., Karaman, G., 1991. The Families and Genera of Marine Gammaridean Amphipoda (except Marine Gammaroids), Part 1.2. *Records of the Australian Museum Supplement* 13, 1–866.
- Bregazzi, P., 1972a. Habitat selection by *Cheirimedon femoratus* (Pfeffer) and *Tryphosella kergueleni* (Miers) (Crustacea: Amphipoda). *British Antarctic Survey Bulletin* 31, 21–31.
- Bregazzi, P., 1972b. Life cycle and seasonal movements of *Cheirimedon femoratus* (Pfeffer) and *Tryphosella kergueleni* (Miers) (Crustacea: Amphipoda). *British Antarctic Survey Bulletin* 30, 1–34.
- Bregazzi, P., 1973. Locomotor activity rhythms in *Tryphosella kergueleni* (Miers) and *Cheirimedon femoratus* (Pfeffer) (Crustacea: Amphipoda). *British Antarctic Survey Bulletin* 33–34, 17–32.
- Dauby, P., Scailteur, Y., Chappelle, G., De Broyer, C., 2001. Potential impact of the main benthic amphipods on the eastern Weddell Sea shelf ecosystem (Antarctica). *Polar Biology* 24, 657–662.
- De Broyer, C., 1983. Recherches sur la systématique et l'évolution des crustacés amphipodes gammarides antarctiques et subantarctiques. Université Catholique de Louvain, Faculté des Sciences, Louvain-la-Neuve.
- De Broyer, C., Jazdzewski, K., 1993. A checklist of the Amphipoda (Crustacea) of the Southern Ocean. In: *Studiedocumenten van het Koninklijk Belgisch Instituut voor Natuurwetenschappen*, vol. 73. Royal Belgian Institute for Natural Sciences, Brussels.
- Fisher, E., Kaufmann, R., Smith, K.J., 2004. Variability of epipelagic macrozooplankton/micronekton community structure in the NW Weddell Sea, Antarctica (1995–1996). *Marine Biology* 144, 345–360.
- Foster, B., 1987. Composition and abundance of zooplankton under the spring sea-ice of McMurdo Sound, Antarctica. *Polar Biology* 8, 41–48.
- Garrison, D., 1991. Antarctic sea ice biota. *American Zoologist* 31, 17–33.
- Graeve, M., Dauby, P., Scailteur, Y., 2001. Combined lipid, fatty acid and digestive tract content analyses: a penetrating approach to estimate feeding modes of Antarctic amphipods. *Polar Biology* 24, 853–862.
- Gulliksen, B., Lønne, O., 1991. Sea ice macrofauna in the Antarctic and the Arctic. *Journal of Marine Systems* 2, 53–61.

- Hellmer, H., Schröder, M., Haas, C., Dieckmann, G., Spindler, M., 2008. The ISPOL drift experiment. *Deep-Sea Research II*, this issue [doi: 10.1016/j.dsr2.2007.12.018].
- Hop, H., Poltermann, M., Lønne, O., Falk-Petersen, S., Korsnes, R., Budgell, W., 2000. Ice amphipod distribution relative to ice density and under-ice topography in the northern Barents Sea. *Polar Biology* 23, 357–367.
- Hopkins, T., 1987. Midwater food web in McMurdo Sound, Ross Sea, Antarctica. *Marine Biology* 96, 93–106.
- Jazdzewski, K., De Broyer, C., Pudlacz, M., Dauby, P., 2000. Amphipods of a stony beach in the maritime Antarctic. *Polskie Archiwum Hydrobiologii/Polish Archives of Hydrobiology* 47, 569–577.
- Kaufmann, R., Smith Jr., K., Baldwin, R., Glatts, R., Robison, B., Reisenbichler, K., 1993. Epipelagic communities in the northwestern Weddell Sea: results from acoustic, trawl, and trapping surveys. *Antarctic Journal of the United States* 28, 138–141.
- Kaufmann, R., Smith Jr., K., Baldwin, R., Glatts, R., Robison, B., Reisenbichler, K., 1995. Effects of seasonal pack ice on the distribution of macrozooplankton and micronekton in the northwestern Weddell Sea. *Marine Biology* 124, 387–397.
- Kiko, R., Michels, J., Mizdalski, E., Schnack-Schiel, S., Werner, I., 2008. Living conditions, abundance and composition of the metazoan fauna in surface and sub-ice layers in pack ice of the western Weddell Sea during late spring. *Deep Sea Research II*, this issue [doi: 10.1016/j.dsr2.2007.12.018].
- Klages, M., 1993. Distribution, reproduction and population dynamics of the Antarctic Gammaridean Amphipod *Eusirus perdentatus* Chevreux, 1912 (Crustacea). *Antarctic Science* 5, 349–359.
- Klages, M., Gutt, J., 1990. Observations on the feeding behaviour of the Antarctic gammarid *Eusirus perdentatus* Chevreux, 1912 (Crustacea: Amphipoda) in aquaria. *Polar Biology* 10, 359–364.
- Lønne, O., Gulliksen, B., 1991. Sympagic macro-fauna from multiyear sea-ice near Svalbard. *Polar Biology* 11, 471–477.
- Marschall, H.-P., 1988. The overwintering strategy of Antarctic krill under the pack-ice of the Weddell Sea. *Polar Biology* 9, 129–135.
- Nygård, H., 2005. Couplings between bottom and ice fauna in a shallow area in Svalbard, Norway. Master's Thesis, Åbo Akademi, Åbo, Finland.
- Richardson, M., Whitaker, T., 1979. An Antarctic fast-ice food chain: observations on the interaction of the amphipod *Pontogeneia antarctica* Chevreux with ice-associated micro-algae. *British Antarctic Survey Bulletin* 47, 107–115.
- Sagar, P., 1980. Life cycle and growth of the Antarctic gammarid amphipod *Paramoera walkeri* (Stebbing, 1906). *Journal of the Royal Society of New Zealand* 10, 259–270.
- Schnack-Schiel, S., Michels, J., Mizdalski, E., Schodlok, M., Schröder, M., 2008. Composition and community structure of zooplankton in the sea ice covered western Weddell Sea in spring 2004—with emphasis on calanoid copepods. *Deep-Sea Research II*, this issue [doi: 10.1016/j.dsr2.2007.12.018].
- Segerstråle, S., 1946. On the occurrence of the amphipod, *Gammarus duebeni* Lillj. in Finland, with notes on the ecology of the species. *Societas Scientiarum Fennica: Commentationes Biologicae* 9, 1–22.
- Segerstråle, S., 1954. The freshwater amphipods, *Gammarus pulex* (L.) and *Gammarus lacustris* G. O. Sars, in Denmark and Fennoscandia—a contribution to the late- and post-glacial immigration history of the aquatic fauna of northern Europe. *Societas Scientiarum Fennica: Commentationes Biologicae* 15, 1–91.
- Smetacek, V., Bathmann, U., Helmke, E., 2005. The expeditions ANTARKTIS XXI/3-4-5 of the research vessel “Polarstern” in 2004. *Berichte zur Polar- und Meeresforschung*, vol. 500. Alfred-Wegener-Institut für Polar- und Meeresforschung, Bremerhaven.
- Stockton, W., 1982. Scavenging amphipods from under the Ross ice shelf, Antarctica. *Deep-Sea Research* 29, 819–835.
- Werner, I., 1997. Grazing of Arctic under-ice amphipods on sea-ice algae. *Marine Ecology Progress Series* 160, 93–99.
- Werner, I., Lindemann, F., 1997. Video observations of the underside of Arctic sea ice—features and morphology on medium and small scales. *Polar Research* 16, 27–36.
- Werner, I., Auel, H., Kiko, R., 2004. Occurrence of *Anonyx sarsi* (Amphipoda: Lysianassidae) below Arctic pack ice—an example for cryo-benthic coupling? *Polar Biology* 27, 474–481.

APPENDIX

1. Co-author statements and signatures (1-10)
2. Additional publications and errata

Norman, L., Thomas, D. N., Stedmon, C. A., Granskog, M. A., Papadimitriou, S., **Krapp**, R. H., Meiners, K. M., Lannuzel, D., van der Merwe, P., & Dieckmann, G. S. (2011). The characteristics of dissolved organic matter (DOM) and chromophoric dissolved organic matter (CDOM) in Antarctic sea ice. *Deep-Sea Research. Part II, Topical Studies in Oceanography*, 58(9–10), 1075–1091.
<https://doi.org/10.1016/j.dsr2.2010.10.030>

Krapp, R. H., Baussant, T., Berge, J., Pampanin, D. M., & Camus, L. (2009b). Erratum to “Antioxidant responses in the polar marine sea-ice amphipod *Gammarus wilkitzkii* to natural and experimentally increased UV levels” [*Aquat.Toxicol.* 94 (2009) 1–7]. *Aquatic Toxicology (Amsterdam, Netherlands)*, 95(2), 162.
<https://doi.org/10.1016/j.aquatox.2009.10.013>

Paper 5

Norman, L., Thomas, D.N., Stedmon, C.A., Granskog, M.A., Papadimitriou, S., Krapp, R.H., ... Dieckmann, G.S. (2011).

The characteristics of dissolved organic matter (DOM) and chromophoric dissolved organic matter (CDOM) in Antarctic sea ice

Deep-Sea Research II, 58, 1075-1091.



Contents lists available at ScienceDirect

Deep-Sea Research II

journal homepage: www.elsevier.com/locate/dsr2

The characteristics of dissolved organic matter (DOM) and chromophoric dissolved organic matter (CDOM) in Antarctic sea ice

Louiza Norman^a, David N. Thomas^{a,*}, Colin A. Stedmon^b, Mats A. Granskog^{c,d}, Stathys Papadimitriou^a, Rupert H. Krapp^e, Klaus M. Meiners^f, Delphine Lannuzel^{f,g}, Pier van der Merwe^{f,h}, Gerhard S. Dieckmannⁱ

^a School of Ocean Sciences, College of Natural Sciences, Bangor University, Menai Bridge, Anglesey LL59 5AB, UK

^b Department of Marine Ecology, National Environmental Research Institute, Aarhus University, Frederiksborgvej 399, 4000 Roskilde, Denmark

^c Arctic Centre, University of Lapland, 96101 Rovaniemi, Finland

^d Norwegian Polar Institute, Polar Environmental Centre, 9296 Tromsø, Norway

^e University Center in Svalbard, P.O. Box 156, N-9171 Longyearbyen, Norway

^f Antarctic Climate and Ecosystems Cooperative Research Centre, Private Bag 80, Hobart 7001, Tasmania, Australia

^g Centre for Marine Science, Private Bag 78, Hobart, Tasmania 7001, Australia

^h Institute of Antarctic and Southern Ocean Studies, University of Tasmania, Private Bag 50, Hobart, Tasmania 7001, Australia

ⁱ Alfred Wegener Institute for Polar and Marine Research, Am Handelshafen 12, D-27570 Bremerhaven, Germany

ARTICLE INFO

Article history:

Received 20 October 2010

Accepted 20 October 2010

Available online 7 January 2011

Keywords:

Sea ice

Antarctic

Coloured dissolved organic matter (CDOM)

Dissolved organic matter (DOM)

Photochemistry

Biogeochemistry

ABSTRACT

An investigation of coloured dissolved organic matter (CDOM) and its relationships to physical and biogeochemical parameters in Antarctic sea ice and oceanic water have indicated that ice melt may both alter the spectral characteristics of CDOM in Antarctic surface waters and serve as a likely source of fresh autochthonous CDOM and labile DOC. Samples were collected from melted bulk sea ice, sea ice brines, surface gap layer waters, and seawater during three expeditions: one during the spring to summer and two during the winter to spring transition period. Variability in both physical (temperature and salinity) and biogeochemical parameters (dissolved and particulate organic carbon and nitrogen, as well as chlorophyll *a*) was observed during and between studies, but CDOM absorption coefficients measured at 375 nm (a_{375}) did not differ significantly. Distinct peaked absorption spectra were consistently observed for bulk ice, brine, and gap water, but were absent in the seawater samples. Correlation with the measured physical and biogeochemical parameters could not resolve the source of these peaks, but the shoulders and peaks observed between 260 and 280 nm and between 320 to 330 nm respectively, particularly in the samples taken from high light-exposed gap layer environment, suggest a possible link to aromatic and mycosporine-like amino acids. Sea ice CDOM susceptibility to photo-bleaching was demonstrated in an *in situ* 120 hour exposure, during which we observed a loss in CDOM absorption of 53% at 280 nm, 58% at 330 nm, and 30% at 375 nm. No overall coincidental loss of DOC or DON was measured during the experimental period. A relationship between the spectral slope (*S*) and carbon-specific absorption (a_{375}^*) indicated that the characteristics of CDOM can be described by the mixing of two broad end-members; and aged material, present in brine and seawater samples characterised by high *S* values and low a_{375}^* ; and a fresh material, due to elevated *in situ* production, present in the bulk ice samples characterised by low *S* and high a_{375}^* . The DOC data reported here have been used to estimate that approximately 8 Tg C yr⁻¹ (~11% of annual sea ice algae primary production) may be exported to the surface ocean during seasonal sea ice melt in the form of DOC.

© 2010 Elsevier Ltd. All rights reserved.

1. Introduction

Sea ice in the polar oceans (Arctic and Southern) and sub-polar seas (e.g., Baltic and White Seas, Hudson Bay) provides a range of physically and geochemically unique habitats, which can support rich and diverse biological assemblages. Sea ice has long been recognised to play a key role in the biogeochemical cycles of ice-covered oceans and seas (Thomas and Dieckmann, 2002a, b; Thomas et al., 2010). The biogeochemical composition of sea ice often yields elevated concentrations of dissolved organic matter (DOM) (Thomas et al., 2010) with distinct optical characteristics as determined on the coloured fraction

* Corresponding author. Tel./fax: +44 1248 382 878.

E-mail addresses: Louisa.Norman@student.uts.edu.au (L. Norman), d.thomas@bangor.ac.uk (D.N. Thomas), cst@dmu.dk (C.A. Stedmon), mats.granskog@npolar.no (M.A. Granskog), s.papadimitriou@bangor.ac.uk (S. Papadimitriou), rkrapp@gmail.com (R.H. Krapp), Klaus.Meiners@acecrc.org.au (K.M. Meiners), delphine.lannuzel@utas.edu.au (D. Lannuzel), pvander@utas.edu.au (P. van der Merwe), Gerhard.dieckmann@awi.de (G.S. Dieckmann).

of DOM, chromophoric dissolved organic matter (CDOM), relative to the surrounding surface waters (Perovich et al., 1998; Belzile et al., 2000; Stedmon et al., 2007).

The marine DOM pool consists of both allochthonous (terrestrial) and autochthonous (marine) material derived from the biosynthesis of organic matter (Nelson and Siegel, 2002). Ubiquitous in all marine environments, CDOM can make up a substantial proportion of the DOM pool in aquatic systems (Thurman, 1985; Coble, 2007), representing up to 60% of the bulk DOC pool (Ertel et al., 1986). The reactivity of CDOM to sunlight has a significant effect on the cycling of both DOM and CDOM (Obernosterer and Benner, 2004) as the absorption of UV radiation by CDOM initiates a set of photochemical reactions, which either directly remineralise the organic matter or leads to the formation of a number of reactive products (Miller and Zepp, 1995; Uher and Andreae, 1997; King et al., 2005; Stubbins et al., 2006; Xie et al., 2009) some of which (i.e. ammonium and phosphate) are biologically labile (Moran and Zepp, 1997; Kitidis et al., 2008).

The optical characteristics of sea ice CDOM are a composite of those of the CDOM present in the surface oceanic water, from which the ice formed, and those of the CDOM in the DOM pool produced in sea ice by the activity of sympagic organisms (Thomas et al., 2001; Granskog et al., 2006; Stedmon et al., 2007). The *in situ* DOM production and its cycling in the often closed environment of sea ice, with little or intermittent accessibility to the pool of nutrients in the surface ocean, can be an important source of nutrients to sympagic assemblages.

One of the unique features of the seasonally ice-covered region of the Southern Ocean is that there are no major terrestrial inputs of DOM, which is in stark contrast to the northern polar and sub-polar regions that are influenced by dense and large river networks (Retamal et al., 2007). Hence, the DOM incorporated in Arctic and sub-Arctic sea ice during ice formation has a substantial river-borne allochthonous component (Benner et al., 2005; Granskog et al., 2006; Stedmon et al., 2007), whereas the DOM incorporated into sea ice formed in the Southern Ocean will be predominantly autochthonous in origin. As a result, the Southern Ocean provides a unique opportunity to investigate the composition and behavior of marine-derived organic matter divorced from terrestrial inputs.

There are very few studies of the optical characteristics of CDOM in sea ice, with none, to our knowledge, in Antarctic sea ice. As mentioned above, the optical properties of CDOM in Baltic sea ice have been shown to differ from that of the under-ice seawater (Ehn et al., 2004; Granskog et al., 2005) as a result of *in situ* (sympagic) CDOM production (Stedmon et al., 2007). Belzile et al. (2000) showed that CDOM was a significant component of the DOM pool attenuating UV light in Arctic first-year sea ice, as did Ehn et al. (2004) and Uusikivi et al. (2010) for the Baltic Sea. Scully and Miller (2000) concluded that melting sea ice would be a source of CDOM to the surface ocean in Baffin Bay (Canadian Arctic), and both Kieber et al. (2009) and Ortega-Retuerta et al. (2010) considered that Antarctic sea ice might be a potential source of CDOM, although this was suggested without direct evidence. The limited number of polar and sub-polar studies have revealed the potential of sea ice as a CDOM reactor and a source of CDOM with distinct optical properties to the surface ocean.

In this study we investigated the optical properties of CDOM in Antarctic sea ice from two regions of the polar Southern Ocean, the Weddell Sea and East Antarctica, in the early spring and early summer. The data were collected from a wide range of sea ice types in respect of age, temperature, and thickness, as well as biological standing stocks. We report on the optical properties of CDOM from directly-sampled sea ice brine, melted (bulk) sea ice from ice cores, the hyposaline water from surface gap layers, and seawater. The relationships between the spectral properties of CDOM and the concentrations of DOC, dissolved organic nitrogen (DON), particulate organic carbon

(POC), particulate nitrogen (PN), and chlorophyll *a* (Chl_a) are examined and discussed in relation to the importance of CDOM in the sea ice, and we assess the potential of sea ice as a source of CDOM to the Southern Ocean.

2. Study sites and sampling

2.1. Study sites

The initial part of the study was conducted in the transition from spring to summer (December 2004) during the interdisciplinary field experiment *Ice Station POLarstern* (ISPOL) (Hellmer et al., 2008). During the experiment, the physical and biogeochemical properties of a single, 10 × 10 km (initial dimensions) ice floe were monitored. The ISPOL floe was located in the western Weddell Sea, where it drifted in a northerly direction at approximately 67–68°S and 55°W (Fig. 1). Samples were taken from first- and second-year ice from the structurally heterogeneous ISPOL floe, as well as from the water of 2 spatially separate gap layers in the upper 10 to 30 cm of the ice column. Details of the physical and chemical features of the floe have been reported elsewhere (Haas et al., 2007; Lannuzel et al., 2008; Papadimitriou et al., 2007, 2009).

The second part of the study was conducted in the transition from winter to spring (September–October 2006) during the *Winter Weddell Outflow Study* (WWOS) on board R.V. *Polarstern* (Lemke, 2009). The cruise track took an east to west transect between 60° to 61°S and 40° to 52°W, and a northeast to southwest transect between 60°S and 65°S, in the north-western Weddell Sea (Hellmer et al., 2009). Brine and ice core samples were obtained at 22 ice stations during a 38-day period (Fig. 1). Physical, chemical, and biological parameters of the WWOS sites have been reported in Haas et al. (2009) and Meiners et al. (2009).

The third part of the study was conducted during the *Sea Ice Physics and Ecosystem Experiment* (SIPEX) onboard the R.S. *Aurora Australis* in the transition from winter to spring (September–October 2007) on 14 ice stations within the 110–130° E region off Eastern Antarctica (Fig. 1). During the SIPEX experiment, the sea ice was thinner than that studied during ISPOL and WWOS, with many of the floes relatively undeformed and less than 60 cm thick. The majority of samples were taken from first-year ice. One station was fast ice, and one station was rafted consolidated pancake sea ice close to the marginal ice zone from which two cores were taken.

2.2. Sampling

Under-ice seawater samples were taken using a Seabird 911+CTD rosette equipped with 12 L Niskin bottles during ISPOL and WWOS, and with a manual, messenger-operated 2 L Niskin bottle during SIPEX. All samples were collected in acid-cleaned 1 or 2 L HDPE bottles.

Ice cores were drilled either manually or using an electric motor, using a KOVACS Mark II (9 cm internal diameter) ice corer, and were immediately sectioned into 10 cm segments directly into acid-cleaned 1L plastic tubs. To maintain consistency all cores were sectioned starting at the bottom of the core and working towards the top. Temperature measurements were taken from a companion core by drilling a small hole at the mid-point of each 10 cm section and inserting a calibrated K–Thermocouple probe on a HANNA Instruments thermometer (HI93530). All ice core sections were then returned to the onboard laboratory and were melted in the dark at +4 °C.

Brine samples were collected using the sackhole sampling method by manually drilling partial bore holes into the ice surface after removing the snow cover and allowing the brine from the surrounding brine channels to percolate into the hole (Gleitz et al., 1995). Between three and six sackholes were drilled on each

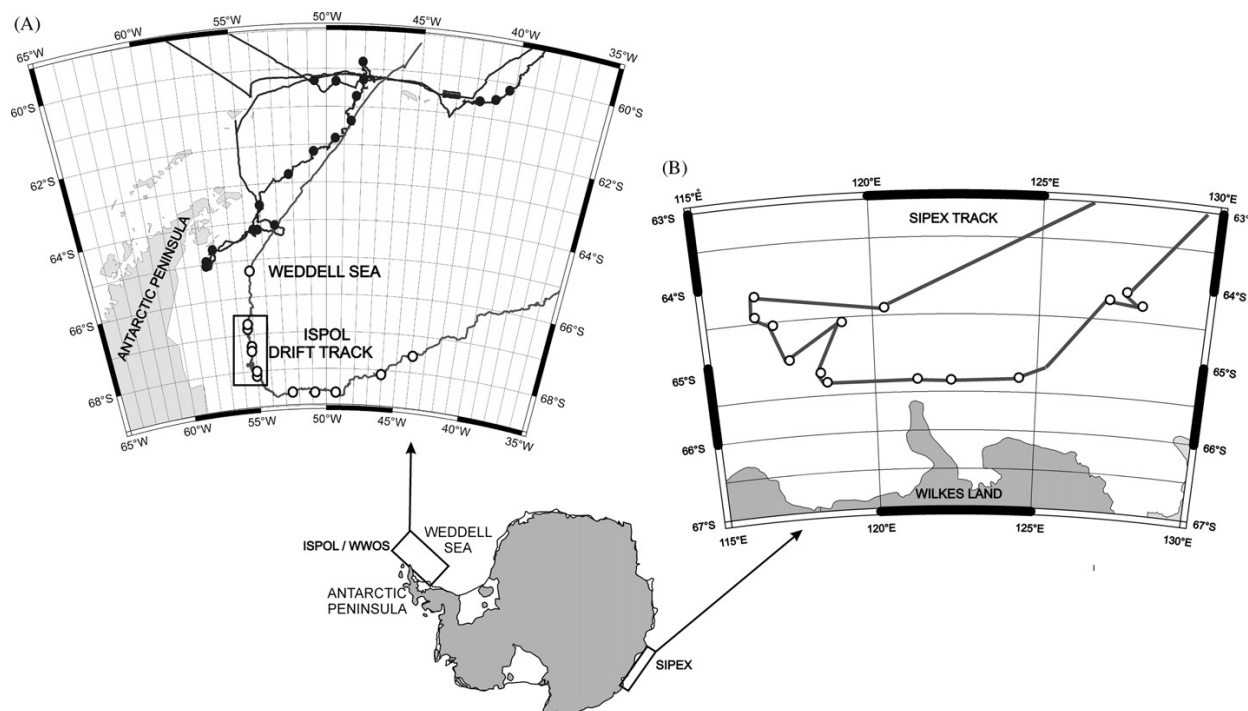


Fig. 1. Cruise tracks and ice stations for (A) the ISPOL drift experiment (27/11/04 to 02/01/05), indicated with open circles, with drift area contained within box, and the WWOS field study (06/09/06 to 13/10/06), indicated with solid circles, both in the Weddell Sea, Antarctica, and (B) the SIPEX field study (11/09/07 to 10/10/07) in the Eastern Antarctic region. The ISPOL/WWOS map was provided by Marcel Nicolaus, Norwegian Polar Institute. The SIPEX map was generated using Online Map Creation.

occasion using a 14 cm (ID) Kovacs Mark V ice corer within approximately a 2 m² ice surface to depths between 16 and 186 cm, but mostly in the 30 to 60 cm range, depending on the thickness of the ice. Ice shavings and slush were removed, and Styrofoam covers were placed over the top of the sackholes to ensure that samples were not compromised by snow, slush, or debris, and to minimise air-brine interaction (Papadimitriou et al., 2007). During ISPOL, sufficient volume of brine was generally collected after 10 minutes, but due to the colder temperatures during the WWOS and SIPEX studies, the time required to collect sufficient brine was 0.5 to 3, and 3 to 7 hours, respectively. The brine samples were collected into acid-cleaned 1L plastic containers using an acid-cleaned 100 mL plastic syringe fitted with a 30 cm length of Teflon tubing. Deeper sackholes were sampled with a stainless steel ladle attached to a pole. The brine temperature was measured *in situ* using a calibrated K-Thermocouple probe on a HANNA Instruments thermometer (HI93530). Sackhole sampling has been shown to be a suitable method for measurements of dissolved constituents in brines but unsuitable for quantitative measurements of the particulate fraction because the latter does not percolate quantitatively with the brine (Weissenberger, 1992; Papadimitriou et al., 2007). The concentrations of Chl_a, POC, and PN measured in sackhole brine samples are therefore underestimates of actual *in situ* concentrations and are reported here only as relative abundance indicators for biomass.

2.3. Samples

The ISPOL samples comprised:

- 1) Seawater samples from four CTD stations at water depths between 5 and 1516 m;

- 2) Seven ice cores from two sites on the floe, five ice cores from a level 50 × 50 m patch of thin first-year ice, and two ice cores from a spatially separate site with thick second-year ice;
- 3) 31 brine samples, 28 hypersaline (salinity > 35) and 3 hyposaline (salinity < 35), 29 from a separate site on the floe with thick first-year ice and two from a location with thick second-year ice;
- 4) 23 hyposaline water samples from two spatially separate gap layers, one overlying thick first-year ice and another overlying second-year ice from which the two ice cores were also obtained as described in 2) above.

The five ice cores from the thin first-year ice described in 2) above were part of a temporal study and were taken at approximately 5 day intervals between 29/11/04 and 30/12/04. The brine samples were collected between 02/12/04 and 29/12/04 at intervals of 3 to 9 days, with a minimum of three sackholes sampled at each sampling event. The biological and geochemical composition of the hypersaline sackhole brines and the hyposaline gap waters from the ISPOL floe has been reported in Papadimitriou et al. (2007, 2009).

The WWOS samples comprised:

- 1) Seawater samples from five CTD stations at water depths between 20 and 5591 m;
- 2) 12 ice cores, 11 from first-year ice and one from second-year ice;
- 3) 118 brine samples, 100 from first-year ice and 18 from second-year ice.

The SIPEX samples comprised:

- 1) 28 under-ice water samples taken at between 1 and 10 m depth;
- 2) 33 ice cores, 30 from first-year ice and three from second-year ice;

3) 38 brine samples, 33 from first-year ice and five from second-year ice.

Fifteen of the ice cores and 16 of the brine samples were taken from sites dedicated to trace iron analysis (van der Merwe et al., 2009). One core was taken from a heavily deformed floe (209 cm thick), and one further core and three brine samples came from an area of land fast ice.

2.4. Photo-bleaching experiment

In addition to field sampling, a CDOM photo-bleaching experiment was set up during ISPOL in order to investigate the changes in brine CDOM during photo-bleaching at *in situ* conditions. Ten borosilicate and 10 quartz 220-mL tubes with stoppers (all pre-combusted at 500 °C for 3 hours) were filled with filtered (using pre-combusted WHATMAN GF/F filters) brine taken from a single sackhole (salinity=55.2). The borosilicate tubes were wrapped in foil to maintain dark conditions and served as control samples, while the quartz tubes were left unwrapped. All vessels were then half-buried in surface snow to minimise temperature variation. Samples for CDOM, DOC, and DON analyses were taken at time zero. Thereafter, two control tubes and two experimental tubes were harvested, thoroughly mixed, and sampled for CDOM, DOC, and DON analyses at 12, 18, 24, 48, and 120 hours. During the experiment light measurements were recorded using a hyperspectral radiometer (TriOS RAMSES ACC-UV) for the UVA (measured between 320 and 400 nm) and UVB (measured between 280 and 320 nm) spectral range, while 2 π quantum sensor (LI-190) was used for the PAR range (400 to 550 nm). Both sensors were placed on the snow surface in proximity to the sample vials, making sure that no shading effects occurred by any of the sensors, cables or connected recorders. The sensors were connected to a PC and a LI-COR datalogger (LI-1400) for control and data storage, respectively. The sampling rates were set to 5 min intervals and the spectral resolution for the radiometer was 2.2 nm. The PAR data are expressed in $\mu\text{mol m}^{-2} \text{s}^{-1}$ while the UVR data are expressed in W m^{-2} .

2.5. Analytical techniques

All salinity measurements were taken at laboratory temperature (17 to 22 °C) using a SEMAT Cond 315i/SET salinometer with WTW Tetracon 325 probe. As the maximum range of the instrument is salinity=70 (measured in PSU), samples with higher salinity were measured after dilution with ultrapure water. The samples for the determination of Chl_a, POC, and PN were collected from an aliquot of known volume on pre-combusted (500 °C, three hours) filters (WHATMAN, GF/F) and were kept at –20 °C until analysis of Chl_a in the onboard laboratory and POC/PN in the Bangor University (ISPOL and WWOS) and University of Tasmania (SIPEX) laboratories. The extracted Chl_a was measured using a Turner Designs 10 AU fluorometer (detection limit of the instrument 0.02 $\mu\text{g L}^{-1}$) following the method of Evans et al. (1987) during ISPOL and WWOS, and Holm-Hansen et al. (1965) during SIPEX. The POC and PN concentrations were determined with a CARLO ERBA NA 1500 Elemental CHN Analyzer (ISPOL and WWOS) and a Thermo Finnigan EA 1112 Series Flash Elemental Analyser (SIPEX) after overnight fumigation with 37% (w/v) HCl to remove the inorganic carbon fraction and oven-drying at 60 °C.

The filtrate provided samples for DOC, DON, and CDOM measurements during ISPOL and WWOS, while, during SIPEX, such samples were obtained by filtering through disposable syringe filters (WHATMAN, GD/X) using an acid-cleaned 20 mL all-plastic syringe. The DON samples were stored at –20 °C in acid-cleaned

20 mL scintillation vials, while the DOC samples were stored acidified with ~20 μL of ultrapure orthophosphoric acid in pre-combusted (500 °C, three hours) 4mL borosilicate vials with Teflon-lined screw caps at –20 °C until analysis in the Bangor University laboratory. The DOC and DON were analysed as described in Papadimitriou et al. (2007).

The CDOM samples were stored refrigerated in the dark in acid-cleaned plastic bottles and were measured within 24 hours of collection. The absorbance of CDOM was measured at room temperature using a dual beam Shimadzu 1601 UV-Vis spectrophotometer over the range 200 to 750 nm at a resolution of 0.5 nm. The optical density acquired from the instrument was converted to the CDOM absorption coefficient ($a_{\text{CDOM},\lambda}$) using the equation

$$a_{\text{CDOM},\lambda} = 2.303 \frac{A(\lambda)}{r} \quad (1)$$

where $a_{\text{CDOM},\lambda}$ = absorption coefficient (m^{-1}), $A(\lambda)$ = optical density at a given wavelength λ , 2.303 = conversion factor from \log_{10} to \log_e units, and r = length of optical path = 0.10 m.

The CDOM absorption spectrum typically declines exponentially with wavelength (λ) when measured from 300 to 650 nm and, hence, can be modeled as an exponential function of λ (Bricaud et al., 1981). The modeled exponential slope of this spectrum (S) offers an indication of CDOM quality because it varies depending on its source (terrestrial or marine), age (fresh or old), and extent of degradation (Carder et al., 1989; Stedmon and Markager, 2001). The absorption at a specific wavelength can be used as an indicator of CDOM concentration. A range of wavelengths have been used in the past here we use 375 nm. The wavelength range from which S is calculated, and the choice of 375 nm, represents a compromise between analytical chemistry where CDOM absorption at UV wavelengths is due to its aromatic content (Chin and Gschwend, 1992), and aquatic bio-optics when predicting penetration of natural light is of interest. Reporting the absorption at 375 nm together with the S value derived from across the whole UVA and visible light range allows others to predict the light attenuation due to CDOM. The carbon-specific CDOM absorption (a_{375}^* , in $\text{m}^2 \text{g}^{-1} \text{C}$) is the absorption normalised to the DOC concentration (expressed in g C m^{-3}) and together with S represents a qualitative measure of CDOM colour.

All concentrations are reported on a per kg solution (mass) basis (C_{mass}) after conversion of the measurements on a per unit volume basis (C_{vol}) as

$$C_{\text{mass}} = \frac{C_{\text{vol}}}{\rho'} \quad (2)$$

with ρ' = sample density at the temperature of sample processing. The density of melted sea ice (ρ'_{melt}), brine (ρ'_b), and gap waters (ρ'_{gap}) in laboratory conditions were calculated by extrapolation of the equation of state for seawater in Millero and Poisson (1981) to the sample salinity, because the major ionic composition of sea ice-derived solutions reflects physical modification of that of oceanic water. The concentrations measured in melted bulk ice were further converted to per kg of brine at *in situ* temperature conditions as

$$C_{b, \text{mass}} = \frac{(C_{\text{vol}}/\rho'_{\text{melt}})\rho_{\text{bulk ice}}}{(V_b/V)\rho_b} \quad (3)$$

where (V_b/V) is the relative brine volume, and $\rho_{\text{bulk ice}}$ and ρ_b are the bulk ice and brine densities, respectively, at *in situ* temperature, all calculated as in Cox and Weeks (1983), using the polynomial functions in Cox and Weeks (1983) for temperatures ≤ -2 °C and Leppäranta and Manninen (1988) for temperatures between 0 > and > –2 °C and an (assumed) relative air volume of 1.5% (C. Haas, pers. comm.). The concentrations directly measured in sackhole brines and those derived from bulk sea ice measurements were

Table 1
Physical parameters measured in sea ice and brines collected during this study.

	ISPOL 27/11/04 - 02/01/05			WWOS 06/09/06 - 13/10/06		SIPEX 11/09/07 - 10/10/07	
	Bulk Ice	Brine	Surface Gap Layers	Bulk Ice	Brine	Bulk Ice	Brine
Thickness (cm)	72 to 226, n=9		1 to 16, n=23	88 to 190, n=12		35 to 133 ^c , n=33	
Depth (cm)		20 to 78, n=36			16 to 66 ^b , n=118		14 to 80, n=41
Temperature (°C)	-2.5 to -1.1 ^a , n=96	-3.4 to -1.3 ^a , n=36	-1.8 to -0.8, n=23	-8.8 to -1.9, n=154	-8.7 to -3.6, n=126	-14.8 to -1.5, n=214	-12.4 to -2.2, n=24
Salinity	1.0 to 9.3, n=96	29.4 to 63.2, n=40	20 to 33, n=23	0.4 to 14.1, n=154	58.1 to 134.0, n=126	2.1 to 18.3, n=251	33 to 179, n=46
V _b /V (%)	2.6 to 31.9, n=95			0.2 to 25.0, n=154		0.2 to 34.8, n=208	

^a The brine samples were derived from the upper layers of thick first-year ice (Papadimitriou et al. 2007), which were colder than the temperature range of the ice cores obtained from spatially distinct, separate patches of thin first-year ice and thick second-year ice on the ISPOL floe.

^b A single brine sample was obtained from a sackhole of 186 cm depth.

^c A single 209-cm-thick ice core was obtained from rafted ice on a heavily deformed floe.

further normalised to a salinity of 35 as

$$C_{b, \text{mass}, S} = \frac{35}{S_b} C_{b, \text{mass}} \quad (4)$$

where S_b is the salinity of the brine, which, for bulk sea ice determinations, was calculated as a function of ice temperature (t , Petrich and Eicken, 2010) as

$$S_b = 1000 \left(1 - \frac{54.11}{t} \right)^{-1} \quad (5)$$

The temperature and salinity of bulk ice, brine, and surface waters, as well as ice thickness and V_b/V from all three studies are given in Table 1. Correlation analysis and analysis of variance were conducted on MINITAB, while regression analysis was based on the geometric mean regression in Ricker (1973). It should be noted that not all analysis were performed on every sample mentioned in Section 2.3 above, therefore numbers of observations quoted in the following results section and accompanying tables may differ.

3. Results

3.1. Physical and biochemical parameters

3.1.1. Seawater

The mean DOC and DON concentrations in seawater varied between expeditions (Table 2), with the SIPEX samples significantly higher than both ISPOL and WWOS ($p < 0.01$) for both parameters. The concentration of POC in the water column was measured during WWOS and SIPEX and was not significantly different between cruises, while PN data were only available for SIPEX. The measured Chl_a concentrations were all less than $0.25 \mu\text{g kg}^{-1}$ during the three studies (Table 2).

3.1.2. Bulk ice

The bulk ice temperature and salinity varied considerably between studies. The warmest ice temperatures and narrowest salinity range were encountered during the ISPOL drift experiment in the spring-summer transition (Table 1). Both the WWOS and SIPEX field studies were conducted during the winter-spring transition, yet

the SIPEX data set exhibited the widest temperature and salinity ranges, including the coldest ice temperature (-14.8°C) and highest bulk ice salinities (18.3) (Table 1).

The DOC, DON, POC, PN, and Chl_a concentrations in the bulk ice samples exhibited a high degree of variability, with their ranges extending over 1 to 3 orders of magnitude for each parameter (Table 2). The mean DOC concentrations were not significantly different across the three studies, with at least 75% of the samples being less than $60 \mu\text{mol kg}^{-1}$ despite the large concentration ranges. The DON concentrations were lower in the SIPEX samples (significant at $p < 0.01$) than both the ISPOL and WWOS samples (Table 2). Based on all available observations from bulk sea ice, $[\text{DOC}] > 200 \mu\text{mol kg}^{-1}$ and $[\text{DON}] > 40 \mu\text{mol kg}^{-1}$ were measured systematically and most frequently in the bottom 10–20 cm of the cores. No other distribution pattern with depth downcore was discernible for these parameters (Fig. 2). When the measured concentrations of DOC and DON were normalised to a salinity of 35 (Gleitz et al., 1995) both constituents were enriched relative to the mean salinity-normalised concentration in the underlying seawater (Table 2). The DOC was positively correlated with DON in all studies (Fig. 3; ISPOL: $r_{\text{linear}}^2 = 0.404$, $p < 0.001$, $n=61$; WWOS: $r_{\text{log-log}}^2 = 0.526$, $p < 0.001$, $n=148$; SIPEX: $r_{\text{log-log}}^2 = 0.318$, $p < 0.001$, $n=138$). The observed DOC to DON ratios were variable within all three datasets, but the mean DOC:DON was not significantly different between them (Table 2).

The mean concentrations of POC and PN measured in the SIPEX bulk ice samples (Table 2) were lower (significant at $p < 0.001$) than those measured during ISPOL and WWOS (Table 2), with the ISPOL and WWOS mean observations being almost 3-fold and 2-fold greater, respectively (Table 2). All datasets yielded positive correlations between POC and PN (Fig. 4; ISPOL: $r_{\text{log-log}}^2 = 0.297$, $p < 0.001$, $n=57$; WWOS: $r_{\text{log-log}}^2 = 0.914$, $p < 0.001$, $n=151$; SIPEX: $r_{\text{log-log}}^2 = 0.830$, $p < 0.001$, $n=110$), with the ISPOL observations exhibiting a greater degree of scatter. Mean POC to PN ratios (Table 2) differed significantly between the studies (all $p < 0.05$).

The Chl_a concentrations in the bulk ice samples were wide ranging in all datasets but especially in the WWOS dataset (Table 2; Fig. 5). The ranges of Chl_a concentration in the ISPOL and SIPEX samples were similar (Table 2), but the mean for the SIPEX samples was almost half that of the ISPOL samples. The majority of the ISPOL and WWOS samples yielded Chl_a concentrations between 1 and $7 \mu\text{g kg}^{-1}$, whereas the majority of SIPEX samples

Table 2
Mean \pm standard deviation, (range), and, number of observations (n) for measured and salinity-normalised concentrations (to a salinity of 35 and indicated by [salinity]) of dissolved constituents, and for measured concentrations of particulate constituents. All concentrations are reported in $\mu\text{mol kg}^{-1}$ solution except for Chla, which is reported in $\mu\text{g kg}^{-1}$ solution, while the DOC:DON and POC:PN are molar ratios.

	ISPOL 27/11/04 - 02/01/05				WVOS 06/09/06 - 13/10/06				SIPEX 11/09/07 - 10/10/07											
	Surface Gap Layers		Brine		Surface Gap Layers		Brine		Surface Gap Layers		Brine		Surface Gap Layers		Brine					
	Seawater	Bulk Ice	Seawater	Bulk Ice	Seawater	Bulk Ice	Seawater	Bulk Ice	Seawater	Bulk Ice	Seawater	Bulk Ice	Seawater	Bulk Ice	Seawater	Bulk Ice				
DOC [measured]	47 \pm 10 (29–66) n=22	47 \pm 31 (20–157) n=68	216 \pm 88 (23–343) n=36	87 \pm 72 (19–324) n=21	37 \pm 15 (14–76) n=12	44 \pm 68 (6–780) n=151	300 \pm 179 (114–970) n=124	53 \pm 10 (38–74) n=28	42 \pm 34 (7–325) n=240	160 \pm 70 (17–306) n=45	DOC [salinity]	48 \pm 10 (29–67) n=22	340 \pm 190 (104–906) n=68	131 \pm 44 (26–208) n=36	102 \pm 78 (26–366) n=21	38 \pm 16 (14–79) n=12	326 \pm 369 (45–2420) n=151	116 \pm 82 (45–475) n=124	254 \pm 224 (24–1547) n=194	60 \pm 31 (14–232) n=45
DON [measured]	2.5 \pm 1.7 (0.5–7.8) n=66	6.1 \pm 5.4 (0.5–29.9) n=85	14 \pm 5 (3–26) n=38	9 \pm 3 (6–15) n=20	3 \pm 1 (2–6) n=19	5.1 \pm 6.1 (0.2–50.2) n=150	18 \pm 12 (1–84) n=126	4 \pm 1 (2–6) n=28	3.7 \pm 3.9 (0.2–37.0) n=242	9 \pm 3 (3–16) n=46	DON [salinity]	2.6 \pm 1.8 (0.5–7.8) n=66	42 \pm 35 (4–156) n=85	9 \pm 4 (1–20) n=38	12 \pm 5 (6–23) n=20	3 \pm 1 (2–6) n=19	40 \pm 49 (1–267) n=150	6.8 \pm 5.2 (0.2–35.4) n=126	21 \pm 19 (1–159) n=200	4 \pm 2 (1–11) n=46
DOC:DON	2.9 \pm 2.5 (6–97) n=17	12 \pm 8 (2–50) n=61	16 \pm 5 (5–26) n=36	11 \pm 9 (3–37) n=36	9 \pm 3 (5–15) n=8	12 \pm 15 (3–145) n=148	21 \pm 27 (6–315) n=124	15 \pm 5 (9–35) n=28	15 \pm 16 (3–169) n=230	18 \pm 10 (3–62) n=45	POC	3.3 \pm 2.1 (0.4–5.8) n=6	128 \pm 178 (6–1195) n=81	64 \pm 26 (6–123) n=30	159 \pm 99 (28–427) n=23	no data	78 \pm 287 (3–3433) n=152	82 \pm 98 (8–537) n=120	41 \pm 54 (8–476) n=110	no data
PN	no data	11.6 \pm 12.2 (0.2–58.9) n=58	6.0 \pm 5.0 (0.9–22.8) n=25	11 \pm 9 (3–41) n=23	no data	9.3 \pm 37.6 (0.4–448.8) n=154	10 \pm 13 (1–70) n=120	0.3 \pm 0.2 (0.2–0.7) n=11	4.2 \pm 8.8 (0.2–74.0) n=110	no data	POC:PN	no data	26 \pm 36 (2–163) n=57	18 \pm 16 (4–79) n=25	15 \pm 5 (8–34) n=23	no data	10 \pm 4 (5–23) n=152	9 \pm 3 (5–29) n=120	19 \pm 12 (3–70) n=110	no data
Chla	< 0.1 n=6	7.9 \pm 15.7 (< 0.1–85.4) n=95	1.1 \pm 0.6 (< 0.1–2.1) n=34	7.2 \pm 11.4 (0.4–44.7) n=17	all < 0.25 n=77	23 \pm 185 (< 0.1–2191) n=142	2.9 \pm 2.8 (< 0.1–15.1) n=91	all < 0.1 n=11	4.0 \pm 10.4 (< 0.1–74.1) n=129	no data										

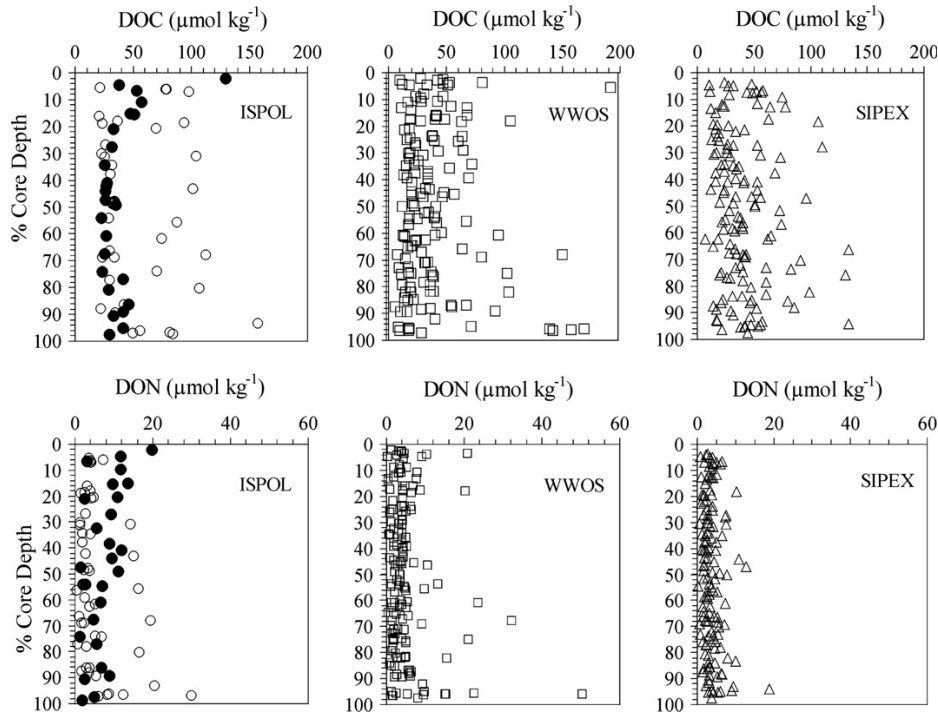


Fig. 2. Profiles of DOC and DON with depth in the ice ($y=0\%$ represents the air-ice or ice-snow interface). In the ISPOL observations, solid circles represent second-year ice with surface and internal communities, and open circles represent first-year ice. For clarity of presentation DOC concentrations $>200 \mu\text{mol kg}^{-1}$ are not included in the figures. The excluded observations were derived from the bottom section (142–155 cm depth below the ice surface) of the core obtained on 03/10/07 during SIPEX ([DOC]=325 $\mu\text{mol kg}^{-1}$) and bottom section (40–43 cm depth) of the core obtained on 05/10/06 during WWOS ([DOC]=780 $\mu\text{mol kg}^{-1}$).

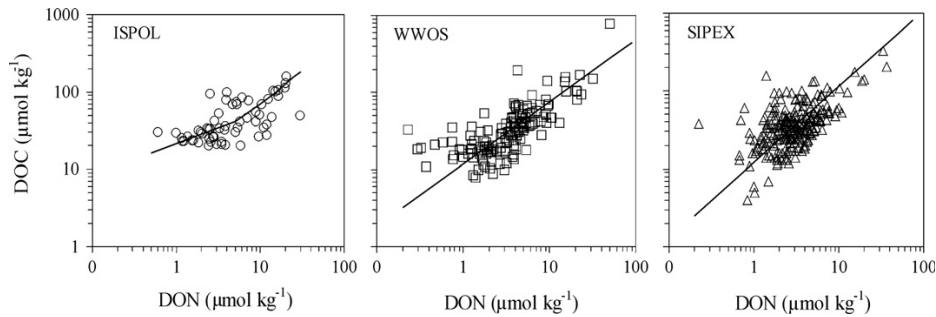


Fig. 3. DOC as a function of DON in bulk ice samples. The solid lines represent linear regressions on untransformed (ISPOL) and log-transformed data (WWOS, SIPEX). Regression equations: $[\text{DOC}] = 13 (\pm 9) + 6 (\pm 1) [\text{DON}]$ (ISPOL), $[\text{DOC}] = 12 [\text{DON}]^{0.9 (\pm 0.1)}$ (WWOS), and $[\text{DOC}] = 12 [\text{DON}]^{1.0 (\pm 0.1)}$ (SIPEX).

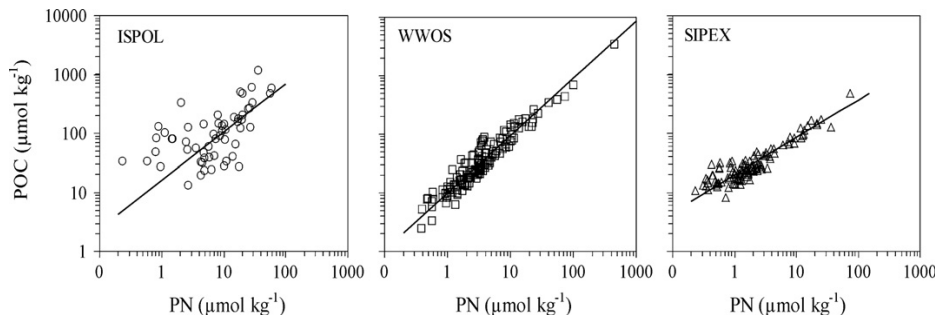


Fig. 4. POC as a function of PN in bulk ice samples. The solid lines represent regressions after log transformation of the data. Regression equations: $[\text{POC}] = 16 [\text{PN}]^{0.82 (\pm 0.19)}$ (ISPOL), $[\text{POC}] = 10 [\text{PN}]^{0.98 (\pm 0.08)}$ (WWOS), $[\text{POC}] = 20 [\text{PN}]^{0.63 (\pm 0.05)}$ (SIPEX).

yielded Chla concentrations $< 1 \mu\text{g kg}^{-1}$. The concentrations measured in the more algal-rich parts of the ice column were also variable between expeditions, with the ISPOL samples yielding Chla concentrations between 10 and $85 \mu\text{g kg}^{-1}$, WWOS from 10 to $2191 \mu\text{g kg}^{-1}$, and SIPEX from 3 to $46 \mu\text{g kg}^{-1}$. This indicates that, at the depth of biomass maximum in sea ice, the algal biomass densities were generally most moderate during the SIPEX study and highest during the WWOS study. The depth profiles of each of the particulate constituents clearly indicated concentration maxima within the bottom 10–20 cm of the cores, except for two second-year ice cores collected during ISPOL, which exhibited localised maximum concentrations higher up in the ice column, where surface and internal communities were present (Fig. 5).

3.1.3. sea ice brine

The temperature of the sea ice brines collected during the three studies ranged between -12.4 and -1.3 °C and their salinities ranged from 29.4 to 179. The highest temperatures and lowest salinities were measured during ISPOL and the lowest temperatures and highest salinities were measured during SIPEX (Table 1). In sea ice, brine salinity (S_b) is reported to be a function of ice temperature (Petrich and Eicken, 2010), and this relationship was evident in the direct observations of S_b and temperature from sackhole brines during each of the studies (Fig. 6; ISPOL: $r^2 = -0.956$, $p < 0.001$, $n = 39$; WWOS: $r^2 = -0.969$, $p < 0.001$, $n = 124$; SIPEX: $r^2 = -0.957$, $p < 0.001$, $n = 34$).

As with the bulk ice samples the DOC, DON, POC, PN, and Chla concentrations in the brine samples exhibited a high degree of

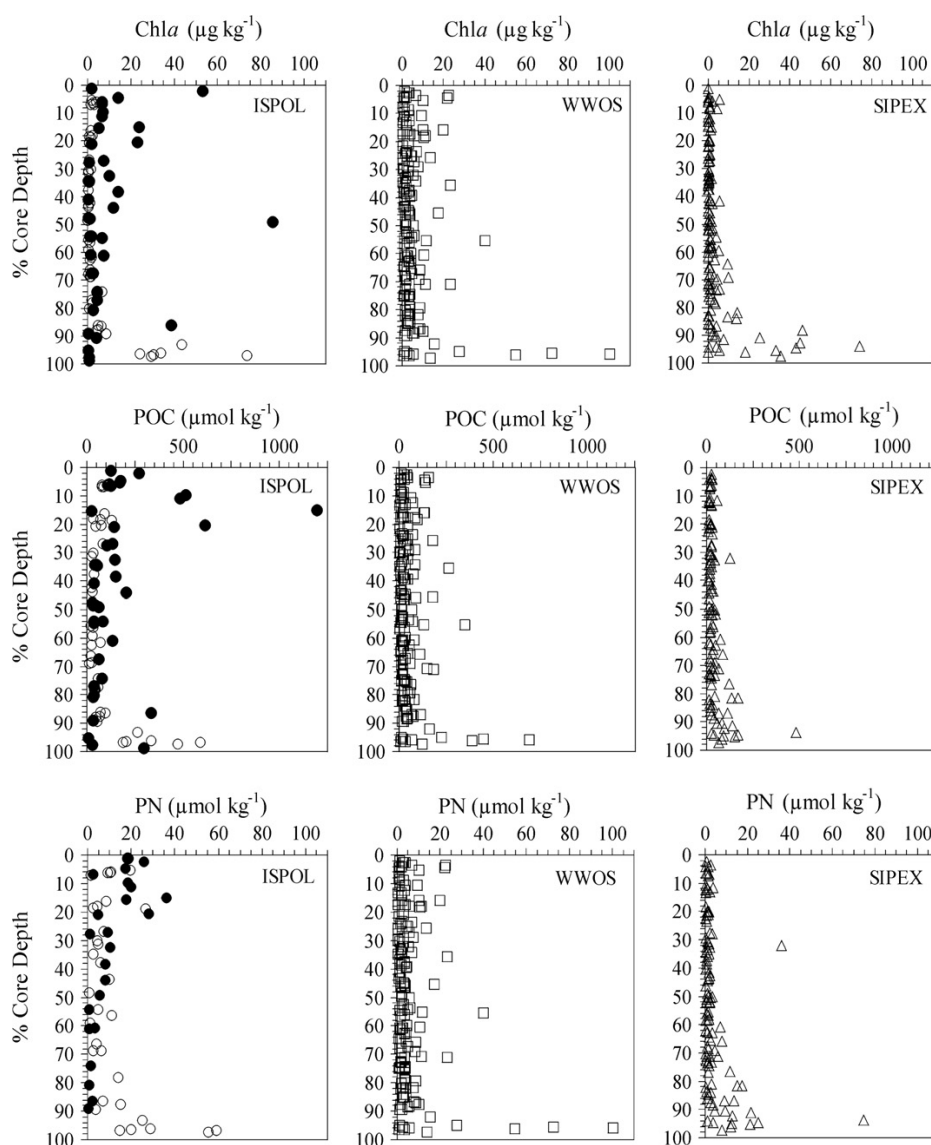


Fig. 5. Ice core profiles of POC, PN, and Chla. In the ISPOL figures, solid circles represent cores from second-year ice with surface and internal communities and open circles represent cores from first-year ice. For clarity of presentation POC concentrations $> 1250 \mu\text{mol kg}^{-1}$, PN concentrations $> 100 \mu\text{mol kg}^{-1}$, and Chla concentrations $> 100 \mu\text{g kg}^{-1}$ are not included in the figures. The excluded observations were derived from the bottom section (142–155 cm depth below the ice surface) of the core obtained on 05/10/06 ([POC]=3433 $\mu\text{mol kg}^{-1}$, [PN]=449 $\mu\text{mol kg}^{-1}$, and [Chla]=2191 $\mu\text{g kg}^{-1}$), and from the bottom section (111–121 cm depth) of the core obtained on 09/10/06 ([Chla]=223 $\mu\text{g kg}^{-1}$), both during WWOS.

variability (Table 2). Mean DOC and DON concentrations were significantly different between the studies (DOC: $p < 0.005$, DON: $p < 0.03$), with the highest means and largest ranges of both parameters occurring in the WWOS brine samples (Table 2). The mean salinity-normalised concentrations of DOC and DON in sackhole brines (normalised to a salinity of 35; Gleitz et al., 1995) were higher than the salinity-normalised concentrations of the underlying seawater during ISPOL and WWOS (Table 2), indicating enrichment of DOC and DON in the sea ice brine beyond that which can be explained by simple physical concentration of these solutes. In contrast, during SIPEX, the mean salinity-normalised concentrations of DOC and DON in sackhole brines ($60 \pm 31 \mu\text{mol kg}^{-1}$ and $3.9 \pm 1.8 \mu\text{mol kg}^{-1}$, respectively) were similar to the mean salinity-normalised seawater concentrations (57 ± 10 and $3.9 \pm 1.0 \mu\text{mol kg}^{-1}$, respectively). The DOC and DON measurements in the brines were positively correlated, (Fig. 7; ISPOL: $r^2=0.808$, $p < 0.001$, $n=31$; WWOS: $r^2=0.772$, $p < 0.001$, $n=122$; SIPEX: $r^2=0.438$, $p=0.031$, $n=29$), and although the observed DOC:DON was variable within all three datasets, the mean DOC:DON did not differ significantly between the datasets (Table 2). Within the ISPOL and SIPEX datasets, there was a small proportion of observations ($< 10\%$) that had a lower DOC:DON (≤ 10) than the majority of samples (range = 14 to 30; Table 2). These observations were excluded from the regression analysis shown in Fig. 7.

The POC and PN concentrations were all elevated in the WWOS brine samples compared to the ISPOL samples (Table 2), but they were not significantly different. The measured concentrations of both parameters were highly variable during both campaigns, although there appeared to be some degree of consistency within locations, particularly during the WWOS field study. The POC and PN of the brines were positively correlated (Fig. 8; ISPOL: $r^2_{\text{linear}}=0.163$,

$p=0.032$, $n=23$; WWOS: $r^2_{\log-\log}=0.907$, $p < 0.001$, $n=120$). The two highest PN observations (19.2 and $22.9 \mu\text{mol kg}^{-1}$) from the ISPOL data set were excluded as the concentrations were 3- to 4-fold higher than any other sample measured and disproportionately influenced the analysis. As with the bulk ice samples, the mean POC:PN differed between the two studies at 18 ± 16 (ISPOL) and 9 ± 3 (WWOS), which may be attributed to the difficulties encountered when sampling particulate matter from sackhole brines.

The Chla concentrations in WWOS brine samples were higher than the ISPOL brine samples (significant at $p < 0.001$), with the majority of the WWOS brine samples yielding Chla concentrations between 2 and $5 \mu\text{g kg}^{-1}$ and all ISPOL samples yielding $< 2.1 \mu\text{g kg}^{-1}$. No Chla data are available from the SIPEX brine samples. As with the POC and PN, the reported Chla concentrations in the brine are only an approximation of the *in situ* concentrations.

3.1.4. Surface gap layers

The biogeochemical composition of the two surface gap layers sampled during the ISPOL study has been reported in Papadimitriou et al. (2009). Briefly, the concentrations of the biogenic dissolved and particulate matter were within the ranges observed in bulk sea ice, with higher DOC, DON, POC, PN, and Chla concentrations in the waters of the thick gap layer overlying second-year ice than those in the water of the thin gap layer overlying thick first-year ice. Additional biogeochemical measurements (pH, dissolved molecular oxygen, major dissolved inorganic nutrients, including total dissolved inorganic carbon), however, indicated comparable autotrophic activity in both gap layers by the surface biological assemblage which extended in the neighboring surface ice layers. Mean values, standard deviations, and ranges are given in Table 2.

3.2. CDOM

The absorption spectra of seawater followed the commonly observed exponential decline with increasing wavelength (Bricaud et al., 1981), but the bulk ice, brine, and gap water samples did not. Many of the bulk ice and brine samples, and all of the gap water samples had a distinct peak at 320–330 nm, with the bulk ice samples also displaying a shoulder between 260 and 280 nm. These features were consistent across all three studies (Figs. 9 and 10). Using 375 nm (a_{375}) as an indicator of CDOM concentration, all studies yielded the highest concentrations in the brine samples, with mean values 4 times greater than in the underlying seawater (Table 3). No significant differences were found in a_{375} between the studies. The carbon-specific CDOM absorption (a_{375}^c) was highest in the bulk ice samples, with a maximum value of $2.38 \text{ m}^2 \text{ g}^{-1} \text{ C}$ (Table 3).

Due to the presence of the shoulders and peaks, none of the gap water spectra, only 12% of the ice spectra, and 47% of the brine spectra could be modeled with an exponential function.

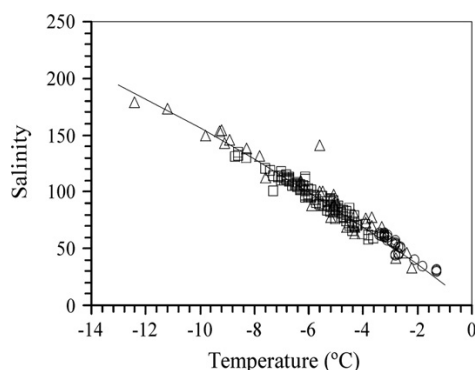


Fig. 6. Salinity as a function of temperature in sea ice brines. The open circles represent ISPOL samples, open squares represent WWOS samples, and open triangles represent SIPEX samples. The solid line represents the functional relationship between the two parameters as described by Petrich and Eicken (2010).

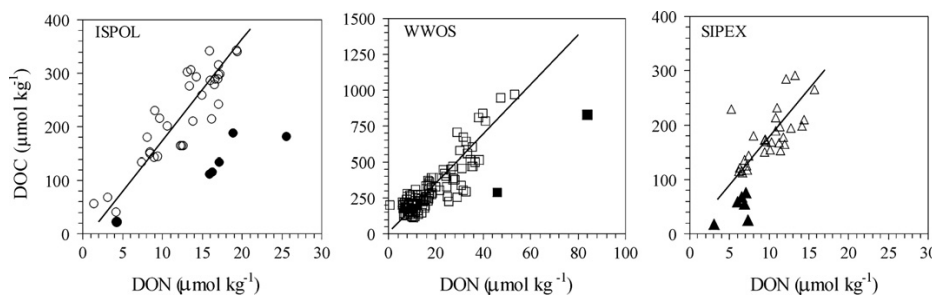


Fig. 7. DOC as a function of DON in sea ice brines. The solid lines represent linear regressions. The solid symbols in all graphs represent observations not included in the regression analysis. Note that the WWOS data is presented on a different scale from the ISPOL and SIPEX data due to the much larger concentration range measured. Regression equations: $[\text{DOC}] = -17 (\pm 42) + 19 (\pm 3) [\text{DON}]$ (ISPOL), $[\text{DOC}] = 15 (\pm 28) + 17 (\pm 1) [\text{DON}]$ (WWOS), $[\text{DOC}] = 1 (\pm 52) + 18 (\pm 5) [\text{DON}]$ (SIPEX).

The *S* values obtained from this sub-set of the data show very similar means and ranges in the seawater and brine samples, whereas the bulk ice samples exhibited a lower mean and minimum value than that of the seawater and brine samples (Table 3). In contrast the a_{375}^* of the bulk ice samples was more than double that of the brine and almost double that of the seawater (Table 3). When *S* was plotted against the a_{375}^* of the brine and seawater samples, all observations followed the same trend, with higher *S* values and low a_{375}^* in seawater and brine and low *S* and high a_{375}^* in bulk sea ice (Fig. 11).

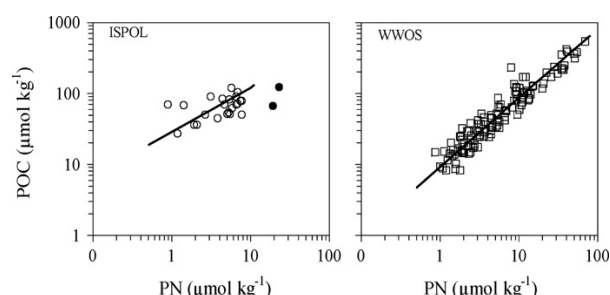


Fig. 8. POC as a function of PN in sea ice brine. The solid lines represent regressions on measured (ISPOL) and log transformed concentrations (WWOS). Solid circles on the ISPOL graph represent observations not included in the regression analysis. Regression equations: $[POC]=14 (\pm 21)+11 (\pm 4) [PN]$ (ISPOL), $[POC]=9 [PN]^{0.97 (\pm 0.08)}$ (WWOS).

3.2.1. Relationships with physical and biogeochemical parameters.

In order to investigate possible relationships between the biogeochemical and physical parameters (DOC, DON, POC, PN, Chl_a, temperature, and salinity) and the optical measurements (CDOM), the absorption spectra of each sample type (seawater, bulk ice, brine, and surface gap layer) were divided into four wavelength bands, and the integrated CDOM absorption coefficient ($a_{CDOM\lambda}$) within those bands was calculated for each sample. Bands 1 (250 to 255 nm) and 4 (390 to 400 nm) represented the background CDOM, band 2 (265 to 270 nm) contained the highest point of the shoulder observed in the bulk ice samples, and band 3 (320 to 330 nm) contained the top of the peak observed in the bulk ice, brine, and gap water samples (see Fig. 9). Between studies the $a_{CDOM\lambda}$ at band 3 in the WWOS bulk ice samples was lower than in both the ISPOL and SIPEX samples (significant at $p=0.001$ and $p < 0.001$, respectively), and in the brine samples the $a_{CDOM\lambda}$ of the SIPEX brine samples was lower than in both ISPOL and WWOS brine samples at all bands (significant at $p < 0.05$) (Table 4). No additional information was gained as to the source of the peaks from the correlation analysis of the wavelength bands with the physical and biochemical parameters.

3.3. Photo-bleaching experiment

3.3.1. Light measurements

The maximum UVR values reached 4.70 W m^{-2} at $t=1 \text{ h}$, and 70.31 W m^{-2} at $t=72 \text{ h}$ (between 1500 and 1600 ship time (UTC -4)) for the UVB and UVA bands, respectively, while the minimum values reached 0.02 W m^{-2} , initially at $t=12 \text{ h}$ and then at each

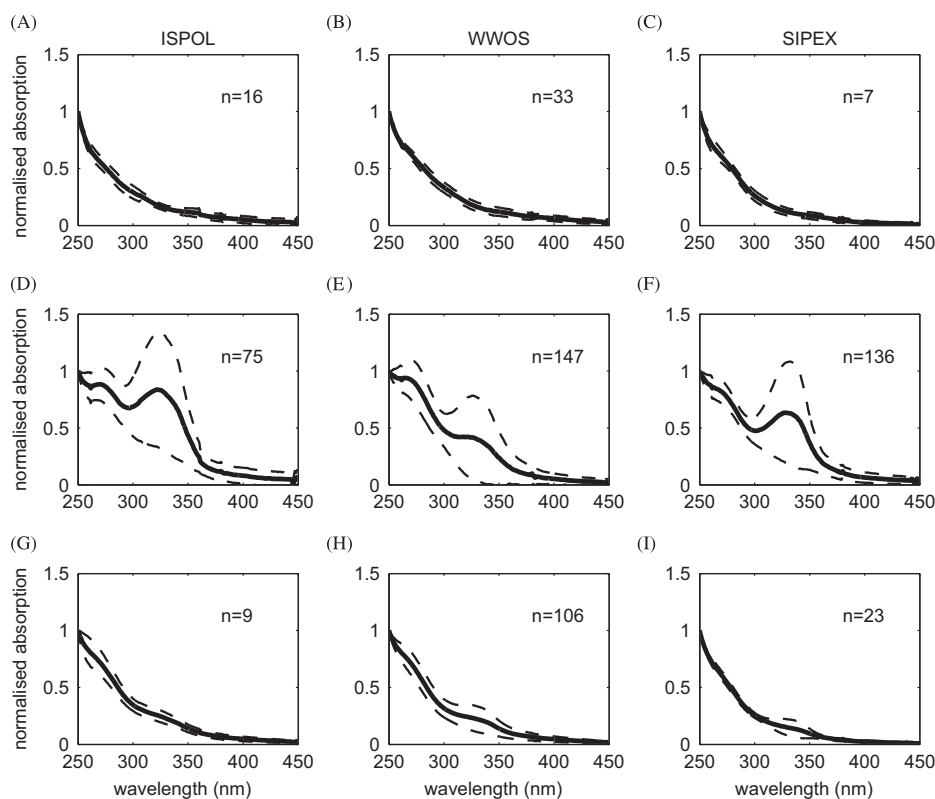


Fig. 9. Seawater, bulk-ice, and brine absorption spectra. Data presented are means and standard deviations of normalised absorption spectra (value at 250 nm normalised to 1). (A), (B), (C)=seawater samples, (D), (E), (F)=ice core section samples, (G), (H), (I)=brine samples.

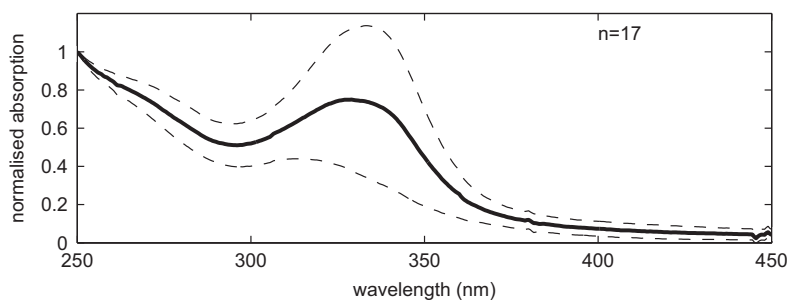


Fig. 10. Absorption spectra from water samples collected from two gap layers during the ISPOL drift experiment in the Weddell Sea between 27/11/04–02/01/05. Data presented are means and standard deviations of normalised absorbance spectra (value at 250 nm normalised to 1).

Table 3

Mean \pm standard deviation, (range), and number of observations (n) for the samples from Antarctic sea ice and surface oceanic waters from which optical measurements of DOM (CDOM) were obtained: CDOM absorption coefficient ($a_{\text{CDOM}\lambda}$) at 375 nm (a_{375}) and average between 320 and 330 nm ($\hat{a}_{320-330}$, corresponding to the peak observed in Figs. 9 and 10), spectral slope (S calculated from the exponential model fit on individual 300–650 nm spectra), carbon-specific absorption (a_{375}^*), and corresponding dissolved organic carbon (DOC) concentrations. For many samples from the brines and ice cores, and for all of the surface gap layer samples it was not possible to model the absorption spectra using an exponential model (see Figs. 9 and 10 for indication of these non-exponential spectral shapes) and S could therefore not be calculated.

	Seawater	Ice	Brine	Surface Gap Layer
a_{375} (m^{-1})	0.11 ± 0.11 (0.01–0.78) n=54	0.14 ± 0.16 (0.00–1.43) n=358	0.41 ± 0.37 (0.00–1.79) n=138	0.28 ± 0.14 (0.07–0.68) n=23
$\hat{a}_{320-330}$ (m^{-1})	0.29 ± 0.55 (0.06–4.23) n=54	0.56 ± 0.46 (0.03–2.83) n=358	1.23 ± 0.99 (0.12–4.52) n=138	1.34 ± 0.77 (0.34–3.37) n=23
S (μm^{-1})	20.9 ± 6.1 (11.1–39.6) n=51	16.2 ± 6.9 (6.5–33.3) n=42	20.2 ± 4.1 (13.7–34.6) n=65	No Data
a_{375}^* ($\text{m}^2 \text{g}^{-1} \text{C}$)	0.19 ± 0.18 (0.04–0.94) n=27	0.33 ± 0.37 (0.00–2.38) n=320	0.13 ± 0.09 (0.00–0.46) n=130	0.56 ± 0.47 (0.08–1.71) n=18
DOC ($\mu\text{mol kg}^{-1}$)	47 ± 14 (14–76) n=43	42 ± 30 (6–192) n=320	271 ± 172 (23–970) n=137	84 ± 75 (18–324) n=20

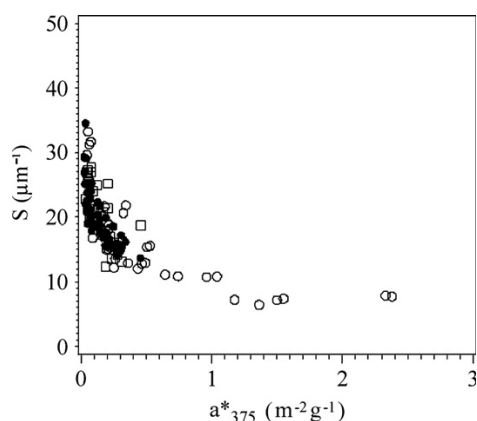


Fig. 11. Spectral slope (S, 300–650 nm) as a function of the carbon-specific absorption coefficient (a_{375}^*). Solid circles represent brine, open circles represent bulk ice, and open squares represent seawater.

24 h interval thereafter, and 0.81 W m^{-2} at $t=12 \text{ h}$ (between 03:00 and 04:00 ship time), respectively (Fig. 12; daily averages given in Table 5). Due to methodological restraints imposed by the type of

sensor used, the PAR data could only be expressed in $\mu\text{mol m}^{-2} \text{ s}^{-1}$. Here the maximum values were around $2500 \mu\text{mol m}^{-2} \text{ s}^{-1}$ at $t=72 \text{ h}$ (local noon), while minimum values reached $\sim 20 \mu\text{mol m}^{-2} \text{ s}^{-1}$ at local midnight (Fig. 12).

3.3.2. Biogeochemical parameters

The shoulders and peaks observed in many of the brine samples were not present in the brine collected for the photo-bleaching experiment. Therefore, in addition to 375 nm it was possible to add two further reference wavelengths of 280 nm and 330 nm to calculate a percentage change in CDOM absorbance over the 120 h experimental period. A clear decrease in $a_{\text{CDOM}\lambda}$ was observed at 280 and 330 nm in the light-exposed brine samples, with little change observed in the dark control samples (Fig. 13). The 120 h exposure to photo-bleaching resulted in a 53% decrease in $a_{\text{CDOM}\lambda}$ at 280 nm and 58% decrease at 330 nm (Table 6; Fig. 14). In contrast, $a_{\text{CDOM}\lambda}$ at 375 nm initially increased by 12% in the light-exposed samples during the first 24 h of the experiment. An overall decrease in $a_{\text{CDOM}\lambda}$ of 30% from the initial concentration was measured at $t=48 \text{ h}$, and no further change was observed at $t=120 \text{ h}$ (Table 6; Fig. 14). The control samples increased throughout the experiment and a 48% increase in $a_{\text{CDOM}\lambda}$ at 375 nm was measured at $t=120 \text{ h}$ (Table 6; Fig. 14). Some variability in DOC

Table 4

Mean \pm standard deviation and (range) for integrated CDOM absorbance coefficients ($a_{\text{CDOM}\lambda}$) within wavelength bands 250 to 255 nm (band 1), 265 to 270 nm (band 2), 320 to 330 nm (band 3) and 390 to 400 nm (band 4) in seawater, bulk ice, brine and gap layer samples. Bands 1 and 4 represent background CDOM, while bands 2 and 3 represent the location of spectral peaks.

	ISPOL 27/11/04 - 02/01/05				WWOS 06/09/06 - 13/10/06			SIPEX 11/09/07 - 10/10/07		
	Seawater, n=10	Bulk Ice, n=74	Brine, n=8	Gap layers, n=20	Seawater, n=32	Bulk Ice, n=142	Brine, n=105	Seawater, n=7	Bulk Ice, n=134	Brine, n=18
Band 1 250 to 255 nm	0.97 \pm 0.18 (0.66–1.18)	0.82 \pm 0.77 (0.13–6.3)	4.3 \pm 2.1 (1.1–6.2)	1.8 \pm 0.50 (0.95–2.92)	0.96 \pm 0.14 (0.71–1.26)	1.0 \pm 1.5 (0.22–16.5)	5.5 \pm 3.6 (2.1–21.1)	1.6 \pm 0.75 (0.98–3.2)	0.95 \pm 0.51 (0.34–3.8)	2.8 \pm 1.2 (0.97–5.5)
Band 2 265 to 270 nm	0.65 \pm 0.14 (0.42–0.79)	0.79 \pm 0.96 (0.11–8.1)	3.5 \pm 1.8 (0.8–5.2)	1.5 \pm 0.54 (0.70–2.8)	0.69 \pm 0.12 (0.45–0.96)	1.1 \pm 1.7 (0.17–19.2)	4.6 \pm 3.5 (1.4–20.2)	1.2 \pm 0.54 (0.68–2.3)	0.82 \pm 0.45 (0.27–3.7)	1.9 \pm 0.84 (0.71–3.9)
Band 3 320 to 330 nm	0.18 \pm 0.04 (0.14–0.26)	0.59 \pm 0.41 (0.07–1.7)	1.1 \pm 0.47 (0.33–1.6)	1.5 \pm 0.68 (0.43–3.2)	0.20 \pm 0.06 (0.06–0.33)	0.39 \pm 0.42 (0.03–2.7)	1.4 \pm 1.0 (0.16–4.5)	0.25 \pm 0.12 (0.12–0.47)	0.62 \pm 0.48 (0.09–2.7)	0.48 \pm 0.27 (0.12–1.1)
Band 4 390 to 400 nm	0.06 \pm 0.03 (0.03–0.12)	0.06 \pm 0.05 (0.00–0.21)	0.23 \pm 0.13 (0.03–0.33)	0.14 \pm 0.07 (0.06–0.40)	0.07 \pm 0.03 (0.01–0.15)	0.07 \pm 0.09 (0.00–0.73)	0.32 \pm 0.28 (0.00–1.2)	0.05 \pm 0.04 (0.01–0.09)	0.07 \pm 0.08 (0.00–0.44)	0.08 \pm 0.05 (0.00–0.2)

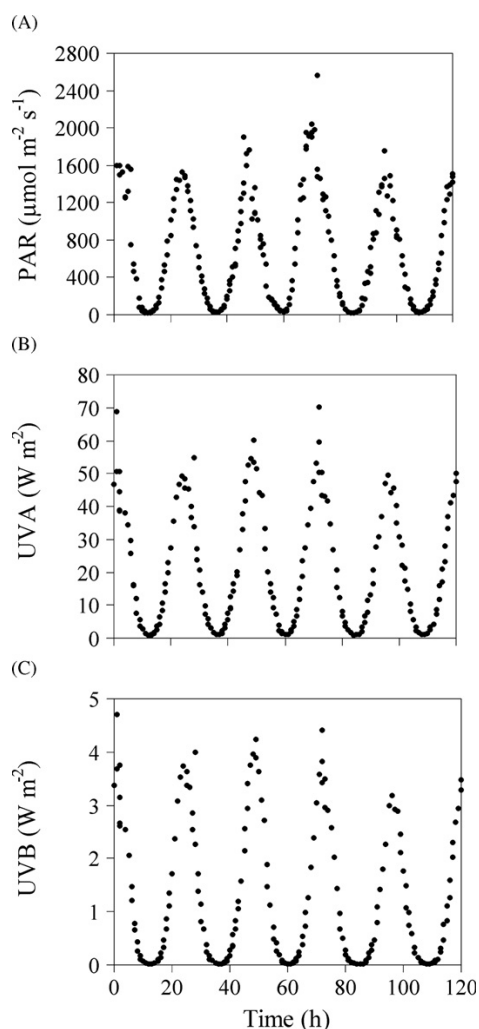


Fig. 12. PAR (A), UVA (B) and UVB (C) measurements during a CDOM photo-bleaching experiment on the ISPOL ice floe between 1500 ($t=0$ h) 06/12/04 and 1500 ($t=120$ h) 10/12/04. PAR data are expressed in $\mu\text{mol m}^{-2} \text{s}^{-1}$, and UVR data are expressed in W m^{-2} . Note difference in scale of Y axis.

Table 5

UVA and UVB daily doses (kJ d^{-1}) during CDOM photo-bleaching experiment on the ISPOL floe. The calculations are based on hourly averages.

Day	UVA (kJ d^{-1})	UVB (kJ d^{-1})
06/12/04	1793.61	114.89
07/12/04	1646.07	117.91
08/12/04	2138.84	127.20
09/12/04	1730.77	99.14
10/12/04	1739.00	99.05

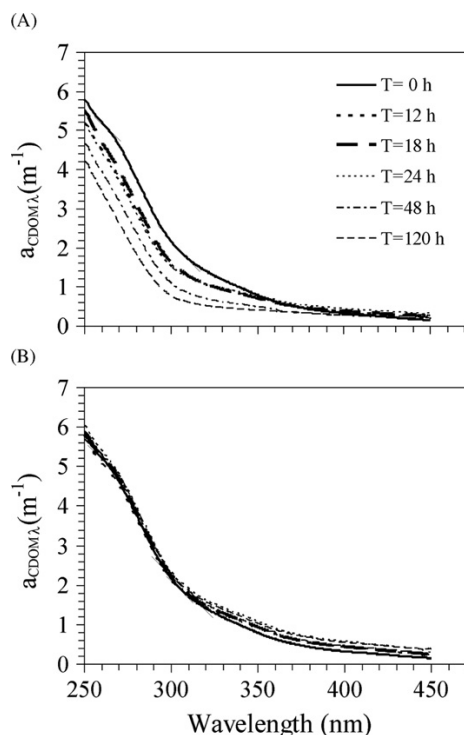


Fig. 13. Changes in CDOM absorbance spectra over time ($t=0$ to $t=120$ h) in sea ice brine exposed to light (A) and dark control (B) *in situ* during a CDOM photo-bleaching experiment set up during ISPOL in order to investigate the bleaching dynamics of brine CDOM. Brine salinity = 55.2.

Table 6

Spectral slope (S , calculated from the exponential model fit on individual 300–650 nm spectra), CDOM absorption coefficient ($a_{\text{CDOM},\lambda}$) at 280 nm (a_{280}), 330 nm (a_{330}), and 375 nm (a_{375}), carbon-specific absorption (a_{375}^*), and corresponding DOC and DON concentrations ($\mu\text{mol kg}^{-1}$) during the CDOM photo-bleaching experiment on the ISPOL floe (brine salinity=55.2).

Treatment	Time Point (hr)	S (μm^{-1})	a_{280} (m^{-1})	a_{330} (m^{-1})	a_{375} (m^{-1})	a_{375}^* ($\text{m}^2 \text{g}^{-1} \text{C}$)	DOC ($\mu\text{mol kg}^{-1}$)	DON ($\mu\text{mol kg}^{-1}$)
Initial Value	0	23.10	3.8	1.2	0.47	0.16	249	18.4
Light Exposed	12	27.78	3.1	0.9	0.48	0.16	251	12.6
	18	28.03	2.9	0.9	0.48	0.16	254	16.2
	24	28.68	2.9	1.0	0.54	0.18	251	12.3
	48	33.82	2.4	0.6	0.33	0.11	257	15.0
	120	35.62	1.8	0.5	0.33	0.11	249	15.2
Dark Control	12	23.31	3.9	1.3	0.58	0.19	252	13.5
	18	23.07	3.9	1.4	0.59	0.19	251	15.9
	24	22.81	3.9	1.3	0.72	0.23	261	14.7
	48	23.12	3.8	1.3	0.70	0.19	261	18.1
	120	23.26	3.7	1.3	0.70	0.24	247	13.9

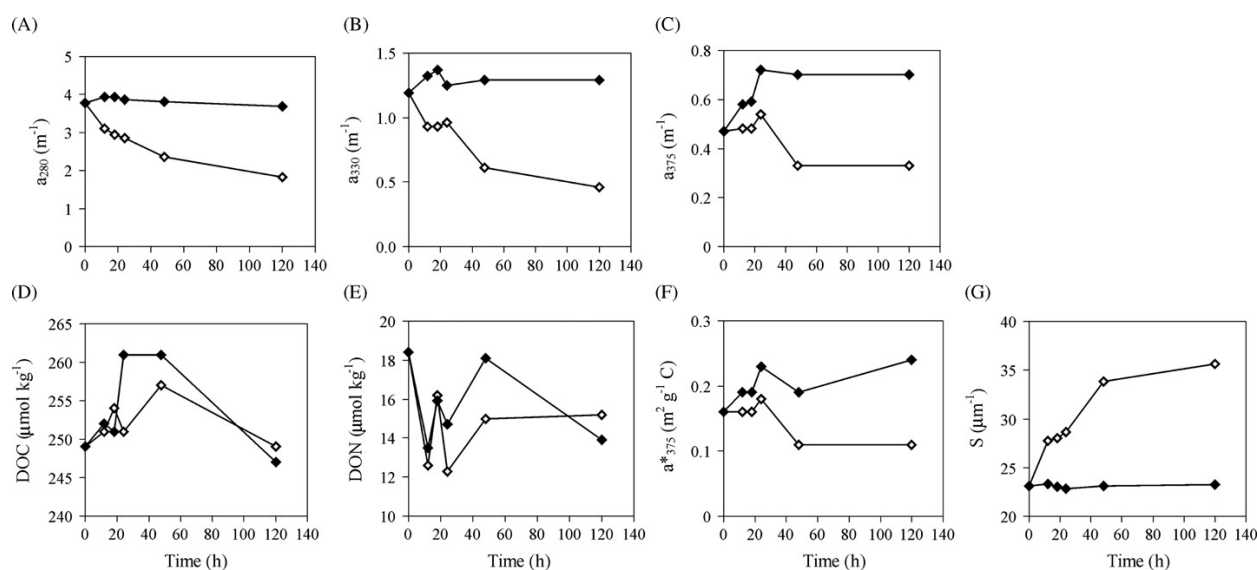


Fig. 14. Changes in $a_{\text{CDOM},\lambda}$ at 280 nm (a_{280}) (A), 330 nm (a_{330}) (B), 375 nm (a_{375}), (C), DOC (D) and DON (E) concentrations ($\mu\text{mol kg}^{-1}$), carbon-specific absorption (a_{375}^*) (F), and spectral slope (G) (S , calculated from the exponential model fit on individual 300–650 nm spectra), over time for a CDOM photo-bleaching experiment set up during ISPOL in order to investigate the bleaching dynamics of brine CDOM. Brine salinity=55.2. Open symbols represent light exposed samples, and filled symbols represent dark (control) samples.

from the initial concentration of $249 \mu\text{mol kg}^{-1}$ was observed in both sample sets, with increases of 3.2% in the light exposed samples, and a 4.8% in the control samples occurring in the first 48 h of the experiment. However, DOC in both sample sets returned to the initial concentration (Light: $249 \mu\text{mol kg}^{-1}$; Control: $247 \mu\text{mol kg}^{-1}$) by the end of the experiment (Table 6, Fig. 14). A loss of DON from the starting concentration of $18.4 \mu\text{mol kg}^{-1}$ was evident in both treatments (Light at $t=120$ h: $15.2 \mu\text{mol kg}^{-1}$; Control at $t=120$ h: $13.9 \mu\text{mol kg}^{-1}$) (Table 6; Fig. 14).

The overall trend of the a_{375}^* in the light-exposed samples was a decline from $0.16 \text{ m}^2 \text{g}^{-1} \text{C}$ at $t=0$ to $0.11 \text{ m}^2 \text{g}^{-1} \text{C}$ at $t=120$ h, save for a small rise at $t=24$ h to $0.18 \text{ m}^2 \text{g}^{-1} \text{C}$. In the dark (control) samples, the overall trend was an increase in a_{375}^* to $0.24 \text{ m}^2 \text{g}^{-1} \text{C}$, suggesting production of light-absorbing carbon-specific CDOM in the control samples during the experimental period (Table 6; Fig. 14). However, the observed variability in DOC concentration was not coincident with the variability of the a_{375}^* in either sample set.

The S value at $t=0$ was $23.1 \mu\text{m}^{-1}$, with the dark (control) samples varying little from this value throughout the duration (120 h) of the experiment (range: 22.8 to $23.3 \mu\text{m}^{-1}$). In contrast, the light-exposed samples exhibited a steady and significant

increase in S ($p=0.006$), with a final value of $35.6 \mu\text{m}^{-1}$ at $t=120$ h (Table 6; Figs. 13 and 14).

4. Discussion

4.1. Biogeochemical parameters

The sources of organic matter (i.e. incorporation from the underlying seawater and *in situ* production) are likely to be broadly the same for each of the studies reported here. It is reasonable to expect that although the quantity of material will be variable depending on seasonal ice growth and decay (e.g., younger ice encountered during SIPEX generally had lower concentrations of the measured parameters than the ISPOL and WWOS ice), the quality of the material will not vary between the studies.

The DOC and POC concentrations in seawater measured during ISPOL and WWOS are within the range previously measured in the Weddell Sea during summer and winter, respectively (Garrison and Close, 1993; Wedborg et al., 1998; Herborg et al., 2001; Ogawa and Tanoue, 2003; Dumont et al., 2009; Ortega-Retuerta et al., 2010).

The SIPEX seawater DOC and POC concentrations are comparable with previously reported concentrations for the same time of year, and from the same area in the Southern Ocean (Dumont et al., 2009). The elevated mean DOC and DON concentrations of the SIPEX samples compared to the ISPOL and WWOS samples may be attributed to the sampling strategy, where full under-ice seawater depth profiles were measured during ISPOL and WWOS, whereas all SIPEX seawater samples were collected at between 1 and 10 m depth. In all three studies, save for a small number of cores exhibiting internal and surface biomass maxima, the highest concentrations of all measured biogeochemical parameters were found in the bottom 10 to 20 cm of the ice column. The WWOS maximum values were all elevated in comparison to ISPOL and SIPEX, indicating that there was considerably more biomass present in the bottom sections of the ice during the WWOS study than during the other two studies.

The mean salinity-normalised bulk ice DOC and DON concentrations were, in all studies, enriched relative to the salinity-normalised concentrations of the underlying seawater, which suggests further *in situ* production that incorporated from the surface ocean as the ice formed. Thomas et al. (2001), Herborg et al. (2001), and Kattner et al. (2004) report mean bulk ice DOC concentrations of 109 μM , 207 μM , and 254 μM in summer sea ice from the Weddell Sea, which are 2- to 5-fold greater than the mean values reported here. Mean brine DOC concentrations reported in Thomas et al. (2001) are also 2- to 4-fold higher than the concentrations reported in this study.

The range of DOC concentrations in the bulk ice reported from the ISPOL study by Dumont et al. (2009) were 106 to 701 $\mu\text{M C}$ as opposed to the much lower range reported here of 20 to 157 μM . The two sets of samples were taken from different areas on the floe, and this variability is an example of the heterogeneity of a single ice floe (Eicken et al., 1991). Similarly, the bulk ice DOC ranges reported here for the SIPEX study and in Dumont et al. (2009) for the ARISE study (2003) were quite different, despite the similar ice conditions (Lannuzel et al., 2007) of the two studies, with the SIPEX mean DOC concentration being half that of the lowest reported measurement from the ARISE ice samples.

All three studies exhibited a large range of DOC to DON ratios in the bulk ice samples, reflected in the relatively low but still significant correlations, with DOC:DON > 50 observed in all studies and DOC:DON > 140 observed in both WWOS and SIPEX studies. All but one of the samples associated with these high DOC:DON values had a DOC concentration that was close to the mean DOC concentrations. This indicates that these high ratios were due to N depletion rather than C enrichment, although no evidence could be found to indicate that DON had been incorporated into the POM. The mean DOC:DON ratios of all three studies were similar to the mean value of 11 reported by Thomas et al. (2001) from samples collected in the southeastern Weddell, Bellingshausen, and Amundsen seas in summer.

The mean concentration and upper concentration range of the POC, PN, and Chl a measured in the bulk ice during SIPEX were all much lower than those measured in the ISPOL and WWOS studies. All the measured biogeochemical parameters from the SIPEX bulk-ice and brine samples had lower concentrations than those of ISPOL and WWOS. The mean POC concentrations measured in the SIPEX samples were also half of that reported in young Weddell Sea winter ice by Garrison and Close (1993), whereas the POC concentrations reported for the ISPOL samples were similar to summer low to medium biomass values reported by Kattner et al. (2004). In addition, the majority of cores collected during SIPEX were < 100 cm with half of these being < 55 cm thick, whereas the cores collected during ISPOL and WWOS were > 70 cm thick, with most being \geq 100 cm thick. The lower biomass and thinner ice during SIPEX indicates an environment of young winter ice growth

with low biomass compared to the older first- and second-year ice from ISPOL and WWOS.

The mean bulk ice POC:PN values reported here in the WWOS samples were similar to the value of 9.5 ± 5.6 reported by Kennedy et al. (2002), with the SIPEX samples being slightly elevated by comparison. In contrast the POC:PN values of the ISPOL samples (mean: 26 ± 36 ; Table 2) were considerably higher. These elevated POC:PN values appear to be a reflection of a mostly non-living as opposed to actively growing community (Kattner et al., 2004), as may be expected in spring/summer ice.

4.2. CDOM absorption and optical properties

The seawater CDOM concentrations (a_{375}) were within the range expected for oceanic waters (Blough and Del Vecchio, 2002), but mean a_{375} in the melted ice cores was lower than the values reported in young Arctic sea ice (Belzile et al., 2000). For the CDOM spectra that could be modeled with an exponential relationship, the resulting S values followed the trend expected from mixing of fresh and old marine CDOM (Stedmon and Markager, 2001), with fresh CDOM having low S values ($\sim 10 \mu\text{m}^{-1}$) and the old marine CDOM having very low concentrations ($a_{375} < 0.05 \text{ m}^{-1}$) and higher S values ($S \sim 20$ to $30 \mu\text{m}^{-1}$). The carbon-specific CDOM absorption was highest in the melted ice cores, with a maximum value of $2.4 \text{ m}^2 \text{ g}^{-1} \text{ C}$. These values are similar to those reported for terrestrial material in the Baltic region and Arctic rivers (Stedmon et al., 2000), which indicates that CDOM production in the ice generates material which is as intense in colour as terrestrial material. For comparison, the seasonal production of CDOM in the surface waters of the North Atlantic generated CDOM with an $a_{375}^* < 0.3 \text{ m}^2 \text{ g}^{-1} \text{ C}$. Plotting the S values versus the carbon specific absorption values reveals the characteristics of CDOM for the two general end-members present (Fig. 11). This indicates that the optical characteristics of the CDOM pool across all samples and locations in the current study can be broadly described by the mixing of two end-members; with fresh material, characterised by low S values and more chromophores (i.e. high a_{375}^*) as one end-member, and older material, typically characterised by high S and low a_{375}^* , as the other. S values have been found to be inversely proportional to the average molecular weight of DOM, with high molecular weight material having low S values and low molecular weight material high S values (Blough and Green, 1995). This indicates that the fresh material referred to above has a high molecular weight DOM. This would be in agreement with the size-reactivity continuum model of Amon and Benner (1996) whose results indicated that the origins of high molecular weight components are generally more recent than those of low molecular weight components. Moreover, the results presented here are also in agreement with those of Belzile and Guo (2006) who showed that low DOC-specific DOM was less coloured and of a lower molecular weight than high DOC-specific DOM.

Peaks in CDOM absorbance spectra similar to those observed here (Figs. 9 and 10) have been identified in both natural and experimental samples. Belzile et al. (2000) reported peaks of this type in ice core samples from the Northern Baffin Bay. Patsayeva et al. (2004) also observed peaks between 270 and 300 nm in brine samples generated in an ice tank experiment, and Ortega-Retuerta et al. (2010) observed peaks below 300 nm in Southern Ocean seawater used in CDOM photochemical experiments, particularly in those where Chl a and bacterial abundance were high. Similar absorbance spectra have also been found to be present in the CDOM produced by cyanobacteria in culture (Steinberg et al., 2004). The shoulders observed in this study between 260 to 280 nm (constrained in band 2 at 265 to 270 nm) are likely to be associated with aromatic amino acids, such as tryptophan and tyrosine, which

exhibit a strong absorbance band at ~ 280 nm, and can contribute significantly to the absorption of UV radiation (Wozniak and Dera, 2007). A number of mycosporine-like amino acids (MAAs), which are UV-absorbing compounds, have been identified with absorbance maxima in the 310 to 360 nm spectral range (Nakamura et al., 1982; Karentz et al., 1991; Shick et al., 1992; Davidson et al., 1994). Riegger and Robinson (1997) observed absorption maxima in the 330 to 333 nm range in 9 out of 11 cultured Antarctic diatom species, which, they suggested, indicated the presence of UV-absorbing compounds, such as MAAs, while Fritsen et al. (2011) have also suggested MAAs as a likely contributor to particulate absorption peaks at ~ 325 nm observed in ice samples from the Bellingshausen Sea. The peaks between 320 and 330 nm measured in this study may therefore be associated with MAAs, as they were markedly high also in samples from the two surface gap layers (Fig. 10), which represents an environment exposed to high solar radiation. MAAs (especially shinorine and palythine) have indeed been shown to contribute significantly to UV absorption in thin snow free sea ice in the Baltic Sea (Uusikivi et al., 2010), with absorption peaks in the 320 to 330 nm range for particulate matter in surface ice layers, indicative of significant production of MAAs by ice algae. In Antarctic phytoplankton, these MAAs are dominated by porphyra-334 with shinorine, mycosporine-glycine, and palythine accounting for the majority of the rest of the MAA pool (Villafañe et al., 1995; Riegger and Robinson, 1997; Ryan et al., 2002). These MAAs are used by many organisms as a chemical sunscreen for protection from UV-radiation and are thought to play a major protective role in ice algal assemblages (Arrigo and Thomas, 2004).

The marked differences between the brine and bulk ice CDOM spectra may be attributed to our sampling strategy, with sackhole brine samples integrating material from an unknown volume of sea ice depending on sackhole depth and sea ice porosity (Papadimitriou et al., 2007). The sackhole brine CDOM spectra from the present study generally represent surface and interior conditions of the sea ice, while the CDOM spectra obtained from ice cores also include bottom ice sections, which often show elevated ice algal biomass as indicated by the Chl *a* concentrations. The bottom ice sections represent sites of high *in situ* DOM production, as indicated by the higher carbon specific absorption values, and fresher, more coloured DOM. In addition, during the melting for bulk ice samples sympagic organisms are released from a higher salinity to a much lower salinity over a period of 24 h. This may result in the loss of intracellular organic compounds, although Thomas et al. (1998, 2001) have argued that these amounts will be low by comparison with the extracellular DOM pool. Nevertheless, melting represents similar conditions to those generated during seasonal ice melt, when the material in sea ice is released to the underlying water.

4.3. CDOM photo-bleaching in sea ice brine.

The photo-bleaching experiment shows that sea ice brine is susceptible to photo-bleaching of the CDOM chromophores over short time scales (i.e. days). This was evident not only in the loss of CDOM concentration, also reported by Ortega-Retuerta et al. (2010, and citations therein) in Antarctic seawater, but also in the large change in *S*, which has been shown to increase as photo-bleaching occurs (Vodacek et al., 1997; Moran et al., 2000). The relatively high photo-bleaching measured during the experiment may suggest that previously the DOM had little earlier exposure to UV radiation; however, Ziegler and Benner (2000) reported losses at 350 nm of 33% (May) and 81% (July) during a 35-h experiment using surface seawater, and Vodacek et al. (1997) reported a reduction of up to 70% of the CDOM absorption and fluorescence (at 355 nm) under high light conditions in surface waters of the Middle Atlantic Bight. In CDOM degradation experiments Hulatt et al. (2009) reported

losses of CDOM absorption at 440 nm of up to 76% over a 16-day period in macroalgae exposed to sunlight. Although the attenuation of light through snow, ice, brine, and water in natural systems may vary from the experimental conditions, the results of Hulatt et al. (2009) indicate that PAR may be as destructive to CDOM chromophores as UVR.

The coincidental loss of DOC as reported by Osburn et al. (2009) was not evident, indicating either a decoupling of CDOM photo-reactivity and DOC photo-remineralisation, or simply that any potential change in the DOC concentration was below the detection limit, occurring on the nM rather μ M concentration scale. The degradation and destruction of CDOM chromophores by photo-bleaching seen here decreases CDOM absorption, increases the penetration of UV radiation (Moran and Zepp, 1997), and initiates the production of a suite of reactive products (Miller and Zepp, 1995; Moran and Zepp, 1997; Uher and Andreae, 1997; Stubbins et al., 2006; Kitidis et al., 2008). Of particular significance to sea ice are the detrimental effects of increased UV radiation on primary production (Arrigo and Brown, 1996), the production of biologically labile products, which may serve as a source of remineralised nutrients (Moran and Zepp, 1997), and the possible photochemical transformations of nitrate and hydrogen peroxide to hydroxyl radicals (Chu and Anastasio, 2003). Observations from snow packs have suggested that the hydroxyl radical may be linked to the production of acetaldehyde and formaldehyde (Couch et al., 2000) and that a reaction between sea ice brine and the OH radical may in part be responsible for polar ozone depletions due to liberation of gaseous halogen species (Peterson and Honrath, 2001; King et al., 2005). King et al. (2005) suggested that first-year sea ice may be an efficient medium for photochemistry, with 85% of all photochemistry occurring in the top 1 m of the ice. This may be of significant importance to the function and structure of organisms which live in this specialized habitat, particularly in young first-year sea ice as was observed during the SIPEX study.

4.4. Potential importance of sea ice-derived CDOM

The measurements from the melted ice cores suggest that, when Antarctic sea ice melts, it might represent a major source of DOM and in particular CDOM to surface waters of the seasonally ice-covered Southern Ocean. This is supported by the findings of Kieber et al. (2009) and Ortega-Retuerta et al. (2010). The effect of this material on the optical properties of the recipient oceanic waters and its importance to the local carbon budget can only be speculated on at this stage, with our data set as a starting point. Using the DOC data for bulk sea ice in Table 3, we can estimate the flux of DOC potentially released from the sea ice annually as a result of sea ice melt. Assuming an area of seasonal ice melt of 16×10^6 km² and an average ice thickness of 1 m (Comiso, 2010), a DOC flux of $0.5 \text{ g C m}^{-2} \text{ yr}^{-1}$ ($42 \text{ mmol C m}^{-2} \text{ yr}^{-1}$) is estimated from the melting sea ice into the surface oceanic mixed layer, which is equivalent to a total areal input of approximately 8 Tg C yr^{-1} . Although this value is low in comparison to the standing stock of DOC in Antarctic surface mixed layer [480 Tg , assuming 50 m mixed layer and average seawater DOC of $50 \mu\text{mol L}^{-1}$ (Kähler et al., 1997; Ogawa and Tanoue, 2003)], this represents a release of not only old DOC that was incorporated into the sea ice during formation, but also new and presumably more labile DOC to the surface waters. In contrast, the standing stock of DOC in the Antarctic surface mixed layer is likely to be older and more refractory. Our annual DOC input estimate of 8 Tg C from sea ice suggests that about 11% of total annual primary production by sea ice algae (70 Tg C yr^{-1} ; Arrigo et al., 2010) is potentially exported to the surface oceanic waters as DOC during the seasonal sea ice melt. For comparison, Arctic river catchments export 16 Tg C to the

Arctic Ocean from a catchment area of similar size to that of the seasonal Antarctic sea ice melt zone (Raymond et al., 2007).

sea ice-derived CDOM is likely to influence the optical properties of the surface Antarctic waters and as a consequence influence primary production within these waters via either UV protection or the attenuation of visible light (Arrigo and Brown 1996), although this might be a transient feature due to the susceptibility of this material to photo-bleaching, as shown in our experiment. Ice melt will also influence the spectral characteristics of CDOM absorption in these surface waters as the material released from the ice has low S values, which equate to a flatter absorption spectrum, i.e. relatively greater absorption of visible wavelengths. Antarctic sea ice therefore represents a productive environment and a likely important source of labile DOC and fresh autochthonous CDOM to surface waters, which in turn influence microbial heterotrophic and autotrophic production, respectively, and thus play a significant role in the cycling of organic matter in the Southern Ocean.

Acknowledgments

CS was supported by the Carlsberg Foundation and the Danish Research Council (grant #272-07-0485). DNT, LN & SP were supported by grants from NERC, The Royal Society and the Leverhulme Trust. MAG was supported by a grant from the Academy of Finland (# 108150). RHK was supported by the German Research Council (DFG; grant #WE2536/6-2). The work during SIPEX was supported by the Australian Government through the Antarctic Climate and Ecosystems Cooperative Research Centre, and by the Australian Antarctic Division through AAS project 2767. We are grateful to the crews of R.V. *Polarstern* and R.S. *Aurora Australis* as well as numerous colleagues, too many to mention, on each trip for their help in making this work possible. In particular we thank H. Betts, E Allhusen, A Scheltz, D.P. Kennedy and R. Thomas for their help in sample analyses and preparation for the cruises. We also thank Lisa Miller and two anonymous reviewers for their useful suggestions on an early version of this manuscript.

References

- Amon, R.M.W., Benner, R., 1996. Bacterial utilization of different size classes of dissolved organic matter. *Limnology and Oceanography* 41, 41–51.
- Arrigo, K.R., Brown, C.W., 1996. Impact of chromophoric dissolved organic matter on UV inhibition of primary productivity in the sea. *Marine Ecology Progress Series* 140, 207–216.
- Arrigo, K.R., Thomas, D.N., 2004. Large scale importance of sea ice biology in the Southern Ocean. *Antarctic Science* 16, 471–486. doi:10.1017/S0954102004002263.
- Arrigo, K.R., Mock, T., Lizotte, M.P., 2010. Primary producers and sea ice. In: Thomas, D.N., Dieckmann, G.S. (Eds.), *Sea Ice 2nd Edition* Wiley-Blackwell, Oxford, pp. 283–325.
- Belzile, C., Johannessen, S.C., Gosselin, M., Demers, S., Miller, W.L., 2000. Ultraviolet attenuation by dissolved and particulate constituents of first-year ice during late spring in an Arctic polynya. *Limnology and Oceanography* 45, 1265–1273.
- Belzile, C., Guo, L., 2006. Optical properties of low molecular weight and colloidal organic matter: Application of the ultrafiltration permeation model to DOM absorption and fluorescence. *Marine Chemistry* 98, 183–196.
- Benner, R., Louchouart, P., Amon, R.M.W., 2005. Terrigenous dissolved organic matter in the Arctic Ocean and its transport to surface and deep waters of the North Atlantic. *Global Biogeochemical Cycles* 19, GB2025. doi:10.1029/2004GB002398.
- Blough, N.V., Green, S.A., 1995. Spectroscopic characterization and remote sensing of nonliving organic matter. In: Zepp, R.G., Sonntag, C. (Eds.), *The Role of Nonliving Organic Matter in the Earth's Carbon Cycle*. John Wiley and Sons, pp. 23–45.
- Blough, N.V., Del Vecchio, R., 2002. Chromophoric DOM in the coastal environment. In: Hansell, D.A., Carlson, C.A. (Eds.), *Biogeochemistry of Marine Dissolved Organic Matter*. Academic Press, London, pp. 509–546.
- Bricaud, A., Morel, A., Prieur, L., 1981. Absorption by dissolved organic matter of the sea (yellow substance) in the UV and visible domains. *Limnology and Oceanography* 26, 43–53.
- Carder, K.L., Steward, R.G., Harvey, G.R., Ortner, P.B., 1989. Marine humic and flavic acids: Their effects on remote sensing of ocean chlorophyll. *Limnology and Oceanography* 34, 68–81.
- Chin, Y.-P., Gschwend, P.M., 1992. Partitioning of polycyclic aromatic hydrocarbons to marine porewater organic colloids. *Environmental Science and Technology* 26, 1621–1626. doi:10.1021/es00032a020.
- Chu, L., Anastasio, C., 2003. Quantum yields of hydroxyl radical and nitrogen dioxide from the photolysis of nitrate on ice. *Journal of Physical Chemistry A* 107, 9594–9602. doi:10.1021/jp0349132.
- Coble, P.G., 2007. Marine optical biogeochemistry: The chemistry of ocean color. *Chemical Reviews* 107, 402–418. doi:10.1021/cr050350+.
- Comiso, J.C., 2010. Variability and trends of the global sea ice cover. In: Thomas, D.N., Dieckmann, G.S. (Eds.), *Sea Ice 2nd Edition* Wiley-Blackwell, Oxford, pp. 205–246.
- Couch, T.L., Sumner, A.L., Dassau, T.M., Shepson, P.B., Honrath, R.E., 2000. An investigation of the interaction of carbonyl compounds with the snowpack. *Geophysical Research Letters* 27, 2241–2244.
- Cox, G.F.N., Weeks, W.F., 1983. Equations for determining the gas and brine volumes in sea ice samples. *Journal of Glaciology* 29, 306–316.
- Davidson, A.T., Bramich, D., Marchant, H.J., McMinn, A., 1994. Effects of UV-B irradiation on growth and survival of Antarctic marine diatoms. *Marine Biology* 119, 507–515.
- Dumont, I., Schoemann, V., Lannuzel, D., Chou, L., Tison, J.-L., Becquevort, S., 2009. Distribution and characterization of dissolved and particulate organic matter in Antarctic pack ice. *Polar Biology* 32, 733–750.
- Ehn, J., Granskog, M.A., Reinart, A., Erm, A., 2004. Optical properties of melting landfast sea ice and underlying seawater in Santala Bay, Gulf of Finland. *Journal of Geophysical Research* 109, C09003. doi:10.1029/2003JC002042.
- Eicken, H., Lange, M.A., Dieckmann, G.S., 1991. Spatial variability of sea ice properties in the northwestern Weddell Sea. *Journal of Geophysical Research—Oceans* 96 (C6), 10603–10615.
- Ertel, J.R., Hedges, J.I., Devol, A.H., Richey, J.E., de Nazaré Góes Ribeiro, M., 1986. Dissolved humic substances of the Amazon River system. *Limnology and Oceanography* 31, 739–754.
- Evans, C.A., O'Reilly, J.E., Thomas, J.P., 1987. *A Handbook for the Measurement of Chlorophyll a and Primary Production*. Biological Investigations of Marine Antarctic Systems and Stocks (BIOMASS). Texas A & M University.
- Fritsen, C.H., Wirthlin, E.D., Momberg, D., Lewis, M.J., Ackley, S.F., 2011. Bio-optical properties of Antarctic pack ice in the early austral spring. *Deep-Sea Research II* 58 (9–10), 1052–1061.
- Garrison, D.L., Close, A.R., 1993. Winter ecology of the sea ice biota in Weddell Sea pack ice. *Marine Ecology Progress Series* 96, 17–31.
- Gleit, M., Rutgers v.d. Loeff, M., Thomas, D.N., Dieckmann, G.S., Millero, F.J., 1995. Comparison of summer and winter inorganic carbon, oxygen and nutrient concentrations in Antarctic sea ice brine. *Marine Chemistry* 51, 81–91.
- Granskog, M.A., Kaartokallio, H., Thomas, D.N., Kuosa, H., 2005. Influence of freshwater inflow on the inorganic nutrient and dissolved organic matter within coastal sea ice and the underlying waters in the Gulf of Finland (Baltic Sea). *Estuarine Coastal and Shelf Science* 65, 109–122.
- Granskog, M., Kaartokallio, H., Kuosa, H., Thomas, D.N., Vainio, J., 2006. Sea ice in the Baltic: A review. *Estuarine Coastal and Shelf Science* 70, 145–160.
- Haas, C., Nicolaus, M., Batzke, A., Willmes, S., Lobach, J., 2007. Changes of sea ice physical properties during the onset of melt. ISPOL Cruise Report. Reports in Polar Research 551 571–102.
- Haas, C., Friedrich, A., Li, Z., Nicolaus, M., Pfaffling, A., Toyota, T., 2009. Regional variability of sea ice properties and thickness in the northwestern Weddell Sea obtained by *in-situ* and satellite measurements. Cruise Report Winter Weddell Outflow Study (WWOS)-ANT XXIII/7. Reports in Polar Research 586, 36–74.
- Hellmer, H.H., Schröder, M., Haas, C., Dieckmann, G.S., Spindler, M., 2008. The ISPOL drift experiment. *Deep-Sea Research II* 55, 913–917.
- Hellmer, H., van Caspel, M., Macrandrer, A., Olbers, D., Sellmann, L., Mata, M., Da Silva Duarte, V., Kerr Duarte Pereira, R., Nuez, N., Schodlok, M., 2009. Water mass variability in the north-western Weddell Sea: A continuation of the DOVETAIL project. Reports in Polar Research 586, 16–21.
- Herborg, L.-M., Thomas, D.N., Kennedy, H., Haas, C., Dieckmann, G.S., 2001. Dissolved carbohydrates in Antarctic sea ice. *Antarctic Science* 13, 119–125.
- Holm-Hansen, O., Lorenzen, C.J., Holmes, R.W., Strickland, J.D.H., 1965. Fluorometric determination of chlorophyll. *ICES Journal of Marine Science (International Council for the Exploration of the Sea)* 30, 3–15.
- Hulatt, C.J., Thomas, D.N., Bowers, D.G., Norman, L., Zhang, C., 2009. Exudation and decomposition of chromophoric dissolved organic matter (CDOM) from some temperate macroalgae. *Estuarine Coastal and Shelf Science* 84, 147–153.
- Kähler, P., Bjørnsen, P.K., Lochte, K., Antia, A., 1997. Dissolved organic matter and its utilization by bacteria during spring in the Southern Ocean. *Deep-Sea Research II* 44, 341–353.
- Karentz, D., McEuen, F.S., Land, M.C., Dunlop, W.C., 1991. Survey of mycosporine-like amino acid compounds in Antarctic marine organisms: Potential protection from ultraviolet exposure. *Marine Biology* 108, 157–166.
- Kattner, G., Thomas, D.N., Haas, C., Kennedy, H., Dieckmann, D.S., 2004. Surface ice and gap layers in Antarctic sea ice: highly productive habitats. *Marine Ecology Progress Series* 277, 1–12.
- Kennedy, H., Thomas, D.N., Kattner, G., Haas, C., Dieckmann, G.S., 2002. Particulate organic matter in Antarctic summer sea ice: concentration and stable isotopic composition. *Marine Ecology Progress Series* 238, 1–13.
- Kieber, D.J., Toole, D.A., Kiene, R.P., 2009. Chromophoric dissolved organic matter cycling during a Ross Sea *Phaeocystis Antarctica* bloom. In: Krupnik, I., Lang, M.A., Miller, S.E. (Eds.), *Smithsonian at the Poles: Contributions to International Polar Year Science – a Smithsonian Contribution to Knowledge*. Smithsonian Institution Scholarly Press, Washington, D.C, pp. 319–333.

- King, M.D., France, J.L., Fisher, F.N., Beine, H.J., 2005. Measurement and modeling of UV radiation penetration and photolysis rate of nitrate and hydrogen peroxide in Antarctic sea ice: An estimate of the production rate of hydroxyl radicals in first-year sea ice. *Journal of Photochemistry and Photobiology A: Chemistry* 176, 39–49.
- Kitidis, V., Uher, G., Woodward, E.M.S., Owens, N.J.P., Upstill-Goddard, R.C., 2008. Photochemical production and consumption of ammonium in a temperate river-sea system. *Marine Chemistry* 112, 118–127.
- Lannuzel, D., Schoemann, V., de Jong, J., Tison, J.-L., Chou, L., 2007. Distribution and biogeochemical behaviour of iron in the East Antarctic sea ice. *Marine Chemistry* 106, 18–32.
- Lannuzel, D., Schoemann, V., de Jong, J., Chou, L., Delille, B., Becquervort, S., Tison, J.-L., 2008. Iron study during a time series in the western Weddell pack ice. *Marine Chemistry* 108, 85–95.
- Lemke, P., 2009. Itinerary and Summary. Cruise Report Winter Weddell Outflow Study (WWOS)-ANT XXIII/7. Reports in Polar Research 586, 10–11.
- Leppäranta, M., Manninen, T., 1988. The brine and gas content of sea ice with attention to low salinities and high temperatures. Finnish Institute Marine Research Internal Report 88-2. Helsinki.
- Meiners, K.M., Papadimitriou, S., Thomas, D.N., Norman, L., Dieckmann, G.S., 2009. Biogeochemical conditions and ice algal photosynthetic parameters in Weddell Sea ice during early spring. *Polar Biology* 32, 1055–1065. doi:10.1007/s00300-009-0605-6.
- Miller, W.L., Zepp, R.G., 1995. Photochemical production of dissolved inorganic carbon from terrestrial organic matter: Significance to the oceanic organic carbon cycle. *Geophysical Research Letters* 22, 417–420.
- Millero, F.J., Poisson, A., 1981. International one-atmosphere equation of state of seawater. *Deep-Sea Research* 28A, 625–629.
- Moran, M.A., Zepp, R.G., 1997. Role of photoreactions in the formation of biologically labile compounds from dissolved organic matter. *Limnology and Oceanography* 42, 1307–1316.
- Moran, M.A., Sheldon, W.M., Zepp, R.G., 2000. Carbon loss and optical property changes during long-term photochemical and biological degradation of estuarine dissolved organic matter. *Limnology and Oceanography* 45, 1254–1264.
- Nakamura, H., Kobayashi, J., Hirata, Y., 1982. Separation of mycosporine-like amino acids in marine organisms using reversed-phase high-performance liquid chromatography. *Journal of Chromatography* 250, 113–118.
- Nelson, N.B., Siegel, D.A., 2002. Chromophoric DOM in the open ocean. In: Hansell, D.A., Carlson, C.A. (Eds.), *Biogeochemistry of Marine Dissolved Organic Matter*. Academic Press, London, pp. 547–578.
- Obernosterer, I., Benner, R., 2004. Competition between biological and photochemical processes in the mineralization of dissolved organic carbon. *Limnology and Oceanography* 49, 117–124.
- Ogawa, H., Tanoue, E., 2003. Dissolved organic matter in oceanic waters. *Journal of Oceanography* 59, 129–147.
- Ortega-Retuerta, E., Reche, I., Pulido-Villena, E., Agustí, S., Duarte, C.M., 2010. Distribution and photoreactivity of chromophoric dissolved organic matter in the Antarctic Peninsula (Southern Ocean). *Marine Chemistry* 118, 129–139. doi:10.1016/j.marchem.2009.11.008.
- Osburn, C.L., Retamal, L., Vincent, W.F., 2009. Photoreactivity of chromophoric dissolved organic matter transported by the Mackenzie River to the Beaufort Sea. *Marine Chemistry* 115, 10–20.
- Papadimitriou, S., Thomas, D.N., Kennedy, H., Haas, C., Kuosa, H., Krell, A., Dieckmann, G.S., 2007. Biogeochemical composition of natural sea ice brines from the Weddell Sea during early austral summer. *Limnology and Oceanography* 52, 1809–1823.
- Papadimitriou, S., Thomas, D.N., Kennedy, H., Kuosa, H., Dieckmann, G.S., 2009. Inorganic carbon removal and isotopic enrichment in Antarctic sea ice gap layers during early austral summer. *Marine Ecology Progress Series* 386, 15–27. doi:10.3354/meps08049.
- Patsayeva, S., Reuter, R., Thomas, D.N., 2004. Fluorescence of dissolved organic matter in seawater at low temperatures and during ice formation. *EARSeL eProceedings* 3, 227–238.
- Perovich, D.K., Roesler, C.S., Pegau, W.S., 1998. Variability in Arctic sea ice optical properties. *Journal of Geophysical Research* 103, 1193–1208.
- Peterson, M.C., Honrath, R.E., 2001. Observations of rapid photochemical destruction of ozone in snowpack interstitial air. *Geophysical Research Letters* 28, 551–514.
- Petrich, C., Eicken, H., 2010. Growth, structure and properties of sea ice. In: Thomas, D.N., Dieckmann, G.S. (Eds.), *Sea ice 2nd Edition* Wiley-Blackwell, Oxford, pp. 23–77.
- Raymond, P.A., McClelland, J.W., Holmes, R.M., Zhulidov, A.V., Mull, K., Peterson, B.J., Striegl, R.G., Aiken, G.R., Gurtovaya, T.Y., 2007. Flux and age of dissolved organic carbon exported to the Arctic Ocean: A carbon isotopic study of the five largest arctic rivers. *Global Biogeochemical Cycles* 21, GB4011. doi:10.1029/2007GB002934.
- Retamal, L., Vincent, W.F., Martineau, C., Osburn, C.L., 2007. Comparison of the optical properties of dissolved organic matter in two river-influenced coastal regions of the Canadian Arctic. *Estuarine, Coastal and Shelf Science* 72, 261–272.
- Ricker, W.E., 1973. Linear regressions in fishery research. *Journal of the Fisheries Research Board Canada* 30, 409–434.
- Riegger, L., Robinson, D., 1997. Photoinduction of UV-absorbing compounds in Antarctic diatoms and *Phaeocystis Antarctica*. *Marine Ecology Progress Series* 160, 13–25.
- Ryan, K.G., McMinn, A., Mitchell, K.A., Trenerry, L., 2002. Mycosporine-like amino acids in Antarctic sea ice algae, and their response to UVB radiation. *Zeitschrift für Naturforschung* 57, 471–477.
- Scully, N.M., Miller, W.L., 2000. Spatial and temporal dynamics of colored dissolved organic matter in the North Water Polynya. *Geophysical Research Letters* 27, 1009–1011.
- Shick, J.M., Dunlap, W.C., Chalker, B.E., Banaszak, A.T., Rosenzweig, T.K., 1992. Survey of ultraviolet radiation-absorbing mycosporine-like amino acids in organs of coral reef holothuroids. *Marine Ecology Progress Series* 90, 139–148.
- Stedmon, C.A., Markager, S., Kaas, H., 2000. Optical properties and signatures of chromophoric dissolved organic matter (CDOM) in Danish coastal waters. *Estuarine Coastal and Shelf Science* 51, 267–278.
- Stedmon, C.A., Markager, S., 2001. The optics of chromophoric dissolved organic matter (CDOM) in the Greenland Sea: An algorithm for differentiation between marine and terrestrially derived organic matter. *Limnology and Oceanography* 46, 2087–2093.
- Stedmon, C.A., Thomas, D.N., Granskog, M., Kaartokallio, H., Papadimitriou, S., Kuosa, H., 2007. Characteristics of dissolved organic matter in Baltic coastal sea ice: Allochthonous or autochthonous origins? *Environmental Science and Technology* 41, 7273–7279. doi:10.1021/es071210f.
- Steinberg, D.K., Nelson, N.B., Carlson, C.A., Prusak, A.C., 2004. Production of chromophoric dissolved organic matter (CDOM) in the open ocean by zooplankton and the colonial cyanobacterium *Trichodesmium* spp. *Marine Ecology Progress Series* 267, 45–56.
- Stubbins, A., Uher, G., Law, C.S., Mopper, K., Robinson, C., Upstill-Goddard, R.C., 2006. Open-ocean carbon monoxide photoproduction. *Deep-Sea Research II* 53, 1695–1705.
- Thomas, D.N., Lara, R.J., Haas, C., Schnack-Schiel, S.B., Dieckmann, G.S., Kattner, G., Nöthig, E.-M., Mizdalski, E., 1998. Biological soup within decaying summer sea ice in the Amundsen Sea, Antarctica. In: Lizotte, M.P., Arrigo, K.R. (Eds.), *Antarctic Sea Ice Biological Processes, Interactions, and Variability*, 73. American Geophysical Union, Antarctic Research Series, pp. 161–171.
- Thomas, D.N., Kattner, G., Engbrodt, R., Giannelli, V., Kennedy, H., Haas, C., Dieckmann, G.S., 2001. Dissolved organic matter in Antarctic sea ice. *Annals of Glaciology* 33, 297–303.
- Thomas, D.N., Dieckmann, G.S., 2002a. Antarctic sea ice – a habitat for extremophiles. *Science* 295, 641–644.
- Thomas, D.N., Dieckmann, G.S., 2002b. Biogeochemistry of Antarctic sea ice. *Oceanography and Marine Biology: An Annual Review* 40, 143–169.
- Thomas, D.N., Papadimitriou, S., Michel, C., 2010. Biogeochemistry of sea ice. In: Thomas, D.N., Dieckmann, G.S. (Eds.), *Sea ice 2nd Edition* Wiley-Blackwell, Oxford, pp. 425–467.
- Thurman, M.E., 1985. *Organic Geochemistry of Natural Waters*. Kluwer Academic Publishers.
- Uher, G., Andreae, M.O., 1997. Photochemical production of carbonyl sulfide in North Sea water: A process study. *Limnology and Oceanography* 42, 432–442.
- Uusikivi, J., Vähätalo, A., Granskog, M.A., Sommaruga, R., 2010. Contribution of mycosporine-like amino acids, colored dissolved and particulate matter on sea ice optical properties and ultraviolet attenuation. *Limnology and Oceanography* 55, 703–713.
- van der Merwe, P.C., Lannuzel, D., Mancuso Nichols, C.A., Meiners, K., Heil, P., Norman, L., Thomas, D.N., Bowie, A.R., 2009. Biogeochemical observations during the winter-spring transition in East Antarctic sea ice: evidence of iron and exopolysaccharide controls. *Marine Chemistry* 115, 163–175. doi:10.1016/j.marchem.2009.08.001.
- Villafañe, V.E., Helbling, E.W., Holm-Hansen, O., Chalker, B.E., 1995. Acclimatization of Antarctic natural phytoplankton assemblages when exposed to solar ultraviolet radiation. *Journal of Plankton Research* 17, 2295–2306.
- Vodacek, A., Blough, N.V., DeGrandpre, M.D., Peltzer, E.T., Nelson, R.K., 1997. Seasonal variation of CDOM and DOC in the Middle Atlantic Bight: Terrestrial inputs and photooxidation. *Limnology and Oceanography* 42, 674–686.
- Wedborg, M., Hoppema, M., Skoog, A., 1998. On the relation between organic and inorganic carbon in the Weddell Sea. *Journal of Marine Systems* 17, 59–76.
- Weissenberger, J., 1992. The environmental conditions in the brine channels of Antarctic sea ice. *Reports on Polar Research* 111, 1–159.
- Wozniak, B., Dera, J., 2007. *Light Absorption in Sea Water*. Springer, New York.
- Xie, H., Bélanger, S., Demers, S., Vincent, W.F., Papakyriakou, T.N., 2009. Photo-biogeochemical cycling of carbon monoxide in the southeastern Beaufort Sea in spring and autumn. *Limnology and Oceanography* 54, 234–249.
- Ziegler, S., Benner, R., 2000. Effects of solar radiation on dissolved organic matter in a subtropical seagrass meadow. *Limnology and Oceanography* 45 (2), 257–266.



Contents lists available at [ScienceDirect](#)

Aquatic Toxicology

journal homepage: www.elsevier.com/locate/aquatox



Erratum

Erratum to “Antioxidant responses in the polar marine sea-ice amphipod *Gammarus wilkitzkii* to natural and experimentally increased UV levels” [Aquat.Toxicol. 94 (2009) 1–7]

Rupert H. Krapp^{a,b,*}, Thierry Baussant^c, Jørgen Berge^b, Daniela M. Pampanin^c, Lionel Camus^d

^a University of Kiel, Institute for Polar Ecology, Wischhofstr. 1-3, Building 12, 24148 Kiel, Germany

^b University Center in Svalbard, Postbox 156, 9171 Longyearbyen, Norway

^c International Research Institute of Stavanger (IRIS), Mekjarvik 12, N-4070 Randaberg, Norway

^d Akvaplan-niva a/s, Polar Environmental Centre, N-9296 Tromsø, Norway

The Corresponding author regrets that during the publication of above article one of the author was misspelled as “Thievery Bassinet” instead of “Thierry Baussant”.

DOI of original article: [10.1016/j.aquatox.2009.05.005](https://doi.org/10.1016/j.aquatox.2009.05.005).

* Corresponding author.

E-mail addresses: rkrapp@ipoe.uni-kiel.de, rupert.krapp@unis.no (R.H. Krapp).

0166-445X/\$ – see front matter © 2009 Elsevier B.V. All rights reserved.

doi:[10.1016/j.aquatox.2009.10.013](https://doi.org/10.1016/j.aquatox.2009.10.013)

